5-2019

AN OXANTHROQUINONE DERIVATIVE DISRUPTS RAS PLASMA MEMBRANE LOCALIZATION AND FUNCTION BY INHIBITION OF ACYLPEPTIDE HYDROLASE AND PERTURBATION OF SPHINGOMYELIN METABOLISM

Lingxiao Tan

AN OXANTHROQUINONE DERIVATIVE DISRUPTS RAS PLASMA MEMBRANE LOCALIZATION AND FUNCTION BY INHIBITION OF ACYLPEPTIDE HYDROLASE AND PERTURBATION OF SPHINGOMYELIN METABOLISM

BY

Lingxiao Tan, B.S.

APPROVED:

John F. Hancock, MA, MB, Bchir, PhD, ScD, MRCP(UK), FRACP.
Advisory Professor

Swathi Arur, Ph.D

Carmen W. Dessauer, Ph.D.

Guangwei Du, Ph.D.

Jeffrey A. Frost, Ph.D.

Dean, The University of Texas MD Anderson Cancer Center UTHealth Graduate School of Biomedical Science

AN OXANTHROQUINONE DERIVATIVE DISRUPTS RAS PLASMA MEMBRANE LOCALIZATION AND FUNCTION BY INHIBITION OF ACYLPEPTIDE HYDROLASE AND PERTURBATION OF SPHINGOMYELIN METABOLISM

A

DISSERTATION

Presented to the Faculty of

The University of Texas

MD Anderson Cancer Center UTHealth

Graduate School of Biomedical Sciences

in Partial Fulfillment

of the Requirements

for the Degree of

DOCTOR OF PHILOSOPHY

by

Lingxiao Tan, B.S.

Houston, Texas

MAY, 2019

DEDICATION

To my parents and my wife

Acknowledgements

First of all, I would love to thank my mentor, Dr. Hancock. Since I joined his lab six years ago, he has served as a perfect example as a scientist with great thinking. His thoughts have carved into my path of life and had a tremendous influence on me. The training that I have received in Dr. Hancock's lab is very comprehensive and I feel very fortunate to have been accepted in his lab.

I would love to thank my committee members, Drs. Frost, Du, Dessauer, and Arur. They have given me very precious advices and ideas. They are very knowledgeable and I enjoy talking with them.

I would love to thank our collaborator, Dr. Cho, Dr. Capon, Dr. Neupane, Dr. Kattan, Dr, Garrido. They performed several key experiments in this study. They also edited the paper before publication and gave me a lot of help in my research. I really enjoyed working with them.

I would love to thank my lab members in providing me a lot of great advices and ideas. Being friends with them gave me a lot of joy.

I would love to thank my fellow students and other friends. They helped me a lot when I have difficulties in my work and study.

AN OXANTHROQUINONE DERIVATIVE DISRUPTS RAS PLASMA MEMBRANE LOCALIZATION AND FUNCTION BY INHIBITION OF ACYLPEPTIDE HYDROLASE AND PERTURBATION OF SPHINGOMYELIN METABOLISM

Lingxiao Tan, B.S.

Advisory Professor: John F. Hancock, MA, MB, Bchir, PhD, ScD, MRCP(UK), FRACP

Abstract

Oncogenic RAS proteins are commonly expressed in human cancer. To be functional, RAS proteins must undergo post-translational modification and localize to the plasma membrane (PM). Therefore, compounds that prevent RAS PM targeting have potential as putative RAS inhibitors. Here we examined the mechanism of action of oxanthroquinone G01 (G01), a recently described inhibitor of KRAS PM localization. We show that G01 mislocalized HRAS and KRAS from the PM with similar potency and disrupted the spatial organization of RAS proteins remaining on the PM. G01 also inhibited recycling of epidermal growth factor receptor and transferrin receptor, but did not impair internalization of cholera toxin, indicating suppression of recycling endosome function. In searching for the mechanism of impaired endosomal recycling we observed that G01 also enhanced cellular sphingomyelin (SM) and ceramide levels and

disrupted the localization of several lipid and cholesterol reporters, suggesting that the G01 molecular target may involve SM metabolism. Indeed, G01 exhibited potent synergy with other compounds that target SM metabolism in KRAS localization assays.

When attached to a biotin moiety, G01 bound acylpeptide hydrolase (APEH) and blocked its enzymatic activity. Inhibition of APEH by ebelactone, an esterase inhibitor, or the knockdown of APEH mislocalized KRASG12V as well as phosphatidylserine from the PM. Together, these results suggest that G01 mislocalizes KRASG12V from the PM by binding to and inhibiting APEH function.

Furthermore, G01 significantly abrogated RAS-RAF-MAPK signaling in MDCK cells expressing constitutively activated, oncogenic mutant RASG12V. G01 also inhibited the proliferation of RAS-less mouse embryonic fibroblasts (MEFs) expressing oncogenic mutant KRASG12V or KRASG12D but not RAS-less MEFs expressing oncogenic mutant BRAFV600E. Consistent with these effects, G01 inhibited the proliferation of KRAS-transformed pancreatic, colon, and endometrial cancer cells. Taken together, these results suggest that G01 should undergo further evaluation as a potential anti-RAS therapeutic.

To enhance the potency of G01 for KRAS inhibition, we synthesized D01 and D02, two derivatives of G01 containing an additional geranyl or farnesyl group, respectively. D01 or D02 mislocalized KRAS more effectively than G01, and disrupted the clustering of KRAS at a much lower concentration than G01. As a consequence, D01 or D02 inhibited MAPK

signaling downstream of oncogenic KRAS, as well as the proliferation of KRAS-dependent pancreatic cancer cells.

Table of Contents

List of Figures

List of Tables

Abbreviation

AMPK: 5′ AMP-Activated Protein Kinase

APEH: Acylpeptide Hydrolase

ASM: Acid Sphingomyelinase

Cer: Ceramide

cGMP: Cyclic Guanosine Monophosphate

CHO: Chinese Hamster Ovary

CI: Combination Index

CTB-647: Cholera Toxin Subunit B, Alexa Fluor 647 Conjugate

EGFR: Epithelial Growth Factor Receptor

EM: Electron Microscopy

eNOS: Endothelial NOS

FB1: Fumonisin B1

FDA: Food and Drug Administration

FTI: Farnesyl Transferase Inhibitor

G01: Oxanthroquinone G01

GAP: GTPase-Activating Proteins

GEF: Guanine Nucleotide Exchange Factors

HK1: Hexokinase 1

HVR: Hypervariable Region

Icmt: Isoprenylcysteine Carboxyl Methyltransferase

MAPK: Mitogen-Activated Protein Kinase

MDCK: Madin-Darby Canine Kidney

MEF: Mouse Embryonic Fibroblast

MOMP: Mitochondrial Outer Membrane Permeabilization

NSAID: Nonsteroidal Anti-inflammatory Drug

PI3K: Phosphoinositol 3-Phosphate Kinase

PKC: Protein Kinase C

PKG: Protein Kinase G

PM: Plasma Membrane

PtdSer: Phosphatidylserine

Rce1: RAS-Converting Enzyme 1

RE: Recycling Endosome

RTK: Receptor Tyrosine Kinase

SM: Sphingomyelin

SPT: Serine-Palmitoyltransferase

STS: Staurosporine

S1P: Sphingosine-1-phosphate

Tf-555: Transferrin From Human Serum, Alexa Fluor 555 Conjugate

TfR: Transferrin Receptor

VEGFR: Vascular Endothelial Growth Factor Receptor

Chapter 1 Introduction

1.1 RAS biological function in normal and cancer cells

RAS proteins are small GTPases that regulate cell growth, proliferation, and differentiation. RAS cycles between the inactive GDP-bound state and the active GTP-bound state in concert with the action of guanine nucleotide exchange factors (GEFs) and GTPase-activating proteins (GAPs). GEFs catalyze the hydrolysis of RAS-bound GDP and thus promote the binding of GTP, whose cellular concentration is much higher than that of GDP [1]. In contrast with GEFs, GAPs are responsible for the inactivation of RAS. Although RAS itself possesses GTPase activity, it is very ineffective at catalyzing the hydrolysis of GTP to GDP, which is performed >1000 fold more efficiently in presence of GAPs [1]. RAS GEFs and GAPs include many proteins. For instance, SOS, the most studied GEF, binds to GDP-bound RAS and activates it by facilitating GDP hydrolysis, or it can bind to GTP-bound RAS and further stimulate RAS activation [2]. SOS activation of RAS happens exclusively on the plasma membrane (PM), and is regulated by GRB2, which recruits SOS to PM-localized RAS [2].

Activated GTP-bound RAS regulate various biological functions by interacting with downstream effectors. Over eleven families of effectors have been identified so far, with some of them contributing to the malignant transformation of cancers. The first RAS effector to be identified in mammalian cells was the serine/threonine kinase RAF, which is also the best studied effector bound to RAS [3]. RAS-GTP binds to three different RAF proteins, CRAF, BRAF, and ARAF. When active, RAF proteins phosphorylate mitogen-activated protein kinase kinases MEK1 and MEK2, which consequently phosphorylate extracellular signal-regulated kinases ERK1

and ERK2. The phosphorylation of ERK1 and ERK2 activates a series of substrates in the cytosol and nucleus. For instance, ERK phosphorylates c-JUN, leading to the activation of the AP1 transcription factor and subsequent expression of many cell cycle regulators [4].

Another well studied RAS downstream effector is the type I phosphatidylinositol 3-kinase (PI3K). The catalytic domain of PI3K binds to RAS, which activates the lipid kinase activity of PI3K [5, 6]. PI3K catalyzes the phosphorylation of phosphatidylinositol-4,5-bisphosphate (PtdIns(4,5)P_2) to phosphatidylinositol-3,4,5-trisphosphate (PtdIns(3,4,5)P_3), a secondary messenger that binds to several downstream enzymes. The most studied of them is AKT, which mediates cell survival by preventing apoptosis [7, 8].

Besides the RAS-RAF-MAPK and RAS-PI3K pathways, RAL represents another critical effector of RAS. The activation of RAL is dependent on the exchange factors RAL guanine nucleotide dissociation stimulator (RALGDS), RALGDS-like gene (RGL/RSB2), and RGL2/RLF. The activation of RAL switches on phospholipase D1 and CDC42/RAC-GAP-RAL binding protein 1 (RALBP1), which act along with AKT to mediate cell cycle arrest and apoptosis [9].

Phospholipase Cε is another important component of the RAS signaling pathway. It hydrolyzes PtdIns(4,5)P_2 to diacylglycerol and inositol-1,4,5-trisphosphate (Ins(1,4,5)P_3) [10], and is responsible for protein kinase C (PKC) activation and calcium mobilization.

A recent unpublished study by Mark R. Philips lab has identified hexokinase 1 (HK1) as a novel effector of RAS. This is the first evidence of RAS directly modulating a metabolic enzyme.

The proper function of RAS is crucial for normal cells, with RAS mutations

instead leading to abnormal development and cancer. RAS was identified initially in oncogenic viruses and was characterized as a 21-kDa protein (p21) [11]. These viruses cause sarcomas both *in vivo* and *in vitro*. In 1982, mutated RAS was discovered in human cancer [12]. Since then, over 500 cancer genes have been identified and validated, however RAS remains the most mutated oncogene [13] and is present in such form in approximately 15% of all human cancers. The most abundant mutation sites are on codons 12, 13, and 61; they block GDP hydrolysis and lock RAS in the GTP-bound active state, leading to constitutive activation of downstream effectors [13-15]. RAS proteins include three isoforms, KRAS, HRAS, and NRAS, which are encoded by separate genes. They contain an almost identical G-domain but very different hypervariable regions (HVRs), which determine the non-redundant biological function of each isoform. Among all RAS isoforms, KRAS is most frequently mutated in human cancers and, therefore, is the most clinically relevant [16, 17].

1.2 Post-translational modification of RAS

To allow them to function, RAS proteins must localize to the inner leaflet of the PM [18]. To localize to the PM, the C-terminus of RAS must be processed correctly after the protein's synthesis. Different RAS isoforms have different C-termini, which implies varying post-translational modifications. A CAAX (where C = cysteine, A = aliphatic amino acid, and X = serine or methionine) motif exists in every RAS isoform. The cysteine of the CAAX motif in all RAS isoforms is prenylated by farnesyltransferase [19]. Then, the AAX of the CAAX motif is cleaved by RAS-converting enzyme 1 (RCE1), and a C-terminal cysteine farnesyl carboxy-

methyl ester is generated by isoprenylcysteine carboxyl methyltransferase (ICMT) [20]. In addition to the farnesyl moiety on the C-terminal cysteine, a second signal, which varies among different RAS isoforms, is required to further stabilize the interaction with the PM. KRAS4B (hereafter referred to as KRAS) contains a positively charged polylysine domain that interacts with the negatively charged phosphatidylserine (PtdSer) on the PM [21]. HRAS and NRAS contain one or two palmitoyl moieties for interaction with the PM [19, 22] and, in the case of NRAS, other hydrophobic residues upstream of the HVR also contribute to the PM interaction [22]. Finally, a minor splice variant of KRAS, KRAS4A, contains both the polylysine domain as well as a palmitoyl moiety for PM interaction [22].

1.3 RAS nanoscale organization on the PM and lipid dependence

RAS interact with PM lipids to form nanoclusters on the PM. About 40% of RAS proteins exist as immobile nanoclusters, whereas the rest are mobile on the PM [23, 24]. The diameter of RAS nanoclusters is about 9 nm and they include 6–7 RAS proteins per cluster. The clusters are constantly assembling and disassembling with a lifetime of 0.1–1 s [24, 25]. Recent studies have reported that the formation of RAS nanoclusters depends on an intermediate RAS dimer [26-30].

Different RAS isoforms assemble into distinct GTP or GDP nanoclusters. As a result, even if they share a conserved G-domain, different RAS isoforms have different biological functions [31]. The structure of the minimal membrane anchor of each isoform determines the localization and spatial segregation of their cognate isoforms on the PM [23]. Additionally, changes in the G-domain conformational

orientation upon GTP loading contribute to the GTP-dependent spatial segregation of RAS. Indeed, this plasticity explains why RAS form different clusters with GTP or GDP loading [32, 33].

These non-overlapping nanoclusters are defined by a distinct lipid composition. First, different RAS isoforms exhibit a different dependency on cholesterol. HRAS-GDP forms cholesterol-dependent nanoclusters. After GTP binding, HRAS forms cholesterol-independent clusters [23]. NRAS, in contrast, forms cholesterol-dependent nanoclusters when it binds GTP but cholesterol-independent nanoclusters when it binds GDP [23]. Finally, KRAS forms cholesterol-independent nanoclusters, irrespective of whether it is loaded with GTP or GDP [23, 24]. Besides cholesterol, anionic lipids also play very important roles in RAS PM binding and clustering. Recently, different RAS isoforms have been reported to associate with different groups of anionic phospholipids [34]. For example, PtdSer is required by KRAS nanoclusters, but not HRAS nanoclusters, and is important for the regulation of KRAS biological functions [34].

1.4 PtdSer-dependent lateral segregation of RAS and its implications for drug discovery

Nanocluster formation of RAS is critical for downstream signal transmission. When active, the nanoclusters of different RAS isoforms interact with a defined set of phospholipids, leading to isoform-specific downstream signaling [35, 36]. Changing the lipid content on the PM abolishes the spatial segregation of RAS and blocks the corresponding biological functions [31]. For instance, overexpression of GFP-HRASG12V disrupts KRAS nanoclustering and inhibits its function, by

altering the distribution of PtdSer on the PM [34]. Disruption of KRAS nanoclustering by HRASG12V selectively targets cancer cells that express oncogenic KRAS [34]. This effect is lipid-regulated and G-domain-independent, as indicated by the fact that overexpression of the C-terminal HVR of HRAS without the G-domain had the same effect on KRAS nanoclustering [34].

Given the abundance of PtdSer on the PM, HRAS overexpression can hardly affect the nanoclustering of KRAS, if all PtdSer participates in KRAS clustering. Indeed, only ~40% of PtdSer molecules are mobile when RAS nanoclusters are being formed [25, 34, 37], and only a fraction of them actually participate in RAS nanocluster formation [34]. Overexpressed HRAS competes with KRAS for a limited PtdSer pool, which explains the HRAS-induced disruption of KRAS nanoclustering [34].

This phenomenon of spatial cross-talk has great significance for the development of anti-RAS pharmacological agents, because the latter can be used to modulate lipid pools and thus control RAS signaling. For example, nonsteroidal anti-inflammatory drugs (NSAIDs) disrupt HRAS and KRAS nanoclusters by stabilizing cholesterol domains. As a result, CRAF activation induced by oncogenic HRAS or KRAS is abolished by NSAIDs [38]. Another example includes pharmacological agents that disrupt sphingomyelin (SM) metabolism. They alter nanoclustering formation and PM interaction of RAS by disrupting PtdSer and cholesterol content on the PM, causing inhibition of RAS function (also discussed in Chapter 1.8) [39-41]. A recent unpublished study by Dharini van der Hoeven showed that the disruption of PM cholesterol by pharmacological agents that altered SM metabolism impaired the membrane localization of epidermal growth factor receptor (EGFR), and inhibited the proliferation of oral cancer cells

overexpressing EGFR.

1.5 Endosomal trafficking of RAS

RAS proteins are localized predominantly on the PM; however, a series of organelles are also targeted by RAS. Among these, the endosome is the most interesting one for its critical role in regulating RAS signaling and function [35].

All RAS isoforms are trafficked through the endosomal system for turnover on the PM. The endosomal trafficking of HRAS and NRAS relies mainly on a cycle of acylation and deacylation. HRAS and NRAS are depalmitoylated by a thioesterase and released into the cytosol due to reduced hydrophobicity. The depalmitoylated HRAS and NRAS are transported to the Golgi complex for a new round of palmitoylation. The repalmitoylated HRAS and NRAS are then trafficked to the PM via membrane carriers that likely involve the recycling endosome (RE) [42-46]. A recent study has shown that vacuolar protein sorting-associated protein 35 (VPS35), a component of the retromer complex, facilitates NRAS recycling from endosomes to the Golgi complex [47]. In addition to post-Golgi trafficking, HRAS and NRAS can be endocytosed in a clathrin-dependent manner [48]. Moreover, ubiquitinylation facilitates the endocytosis and sorting of these two RAS isoforms [49].

Compared to HRAS and NRAS, KRAS interacts more weakly with the PM, because interaction between the polybasic domain and the PM is not as strong as that between the palmitoyl group and the PM. Given the weaker interaction, KRAS dissociates more easily from the PM [50, 51]. The endocytosed KRAS dissociates from the vesicles and is released into the cytosol, where it diffuses freely until it

associates with another membrane. Due to the extent of endomembranes, KRAS ends up binding to all cellular membranes before it is trafficked back to the PM [51].

Prior to reaching again the PM, KRAS needs to diffuse back into the cytosol. The diffusion is facilitated by a cytosolic solubilization factor, PDEδ, which captures KRAS in the cytosol [51]. PDEδ is essential for the trafficking of KRAS to the PM, but it is not sufficient. The ARF-like GTPase ARL2 is required for the release of KRAS from PDEδ following binding to the allosteric site and a change in the conformation of PDEδ [51]. Because ARL2-GTP is concentrated in the perinuclear area, KRAS is released mostly in this region, where it can easily interact with RAB11-positive RE vesicles enriched with negatively-charged PtdSer. Finally, KRAS is trafficked back to the PM via the RE [51].

1.6 Blocking RAS PM localization inhibits RAS function

Blocking RAS PM localization abrogates RAS biological function, as effector activation occurs exclusively on the PM [18]. So far, most studies have focused on pharmacological agents responsible for disrupting the post-translational modification of RAS.

Farnesyltransferase inhibitors (FTIs) prevent HRAS from interacting with the PM by hindering the attachment of farnesyl to the CAAX cysteine. Two FTIs, lonafarnib and tipifarnib, have been shown to be effective against HRAS-driven tumors in mouse studies and clinical trials [52]. However, KRAS and NRAS can become geranylgeranylated and remain fully functional during FTI treatment [53, 54]. Therefore, FTIs are only applicable to mutant HRAS therapy, which is rare among cancers with mutated RAS.

Another group of inhibitors of RAS post-translational modifications includes RCE1 and ICMT inhibitors [55-59]. However, these two enzymes are critical for the regulation of many other cellular functions and, therefore, inhibitors of these two enzymes are toxic to normal patient tissues. In the case of HRAS and NRAS, inhibitors of palmitoylation have also been considered as putative anti-RAS therapeutics [43]. However, the application of these inhibitors has been limited because the majority of RAS-dependent cancers contains mutant KRAS.

Other post-translational modifications of RAS that determine its localization on the PM have also been proposed as therapeutic targets. PKC alpha (PKCα) or protein kinase G (PKG) activation induces the intracellular redistribution of KRAS, because both kinases phosphorylate KRAS on S181 [60, 61]. The negatively charged phosphoryl group neutralizes the electrostatic interaction between the polybasic domain and PtdSer. Therefore, phosphorylated S181 prevents KRAS from binding to the anionic lipids on the RE [61]. Based on this phenomenon, bryostatin, a PKCα agonist, has been reported to effectively inhibit RAS PM localization and function in mouse xenograft models [60]. Recent studies have shown that activation of PKG through the 5' AMP-activated protein kinase (AMPK)-endothelial NOS (eNOS)-cGMP secondary messenger pathway blocks RE-mediated KRAS recycling [61]. Hence, mitochondrial inhibitors that induce the AMPK-eNOS-cGMP secondary messenger pathway have additional potential as anti-RAS therapeutics [61].

Finally, blocking the function of key proteins in the endosomal trafficking of RAS also inhibits its interaction with the PM. Knockdown or inhibition of PDEδ prevents PM enrichment of KRAS [51, 62]. Knockdown of RAB11, a critical small

GTPase regulating RE function, or expression of dominantly negative RAB11 also disrupts the cellular localization of KRAS [51].

1.7 Other strategies for RAS inhibition

Besides inhibition of RAS PM localization, other approaches aimed at inhibiting the biological function of RAS have been explored. These approaches include direct inhibition of RAS, inhibition of RAS effectors, identification of protein targets that have synthetic lethal interactions with RAS, and targeting RAS-driven metabolic changes [13].

1.7.1 Direct inhibition of oncogenic RAS function

Wild-type RAS proteins require the cycling between inactive and active forms to function normally, whereas mutated RAS are locked in the GTP-bound state. Therefore, efforts have been made to find GTP-competitive inhibitors. However, this attempt has failed because GTP binds RAS with picomolar affinity. In addition, no molecules that could function as GAPs for mutant RAS have been found either [63].

Several binding pockets of RAS have been identified using computational approaches. A number of inhibitors that bind these pockets have the ability to inhibit the formation of RAS-RAF complexes. For instance, sulindac analogs bind to the RAF-binding domain of RAS and thus prevent formation of the RAS-RAF complex [64, 65]. Sulindac inhibits mitogen-activated protein kinase (MAPK) signaling as well as the proliferation of RAS-transformed cancer cells [66]. However, these analogs are not potent enough for clinical use.

In addition to inhibitors of the RAS-RAF complex, some RAS-binding chemical compounds disrupt RAS-GEF binding. Among these compounds, the most promising is a peptide (HBS3) that is based on the structure of the alpha helix of SOS1. HBS3 binds to RAS in the cleft near the SI and SII regions, effectively inhibiting binding of SOS1 to RAS. MAPK signaling downstream of RAS is inhibited by this peptide whose dissociation constant (K_d) is 158 μM [67].

Recent studies have identified several compounds that bind specifically to certain mutant forms of RAS. For instance, an inhibitor that binds specifically to KRASG12C was identified for treating non-small-cell lung cancer as KRASG12C is the most frequent RAS mutation in this type of cancer. By targeting selectively KRASG12C-expressing cancer cells the inhibitor interferes with SOS1-regulated nucleotide exchange as well as RAS-RAF complex formation [68].

1.7.2 Inhibition of RAS effectors

Inhibition of RAS downstream effectors has been the most successful approach so far for blocking RAS signaling. The most well characterized inhibitors have targeted RAF-MEK-ERK signaling.

The RAF-MEK-ERK signaling pathway was initially thought to be simple and unidirectional. However, it turns out that the RAF-MEK-ERK cascade is regulated by several inputs and outputs, feed-forward and feedback mechanisms [69], which has complicated the development of inhibitors targeting this pathway.

Four RAF inhibitors have been approved by the US Food and Drug Administration (FDA). One of these inhibitors, sorafenib, not only inhibits RAF function, but also blocks members of the vascular endothelial growth factor receptor (VEGFR) family [70, 71] and thus VEGFR-mediated tumor angiogenesis.

Two other FDA-approved ATP-competitive RAF inhibitors are vemurafenib and dabrafenib, which paradoxically activated ERK signaling when tested in RAS-mutant cancers [72-75]. Furthermore, these inhibitors promote RAF dimerization, which activates RAF function [76, 77]. Current efforts are focusing on a new generation of RAF inhibitors that do not enhance RAF dimerization.

More than a dozen MEK inhibitors have also been evaluated clinically. One of these, trametinib, has been approved by the FDA for treatment of metastatic melanoma harboring a BRAF mutation. One of the advantages of MEK inhibitors is that they are highly selective. However, sometimes the inhibitors are not effective because they block ERK feedback inactivation of RAF. In addition, RAS-mutant cancers are sometimes characterized by an increased activation of receptor tyrosine kinases (RTKs) upstream of RAS. Activated RTKs can enhance ERK activity to a level that is above the suppression threshold. As a consequence, therapeutic responses are not observed due to overactivation of RTKs [78].

Several ERK inhibitors are also under evaluation. The inhibition of ERK, however, blocks ERK feedback inactivation of RAF the same way as MEK inhibitors do, which prolongs MEK activation. Furthermore, a recent study shows that protective autophagy, which is a cellular process of self-consumption, can be induced by inhibition of the RAS-RAF-MAPK pathway. This process helps the cells avoid the harm caused by inhibitors of the RAS-RAF-MAPK pathway [79]. Therefore, a combination of inhibitors of different protein targets in various pathways may be tested in the future for more effective RAS inhibition in human cancers.

1.7.3 Identification of synthetic lethal interactions

There are two types of synthetic lethal interactions. The first type of potential synthetic lethal targets includes pathways that are responsible for relieving stress induced by oncogenes. For instance, in oncogenic KRAS-dependent cancers, cells produce more proteins than normal cancer cells. These cells with mutated KRAS are therefore under proteotoxic stress, and proteasomes are critical for relieving this condition. When such KRAS-dependent cancer cells are treated with proteasome inhibitors, they become vulnerable to proteotoxicity, whereas cancer cells with wild-type KRAS are less responsive to proteasome inhibitors [80-82].

Another type of synthetic lethal targets includes proteins in pathways that are required to compensate for changes caused by oncogenic pathways. For instance, in BRCA1- and BRCA2-mutant breast cancer cells, DNA homologous recombination repair is damaged by BRCA1 and BRCA2 mutations. As a result, poly(ADP-ribose) polymerase (PARP) becomes indispensable for these cells because PARP regulates non-homologous end-joining DNA repair. Therefore, PARP inhibitors show a potent effect on inhibition of BRCA-mutant breast cancer [13].

1.7.4 Targeting RAS-driven metabolic changes

Metabolic changes and adaptations represent a hallmark of cancer. RAS-driven metabolic changes are critical for the development of cancers, their maintenance and their growth. Therefore, targeting these metabolic pathways represents a possible therapeutic approach against cancers that are dependent on oncogenic RAS.

The first such strategy is to target metabolic recycling processes. In cancers driven by oncogenic RAS, autophagy and macropinocytosis are required for the

maintenance of cancer cells, because aggressive cancers require vast amounts of energy for growth and metastasis. Autophagy and macropinocytosis satisfy the energy requirement of RAS-dependent cancer cells. Therefore, inhibitors of these two biological processes have been tested as tumor suppressors. At present, autophagy inhibitors, such as chloroquine and its derivative hydroxychloroquine (HCQ), are being tested in clinical trials involving several types of cancers, including pancreatic cancers with KRAS mutations [83, 84]. Recent studies have revealed that ERK inhibition increases the dependence of pancreatic cancer cells on autophagy, suggesting the important role of autophagy in the RAS signaling pathway [85]. Furthermore, because both autophagy and macropinocytosis require normal lysosome function, lysosome inhibitors are also potential pharmacological agents that inhibit metabolic recycling in RAS-dependent cancers.

The second strategy is to target metabolic changes, such as glucose metabolism. Mutant KRAS enhances glucose metabolism in cancer cells by altering the rate-limiting enzymes. As a result, more glycosylation and ribose precursors required for DNA and RNA synthesis are produced, thus sustaining the aggressive proliferation of cancer cells. Knockdown of these rate-limiting enzymes has been shown to effectively inhibit KRAS-dependent pancreatic cancer cells *in vivo* and *in vitro* [86].

1.8 SM metabolism is crucial for cancer cell survival as well as RAS function

Sphingolipids are components of the cell membrane and regulate a number of biological functions, such as cell growth, proliferation, and migration [87]. In

cancer cells, SM metabolism plays key roles in regulating cell death. First, ceramide induces apoptosis in cancer cells, possibly by facilitating mitochondrial outer membrane permeabilization (MOMP), an initiation step in mitochondria-induced apoptosis [88]. In this process, ceramide is responsible for forming channels on the planar phospholipid membranes and outer membranes of mitochondria that allow the passage of proteins released by MOMP from mitochondria to the cytosol for cell apoptosis [88]. Second, ceramide induces tumor cell necroptosis by interacting with the phosphatase 2A inhibitor I2PP2A and activating the tumor suppressor serine/threonine-protein phosphatase 2A (PP2A) [89, 90]. Finally, ceramide induces autophagy by targeting autophagosomes to mitochondria, whereas accumulation of SM in cells hinders the maturation of autophagosomal membranes [91, 92]. These observations suggest that different sphingolipids play different roles in autophagy.

While ceramide induces cancer cell death, sometimes cancer cells find ways to evade this effect. The most outstanding example is the sphingosine-1-phosphate (S1P)-induced anti-apoptotic effect [91, 92]. When cancer cells are under stress such as chemotherapy, ceramide and sphingosine are generated to manage cell death. However, the conversion of ceramide to S1P makes cancer cells escape death, leading to S1P-dependent cancer cell survival. Therefore, therapeutic strategies have been developed to target pro-survival S1P-S1P receptor signaling [93].

SM metabolism has been reported in recent years as a regulator of KRAS PM localization and function. We have described several classes of chemical compounds that inhibit oncogenic KRAS PM localization and function by disrupting SM metabolism. The most outstanding compounds include fendiline and

staurosporine (STS).

Fendiline is a clinically obsolete FDA-approved calcium channel blocker [94]. However, fendiline mislocalizes oncogenic KRAS from the PM through a mechanism unrelated to calcium channel blocking [41], which involves instead inhibition of acid sphingomyelinase (ASM) [39, 40]. ASM is responsible for catalyzing the breakdown of SM. Inhibition of ASM by fendiline causes SM accumulation in the lysosomal compartment, which in turn reduces the amount of PtdSer and cholesterol on the PM [39, 40]. As a result of the loss of PtdSer from the PM, PM localization of KRAS is blocked and its spatial organization on the PM is disrupted.

STS was previously reported as a PKC inhibitor. However, KRAS mislocalization by STS is not related to PKC [95]. We believe that STS mislocalizes KRAS by disrupting SM metabolism. STS decreases the cellular level of ORMDL, a protein that negatively regulates serine-palmitoyltransferase (SPT) [96]. Because SPT catalyzes the synthesis of ceramide, the precursor of SM, STS enhances the cellular level of SM [96]. Increased SM causes mislocalization of PtdSer and cholesterol from the PM, thus critically affecting oncogenic KRAS and HRAS PM binding and clustering [96].

A recent study on a series of ASM inhibitors has reported that imipramine, desipramine, and amitriptyline lead to the same mislocalization of KRAS as fendiline [39]. These FDA-approved antidepressants can be potentially employed as anti-RAS pharmacological agents. In addition, we have shown that knocking down several key enzymes in SM synthesis and turnover pathways blocks KRAS PM localization and function to a varying extent [39]. Therefore, pharmacological tools that modulate SM metabolism may be utilized in oncogenic KRAS-expressing

cancers.

Chapter 2 Methods and Materials

This chapter is based upon: Tan L, Cho KJ, Neupane P, Capon RJ, Hancock JF: An oxanthroquinone derivative that disrupts RAS plasma membrane localization inhibits cancer cell growth. J Biol Chem. 2018 Aug 31;293(35):13696-13706. The journal does not require permission to reuse publications of the authors for dissertation.

2.1 Materials

Oxanthroquinone deratives were synthesized as described previously [97] by Robert J. Capon (University of Queensland) and dissolved in dimethyl sulfoxide (DMSO). Cell culture media and fetal bovine serum (FBS) were purchased from HyClone unless described otherwisely. Rabbit anti-acylpeptide hydrolase (APEH) antibody (PA5-11354) was purchased from Thermo Fisher Scientific. Rabbit anti-RAB11 (3539), Rabbit anti-phospho-p44/42 mitogen-activated protein kinase (MAPK) (ppERK1/2) (Thr202/Tyr204) (9101), rabbit anti-ERK (4695) antibodies were purchased from Cell Signaling Technology (Beverly, MA). Mouse anti-β-actin (A1978) antibody was purchased from Sigma Aldrich. Rabbit anti-mGFP antibody for immunogold labeling was generated in house. Transferrin from human serum, Alexa Fluor™ 555 Conjugate (T35352), Cholera Toxin Subunit B (Recombinant), Alexa Fluor™ 647 Conjugate (C34778), and Wheat Germ Agglutinin, Alexa Flour™ 488 Conjugate (W11261) were purchased from Thermo Fisher Scientific.

2.2 Cell culture

BxPC3, MiaPaCa-2, MOH were provided by Craig Logsdon, KLE, Hec-1a cells by Karen Lu, Hec-1b cells by Bryan Hennessey, and Hec-50 cells by Russell

Broaddus, all at MD Anderson Cancer Center, Houston, TX. Other cell lines were purchased from the American Type Culture Collection (ATCC) or provided by the NCI Ras Initiative. The Madin-Darby canine kidney (MDCK), A431 cell line and RAS-less mouse embryonic fibroblasts (MEFs) were maintained in Dulbecco's modified Eagle medium (DMEM) supplemented with 2mM L-glutamine and 10% FBS. Chinese hamster ovary (CHO) cells were maintained in Ham's F-12K medium (ATCC) supplemented with 10% FBS 2mM L-glutamine. BxPC3, MOH, NCI-1975, NCI-23, NCI-2122, NCI-441, NCI-H508 cells were grown in RPMI-1640 supplemented with 10% FBS. MiaPaCa-2 cells were grown in DMEM supplemented with 10% FBS and 2.5% horse serum. KLE and Hec-50 cells were maintained in DMEM-F-12 medium supplemented with 10% FBS. Hec-1a and Hec-1b cells were grown in McCoy's 5a medium supplemented with 10% FBS. SK-CO-1 cells were maintained in Eagle's MEM supplemented with 10% FBS. CaCO-2 cells were grown in Eagle's MEM supplemented with 20% FBS. SW948 cells were grown in Leibovitz's L15 medium with 10% FBS. TLA293t cells were maintained in DMEM supplemented with 10% FBS.

2.3 Transfection and selection of monoclonal stable cell lines

Cells were seeded and reached 90% confluency before transfection. Cells were then treated with Opti-MEM reduced serum medium containing 4 μg plasmid DNA and 10 μl Lipofectamine 2000 (11668019, Thermo Fisher Scientific) for 24 h. The cells were selected in cell growth medium with antibiotics for 7 days. Only one single cell was seeded onto each well in several 96-well plates. Cell were

maintained and observed under a fluorescence microscope. The cell colonies with homogeneous fluorescence-tagged proteins were selected and further cultured.

2.4 Lentiviral infection

2.4.1 Lentivirus production in TLA293t cells

TLA293t cells were seeded onto 6-well plates and reached 70% confluency before transfection. The lentiviral DNA plasmid mix was transfected into cells as described in 2.3. TLA293t cells were cultured in Opti-MEM reduced serum medium for 24 h and then growth medium for 40 h. The growth medium was collected by centrifuge at 3000 rpm for 15 min. The concentration of virus was determined.

2.4.2 Lentiviral infection

Cells were seeded on 6-well plates and reached 90% confluency before infection. The virus media were added to cells with 8ug/ml polybrene. Fresh media with antibiotics were added to the cells 24 h later. The cells were selected with 5ug/ml puromycin for 5 days. If necessary, monoclonal stable cell lines were selected as described in 2.2.

2.5 Fluorescence microscopy

Cells were grown on coverslips and fixed with 4% paraformaldehyde (PFA). The coverslips were mounted in mowiol and imaged in a confocal microscope (Nikon A1R) using a 60X or 100X objective. The manders coefficient plugin from ImageJ was used for quantification.

2.6 Electron microscopy

MDCK cells expressing mGFP tagged protein were seeded on fibronectin coated, gold electron microscopy (EM) grids (IGG200, Ted Pella Inc). Cells were grown on the grids for 48 h. Apical PM was removed by placing a Whatman filter paper soaked in PBS onto the cells for 5 min, applying brief pressure and then removing the PBS-soaked filter paper. The cytosolic surface of the adherent basal PM was exposed because the apical PM was removed. The cytosolic leaflet of the basal PM was washed, fixed with PFA and glutaraldehyde, and labeled with anti-GFP antibody conjugated to 4.5-nm gold particles. Digital images of intact immunogold-labeled PM sheets were obtained via a JEOL 1400 transmission EM at 100,000x magnification. Intact 1 μm^2 areas of the PM sheet were identified and the (x,y) coordinates of the gold particles were determined using ImageJ. Univariate K-functions [98] were calculated as described previously and standardized on the 99% confidence interval (CI) [23, 99, 100]. Bootstrap tests to examine differences between replicated point patterns were constructed as described previously, and statistical significance evaluated against 1000 bootstrap samples [24, 100].

2.7 Western blotting

Cells were washed in ice-cold phosphate-buffered saline (PBS) and lysed for 10 min on ice in buffer containing 50 mM TrisCl (pH 7.5), 75 mM NaCl, 25 mM NaF, 5 mM $MgCl_2$, 5 mM EGTA, 1 mM dithiothreitol, 100 μM Na_3VO_4, 1% NP40, and protease inhibitors. The resulting whole cell lysate was centrifuged at 14,000 rpm for 20 min to remove cell debris and 20μg of the supernatant analyzed by SDS-PAGE. After SDS-PAGE, proteins were transferred to PVDF membranes using

semidry Western transfer. After incubation with primary and secondary antibodies the protein of interest was visualized using enhanced chemiluminescence (SuperSignal; Pierce) with ChemiDoc MP System (Bio-rad) and quantified with ImageJ.

2.8 Cell proliferation assay

Tumor cells or RAS-less MEFs were seeded in 24-well plates. After 24 h, cells were treated with vehicle (DMSO) or 5 μM G01 for 72 h. The cells were trypsinized and counted. The cell number of G01-treated cells was normalized to that of the DMSO-treated cells.

2.9 Lysenin staining

Maltose binding protein (MBP)-GFP-Lysenin fragment (amino acid residues 161 to 297) was purified as described previously [39, 40]. For lysenin staining, MDCK cells were fixed with 4% PFA, permeabilized or not permeabilized with 0.05% saponin, and then incubated with 60 μg/ml MBP-GFP-lysenin for 15 min.

2.10 Pull-down assay

2.10.1 Determining relative RAB11-GTP level with GST-FIP3

GST tagged FIP3 fragment (Kindly provided by Emilio Hirsch, Italy) was produced as previously described [101]. Cells with or without drug treatment were lysed and incubated with GST-FIP3 for protein binding. Glutathione agarose beads were added to cells lysate and incubated. The relative amount of RAB11A-GST were examined with immunoblotting.

2.10.2 Identifying binding target of G01 with G01 with biotin moiety

G01 with biotin moiety (B-G01) were added to CaCO-2 cell lysate and incubated for 1 h at room temperature. B-G01 bound with protein targets was then pulled down by streptavidin beads. The samples were analyzed by silver staining. The bands of interest were cut and analyzed by mass spectrometry in Clincal and Translational Proteomics Service Center Center for Precision Biomedicine, Institute of Molecular Medicine, Houston, Texas. The protein targets were confirmed by immunoblotting with their antibodies.

2.11 Enzyme assays

The relative APEH activity was measured by spectrophotometer. The enzyme substrate acetyl-Alanine-p-nitroaniline (Ac-Ala-pNA) was synthesized by Bachem. MDCK cells were seeded and treated with other chemical compounds for 48 h. Cells were lysed and protein concentrations were determined. The samples each containing 250 μg proteins were incubated with DMSO or chemical compounds for 1h at room temperature. The samples were then heated at 37°C for 2 min before 1mM ac-Ala-pNA was added. The samples were shaken at 37°C. Absorbance under 410nm was measured at different time points.

2.12 Statistical analysis

Prism (Version 5.0c, GraphPad Software) was used for one-way ANOVA and two-tailed Student's *t* tests.

Chapter 3 G01 inhibits RAS PM localization and function

This chapter is based upon: Tan L, Cho KJ, Neupane P, Capon RJ, Hancock JF: An oxanthroquinone derivative that disrupts RAS plasma membrane localization inhibits cancer cell growth. J Biol Chem. 2018 Aug 31;293(35):13696-13706. The journal does not require permission to reuse publications of the authors for dissertation.

3.1 Introduction

RAS localization as well as clustering formation on the PM is crucial for the downstream signaling [18]. Hence, inhibitors that disrupt cellular distribution or PM clustering of RAS are possible to inhibit RAS function. In a high-content screening for inhibitors of KRAS binding, a *Streptomyces* sp. (MST-134270) was isolated and used as a source of metabolites. Several new polyketides were isolated, including oxanthroquinone. Based on the original structure of oxanthroquinone, a series of derivatives were synthesized. These derivatives mislocalized oncogenic KRAS with different potencies. The most potent of them was 3-O-methyl oxanthroquinone ethyl ester (Figure 1A), hereafter referred to as G01 [97]. We selected G01 for further analysis in this study. We investigated whether G01 inhibited the localization and cluster of RAS on the PM. We also determined whether G01 inhibited the function of RAS as well as oncogenic KRAS-dependent cancer cell proliferation.

3.2 Results

3.2.1 G01 mislocalizes oncogenic KRAS, KRAS4A and HRAS from the plasma membrane

We reported previously the synthesis of a series of oxanthroquinone derivatives based on the original microbial polyketide structures identified in a high content screen for inhibitors of KRAS PM binding [97]. The most potent synthetic compound was 3-O-methyl oxanthroquinone ethyl ester, with a structure as shown in Figure 1A, and hereafter referred to as G01 [97]. We selected G01 for further analysis. We first examined the RAS isoform specificity of G01. Madin-Darby canine kidney (MDCK) cells stably co-expressing mGFP-KRASG12V, or mGFP-HRASG12V, or mGFP-KRAS4AG12V, and mCherry-CAAX, a general endomembrane marker, were treated with different concentrations of G01 for 48h, and analyzed by confocal microscopy [102]. The extent of RASG12V mislocalization was calculated using manders coefficients, which quantify the fraction of mGFP-RASG12V co-localizing with mCherry-CAAX. The greater the value of the Manders coefficient, the more extensive is the displacement of mGFP-RASG12V from the PM [95]. The results show that G01 mislocalizes oncogenic KRAS, HRAS, and KRAS4A from the PM with approximately equal potencies, the dose response curves yielding IC_{50}s of ~1μM (Figure 1, B and C).

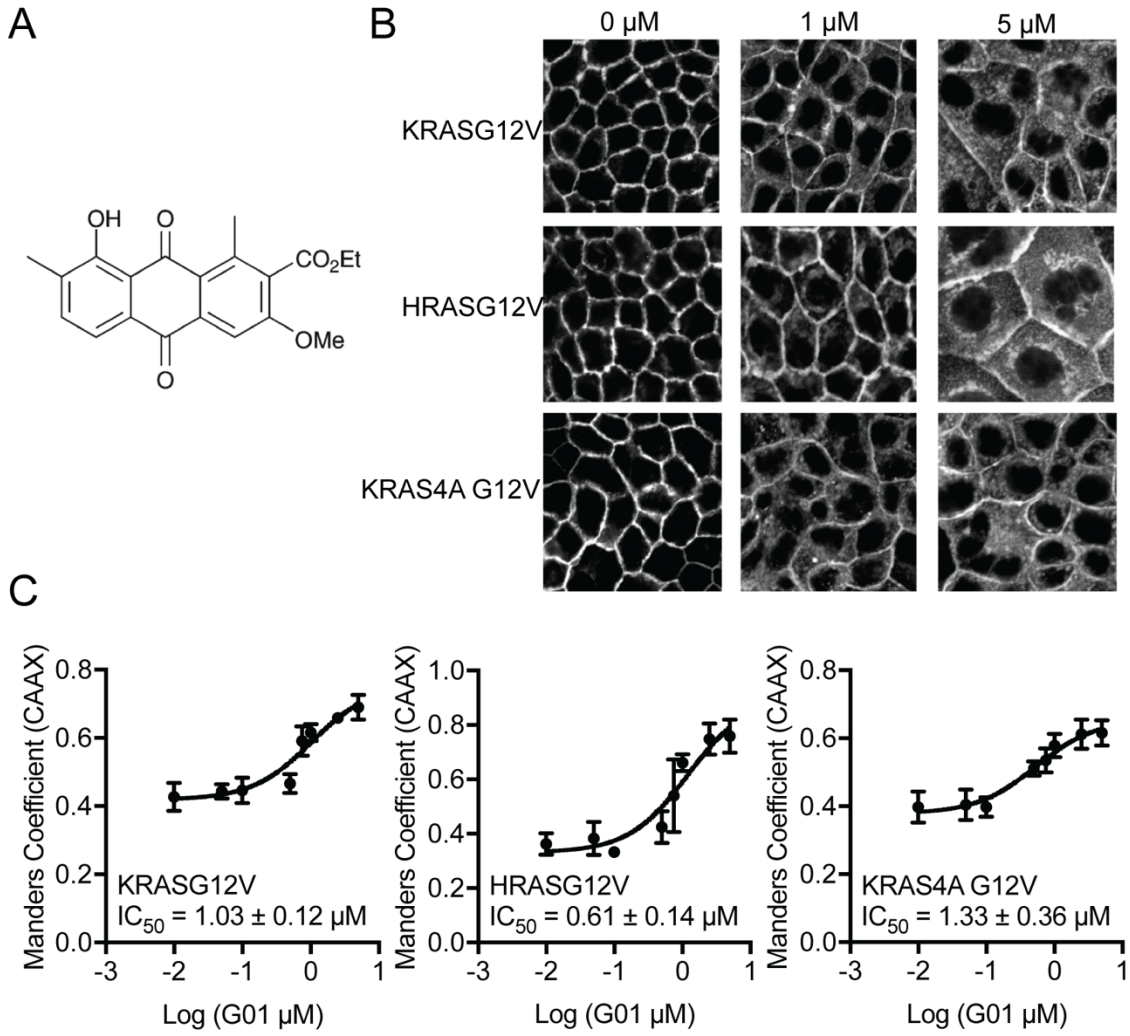

Figure 1. Mislocalization of KRASG12V, HRASG12V, KRAS4A G12V from the PM is induced by G01. (A) Structure of G01. (B) MDCK cells stably coexpressing mCherry-CAAX, an endomembrane marker, and mGFP-KRASG12V, or mGFP-HRASG12V, or mGFP-KRAS4A G12V were seeded on coverslips and treated with vehicle (DMSO) or G01 for 48 h. Cells were imaged in a confocal microscope. Representative images of vehicle (DMSO), 1 μM and 5 μM G01 treatments are shown. (C) The extent of RAS mislocalization was quantified with Manders coefficients, which evaluate the extent of colocalization of mCherry-CAAX and mGFP-RASG12V. Estimated IC_{50} values for G01 on each cell line were obtained from the respective Manders coefficient (± s.e.m. *n*= *3*) dose-response plots.

3.2.2 G01 impairs spatial organization of RAS on the PM

In addition to PM subcellular localization, the lateral spatial organization of RAS proteins into nanoclusters on the PM is critical for RAS signal transmission [103]. To quantify the effect of G01 on RASG12V nanoclustering, intact basal PM sheets from MDCK cells expressing mGFP-KRASG12V, mGFP-HRASG12V or mGFP-KRAS4AG12V treated with G01 for 48h, were labeled with gold-conjugated anti-GFP antibodies and analyzed by electron microscopy (EM). Spatial mapping of each RAS protein on the PM revealed significant decreases in the peak values of the *L(r)–r* clustering statistic, *Lmax*, (Figure 2A), indicating a reduction in the amount of nanoclustered KRASG12V, HRASG12V and KRAS4AG12V on the PM. We also observed a significant reduction in anti-GFP immunogold labeling of each RAS isoform after G01 treatment, again showing that G01 significantly depleted KRAS, HRAS and KRAS4A from the inner leaflet of the PM (Figure 2B), concordant with the confocal imaging results (Figure 1, B and C).

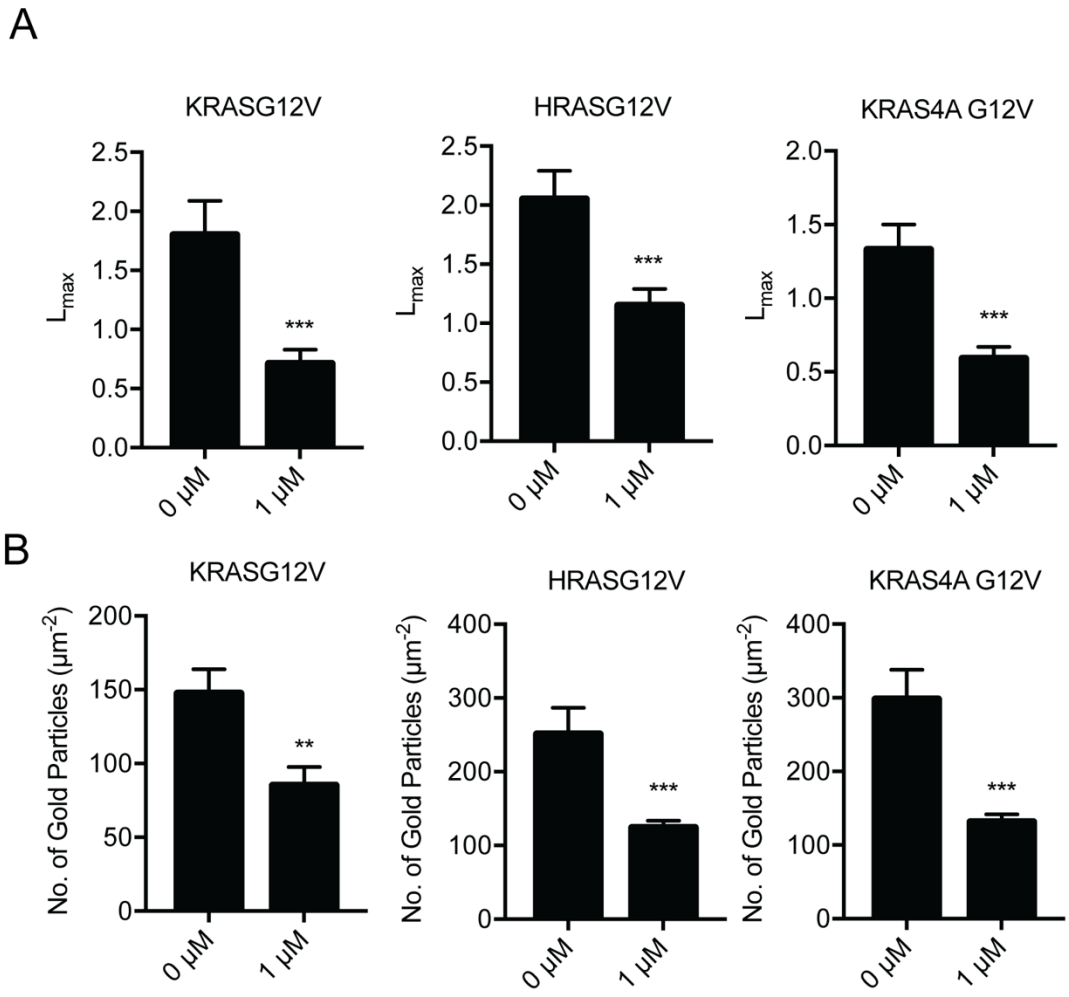

Figure 2. G01 disrupts the PM nanoscale organization of KRASG12V, HRASG12V and KRAS4A G12V. (A) Basal PM sheets were generated from MDCK cells stably expressing mGFP-KRASG12V or mGFP-HRASG12V or mGFP-KRAS4A G12V treated with vehicle (DMSO) or 1 μM G01 for 24 h and imaged by EM after labeling with anti-GFP antibody conjugated to 4.5 nm gold. The extent of clustering of the gold particles was analyzed using Ripley's K-function expressed as $L(r)$ - r functions and normalized on the 99% confidence interval (CI). The maximum value of $L(r) - r$, defined as L_{max} is used as a summary statistic. Values of L_{max} above the CI indicates nanoclustering, with the extent of clustering being reflected by the L_{max} value. At least 12 PM sheets were evaluated

for each condition and RAS isoform. Significant differences from the control pattern for G01-treated cells were assessed using bootstrap tests (***, $P < 0.001$). (B) Average mean (± s.e.m. $n \geq 12$) gold labeling density on the PM sheets was calculated and the statistical significance of differences in gold labeling density was evaluated using Student's *t* test (**, $P < 0.01$; ***, $P < 0.001$).

3.2.3 ERK signaling downstream of oncogenic RAS is abrogated by G01

RAS PM localization and nanocluster formation are critical for signal transmission [18]. Thus G01 concentrations that significantly mislocalized KRASG12V or HRASG12V or KRAS4A G12V also suppressed ppERK levels in MDCK cells stably expressing each oncogenic RAS isoform (Figure 3, A to C). Thus oncogenic RAS-MAPK signaling is abrogated by G01. As we did not observe significant changes in oncogenic RAS levels, ppERK was not lowered by a decrease in oncogenic RAS in G01-treated cells (Figure 4, A to C).

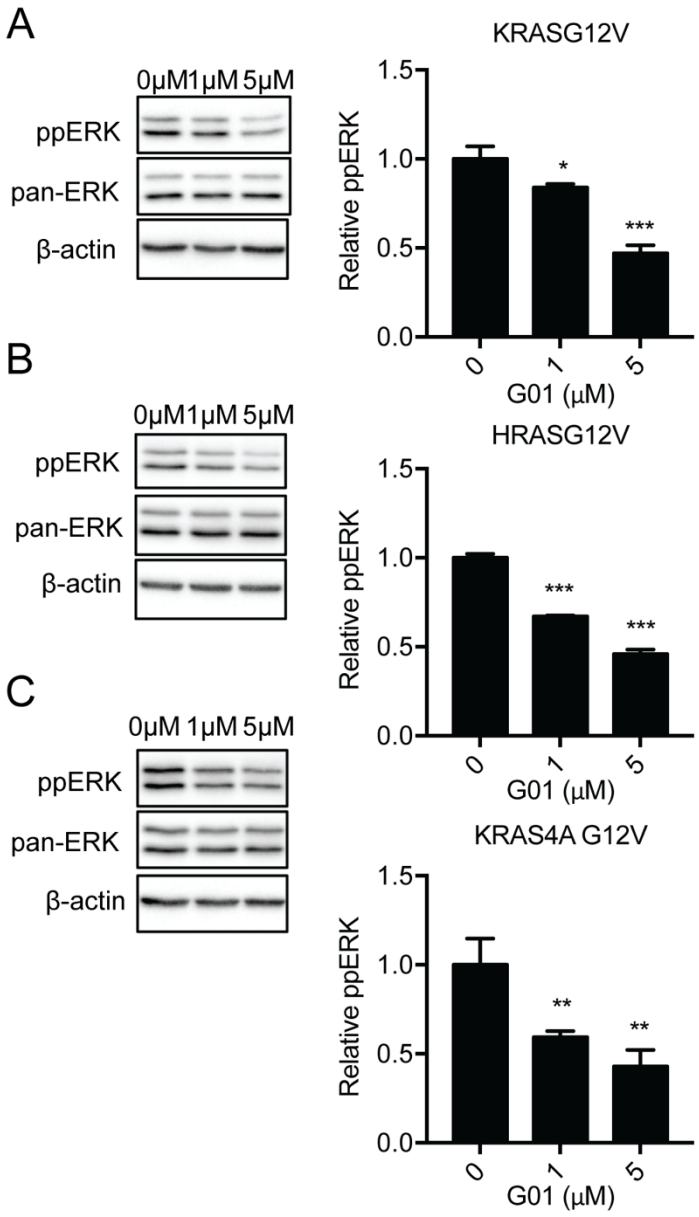

Figure 3. G01 inhibits oncogenic RAS signaling. MDCK cells stably expressing mGFP-KRASG12V (A), or mGFP-HRASG12V (B), or mGFP-KRAS4A G12V (C) were treated with vehicle (DMSO) or G01 for 48 h. Levels of ppERK were measured by quantitative immunoblotting and normalized to the total level of ERK. Representative western blots are shown. The significance of differences between mean (± s.e.m. *n*= *3*) drug-treated and control ppERK levels were assessed using one-way ANOVA (*, $P < 0.05$; **, $P < 0.01$; ***, $P < 0.001$).

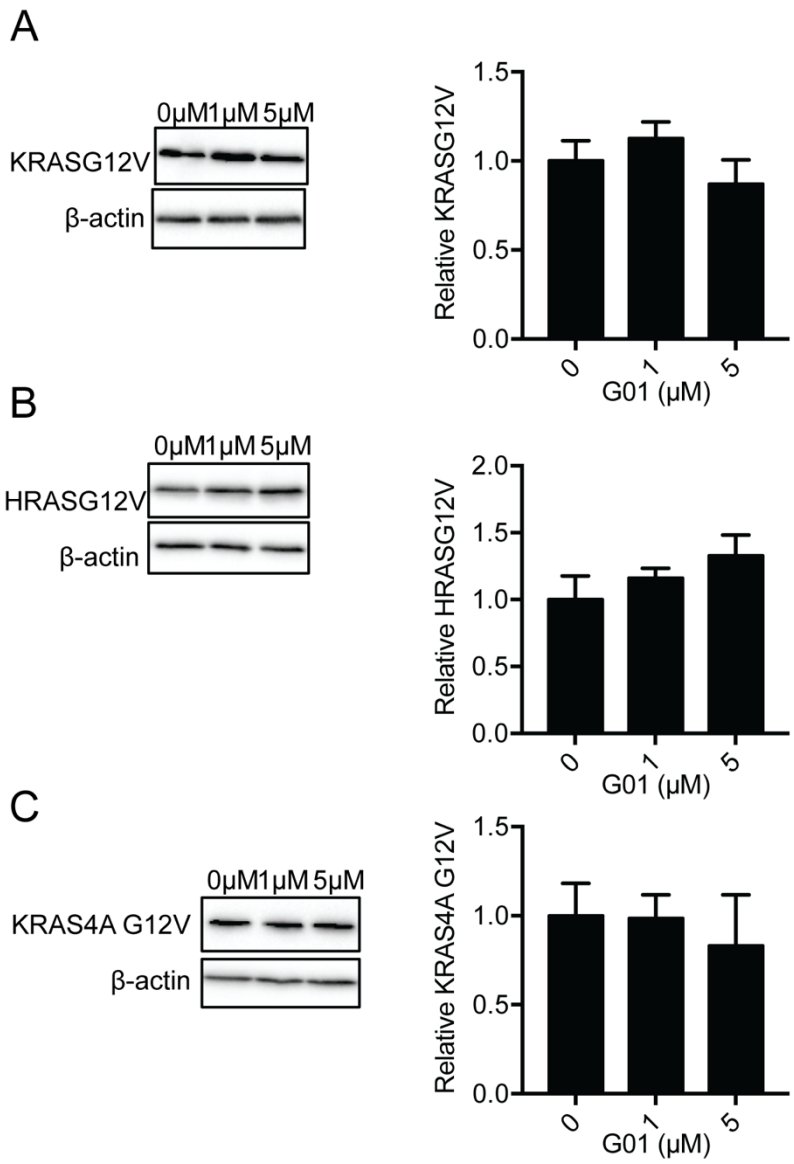

Figure 4. G01 does not affect RASG12V cellular level. MDCK cells stably expressing mGFP-KRASG12V (A), or mGFP-HRASG12V (B), or mGFP-KRAS4A G12V (C) were treated with vehicle (DMSO) or G01 for 48 h. Levels of RASG12V were measured by quantitative immunoblotting. Representative western blots are shown. The significance of differences between mean (± s.e.m. *n*= *3*) drug-treated and control ppERK levels were assessed using one-way ANOVA.

3.2.4 G01 inhibits the proliferation of RAS-less mouse embryonic fibroblasts and KRAS-transformed tumor cell lines

We first tested the effect of G01 on the proliferation of RAS-less mouse embryonic fibroblasts (MEFs) expressing KRASG12V or KRASG12D or BRAFV600E. These are cell lines generated from KRAS-floxed, NRAS-null and HRAS-null mice and express a single transgene that activates the RAS signaling pathway [104]. Interestingly, 5 μM G01 treatment for 72 h, significantly inhibited proliferation of KRASG12V and KRASG12D RAS-less MEFs, but not BRAFV600E RAS-less MEFs (Figure 5A). This result suggests that G01 inhibits cell growth at the level of KRAS but not RAF, consistent with an effect on KRAS PM binding. Finally, we tested the efficacy of G01 on a panel of 14 pancreatic, lung, endometrial, and colon tumor cell lines, which express wild-type or oncogenic mutant KRAS. G01 more potently inhibited the proliferation of pancreatic, endometrial, and colon tumor cells that expressed oncogenic KRAS (Figure 5B). G01 also inhibited the proliferation lung tumor cell lines, but without evidence of increased potency in lines expressing oncogenic mutant KRAS rather than wild-type KRAS (Figure 5B).

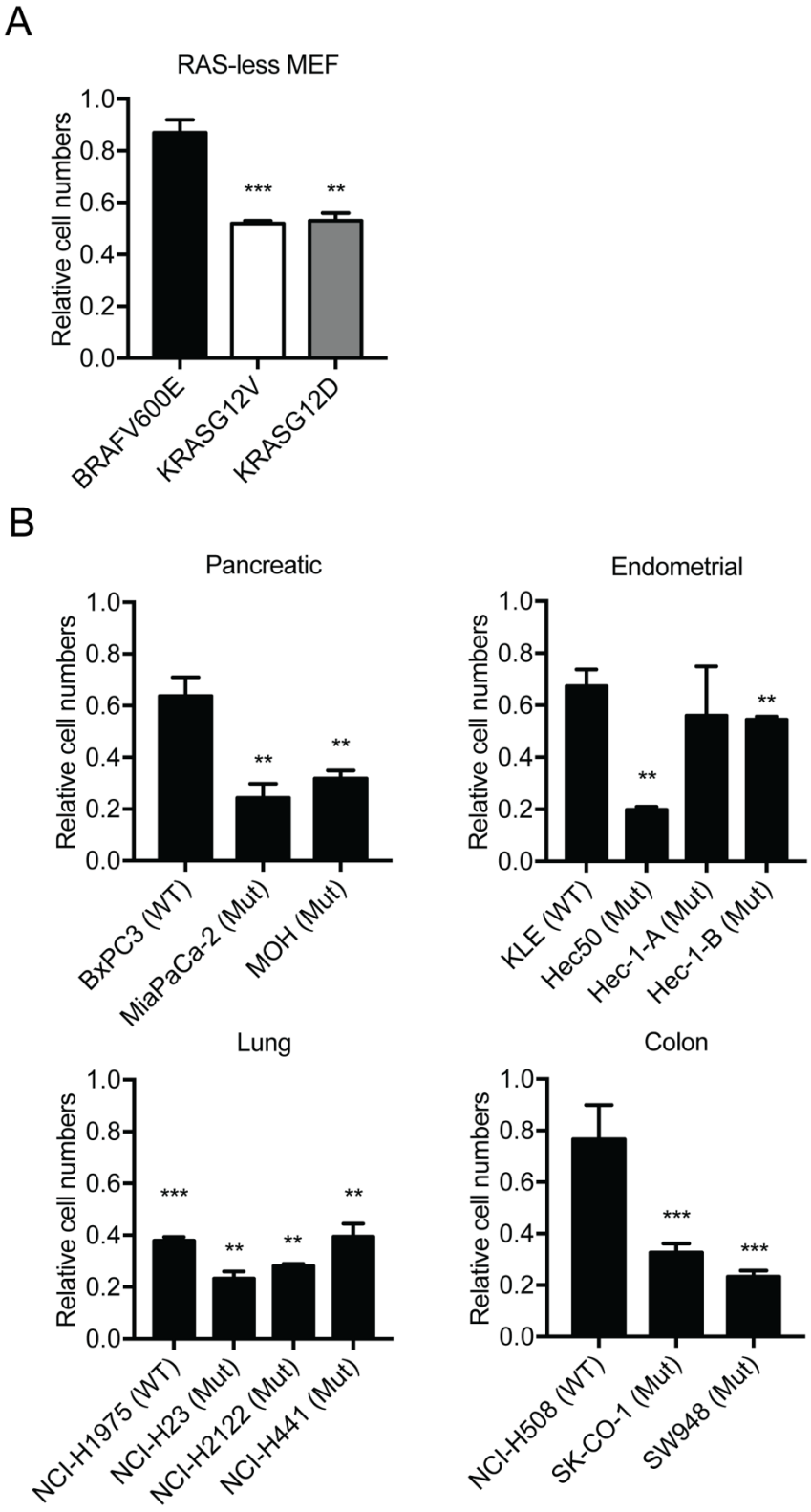

Figure 5. G01 inhibits the proliferation of oncogenic KRAS dependent cell lines. (A) RAS-less MEF cells rescued by expressing KRASG12V, or KRASG12D,

or BRAFV600E were seeded in 24-well plates and treated with vehicle (DMSO) or 5 μM G01 for 48 h. The cells were detached and counted. For graphing cell numbers were normalized to the respective mean of number of vehicle (DMSO) treated cells. The statistical significance of differences in actual cell numbers between control and treated cells (± s.e.m. *n*= *3*) were evaluated by Student's *t* (**, $P < 0.01$; ***, $P < 0.001$). (B) A panel of wild-type (WT) or oncogenic mutant (Mut) KRAS-expressing tumor cells and treated for 72 h with vehicle (DMSO) or 5 μM G01. The cells were detached and counted. For graphing cell numbers were normalized to the respective mean of number of vehicle (DMSO) treated cells. The statistical significance of differences in actual cell numbers between control and treated cells (± s.e.m. *n*= *3*) were evaluated by Student's *t* test (**, $P < 0.01$; ***, $P < 0.001$). Results with pancreatic, endometrial, lung, and colon tumor cells are shown respectively.

3.3 Discussion

We show here, using fluorescence and electron microscopy that G01 potently mislocalizes oncogenic KRAS, HRAS and KRAS4A from the PM to endomembranes. G01 also disrupts KRAS, HRAS and KRAS4A nanocluster formation. Concordant with previous work showing that RAS PM localization and nanocluster formation is crucial for biological function, G01-induced changes to RAS cellular localization and PM spatial organization significantly abrogated RAF-MAPK signaling downstream of oncogenic KRAS, HRAS and KRAS4A. G01 also inhibited the proliferation of RAS-less MEF cells expressing oncogenic KRAS but not that of RAS-less MEFs expressing oncogenic BRAF, confirming that inhibition

was effected at the level of RAS. In cancer cell proliferation assays, G01 more potently inhibited the proliferation of pancreatic, colon, endometrial tumor cell line that are oncogenic KRAS dependent, but had less activity against the tumor cell lines that expressed wild-type KRAS or were KRAS independent. This selectivity for KRAS function was not observed in the small set of lung cancer cell lines we examined, perhaps indicating that wild type RAS signaling, which would also be suppressed by G01, is required to support the transformed phenotype in these lung cancer cell lines. Taken together, we conclude that G01 is a novel inhibitor of RAS PM localization and function.

Chapter 4 G01 disrupted SM metabolism as well as RE function

This chapter is based upon: Tan L, Cho KJ, Neupane P, Capon RJ, Hancock JF: An oxanthroquinone derivative that disrupts RAS plasma membrane localization inhibits cancer cell growth. J Biol Chem. 2018 Aug 31;293(35):13696-13706. The journal does not require permission to reuse publications of the authors for dissertation.

4.1 Introduction

Although we have evidence showing that G01 inhibits oncogenic RAS PM localization and function, the mechanism of action of G01 for KRAS mislocalization was not understood. SM metabolism maintains the PM localization of PtdSer and cholesterol, which are critically important for the PM localization and clustering of K- and H-RAS [39, 40]. Therefore, we tested whether G01 disrupted SM metabolism. In addition, because all RAS isoforms traffic via the RE to the PM [46, 51], we investigated whether G01 disrupted RE function. Finally, we synthesized G01 with a PEG linker and a biotin moiety for identification of the protein target that binds to G01.

4.2 Results

4.2.1 G01 enhances cellular levels of SM and ceramide

Recent studies have implicated SM metabolism in the maintenance of normal PM lipidomic content and organization that are critical for both KRAS and HRAS membrane binding and nanoclustering [39, 40]. To determine whether G01 disrupts SM metabolism, we first measured SM and ceramide (Cer) levels using whole cell lipidomics. MDCK cells treated with G01 for 48h exhibited significantly

increased SM and Cer levels (Figure 6A). The enhancement in SM level was confirmed by staining with mGFP-lysenin that specifically binds SM. MDCK cells were treated with G01 for 48h and incubated with mGFP-lysenin with and without membrane permeabilization. Images were obtained with a confocal microscope. Concordant with the lipidomic analysis, G01 enhanced mGFP-lysenin staining of the exofacial leaflet of the PM as well as intracellular membranes (Figure 6, B and C). Disrupted SM metabolism may result in mislocalization of PtdSer and cholesterol from the PM [96]. MDCK cells stably co-expressing mCherry-CAAX and mGFP-LactC2, a probe for PtdSer, were treated with G01 for 48h and analyzed by quantitative confocal microscopy. The results show that G01 disrupts the PM localization of mGFP-LactC2, and by inference PtdSer, albeit with a potency much lower than that against RAS (Figure 6D). Similarly, when MDCK cells stably co-expressing mCherry-D4H, a cholesterol probe, were treated with G01 for 48h, the mCherry-D4H probe was mislocalized from the PM and accumulated in intracellular puncta, but again this effect was only observed with higher concentrations of G01 (Figure 6E).

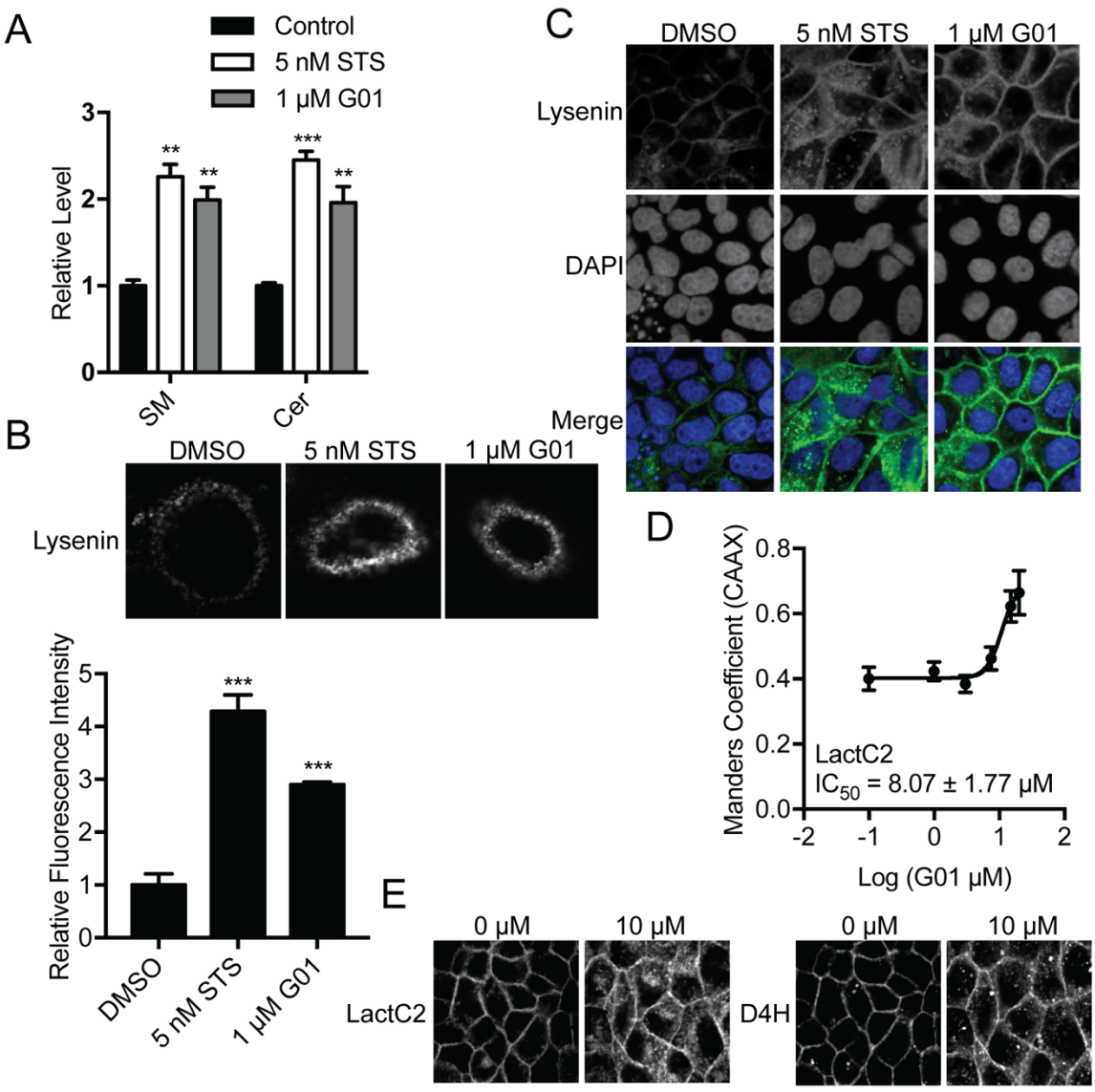

Figure 6. SM metabolism is disrupted in G01-treated cells. (A) MDCK cells stably expressing mGFP-KRASG12V, or wild-type MDCK cells were grown in the presence of vehicle (DMSO) or 5nM STS or 1 μM G01 for 48 h. Whole cell lysates were prepared and total SM and Cer levels were measured. The graph shows SM and Cer levels relative to control, the significance of differences were assessed in one-way ANOVA using the actual mean lipid pmol values (± s.e.m. *n=3*) (**, $P < 0.01$; ***, $P < 0.001$). (B) Wild-type MDCK cells were treated with G01 for 48 h, stained with mGFP-lysenin and imaged in a confocal microscope with fixed

imaging parameters to assess comparative fluorescent intensities. The PM mGFP fluorescence intensity was quantified using the region of interest tool in ImageJ. The values of fluorescence intensity were normalized to the mean of those in vehicle (DMSO) treated group (± s.e.m. $n \geq 20$)). The statistical significance of differences in relative fluorescence intensity was assessed by one-way ANOVA (***, $P < 0.001$). (C) Wild-type MDCK cells were treated with G01 for 48 h and permeabilized, stained with GFP-lysenin and 4',6-diamidino-2-phenylindole (DAPI). Cells were imaged in a confocal microscope with fixed imaging parameters. Representative images were shown. (D) MDCK cells stably coexpressing mGFP-LactC2 and mCherry-CAAX were treated with G01 for 48 h. Cells were fixed and imaged in a confocal microscope. Colocalization between mGFP-LactC2 and mCherry-CAAX was quantified by Manders coefficients. The IC_{50} value was estimated from the Manders coefficient (± s.e.m. $n= 3$) dose-response plot. (E) MDCK cells stably coexpressing mGFP-LactC2 and the cholesterol probe, mCherry-D4H, were treated with G01 for 48 h. Cells were fixed and imaged in a confocal microscope. Representative images are shown.

4.2.2 G01 synergizes with other compounds that disrupt SM metabolism

To explore the potential molecular mechanism of action of G01, we tested for synergism between G01 and three other compounds that disrupt SM metabolism: fumonisin B1 (FB1), STS and R-fendiline. The premise being compounds that have different molecular targets in a common metabolic pathway that is involved in maintaining KRAS PM localization may exhibit synergism for KRAS redistribution.

FB1 is a Cer synthase inhibitor that decreases cellular SM and Cer levels [96]. STS when used at very low concentrations, well below the IC_{50} for PKC inhibition [39, 40], increases the rate of SM synthesis by decreasing the level of ORMDL proteins, which negatively regulate the enzyme serine-palmitoyltransferase [96]. R-fendiline is an inhibitor of ASM. R-fendiline treatment therefore elevates the SM content of the endolysomal system [39, 40]. We treated MDCK cells coexpressing mGFP-KRASG12V and mCherry-CAAX with various concentrations of G01, in the presence of a fixed low concentration (10μM) of FB1 for 48h and imaged the cells using confocal microscopy, Manders coefficients were measured and IC_{50}s were calculated. G01 alone mislocalizes KRASG12V with an IC_{50} of ~1μM, while FB1 improves the IC_{50} to ~0.2μM (Figure 7A). To formally quantify synergism, we calculated a combination index (CI) using the Chou-Talalay method. By this method a CI of 1 indicates an additive effect, a CI < 1 indicates synergism and a CI > 1 indicates antagonism [105]. This analysis confirms that G01 synergizes with FB1 for KRAS mislocalization over most of the G01 concentration range tested (Table 1A). Reciprocally, a low dose of G01 shifted the dose response curve of FB1 to the left indicating a reduced IC_{50} (Figure 7A). Chou-Talalay analysis again confirmed synergism over most of the FB1 concentration range tested (Table 1A). Similar experiments with G01 and STS, G01 and R-fendiline showed strong synergism between each pair of compounds for KRAS mislocalization from the PM (Figure 7, B and C; Table 1, B and C). These results strongly suggest that the molecular target of G01 impacts SM metabolism but is likely different from the enzymes inhibited by FB1, STS and R-fendiline.

Given that G01 synergizes with compounds that perturb SM metabolism for KRASG12V mislocalization, we also tested RAS-RAF-MAPK signaling in MDCK

cells expressing KRASG12V treated with synergistic drug combinations. Concordant with the mislocalization data shown in Figure 7, treatment with 10μM FB1 or 0.5μM G01 alone had no effect on pp-ERK levels, whereas the drug combination significantly inhibited RAS-RAF-MAPK signaling (Figure 8A). Similar results were obtained with low doses of G01 combined with low doses of STS, or R-fendiline, that singly had no effect on RAS-RAF-MAPK signaling, but which in combination synergized to reduce ppERK levels (Figure 8, B and C).

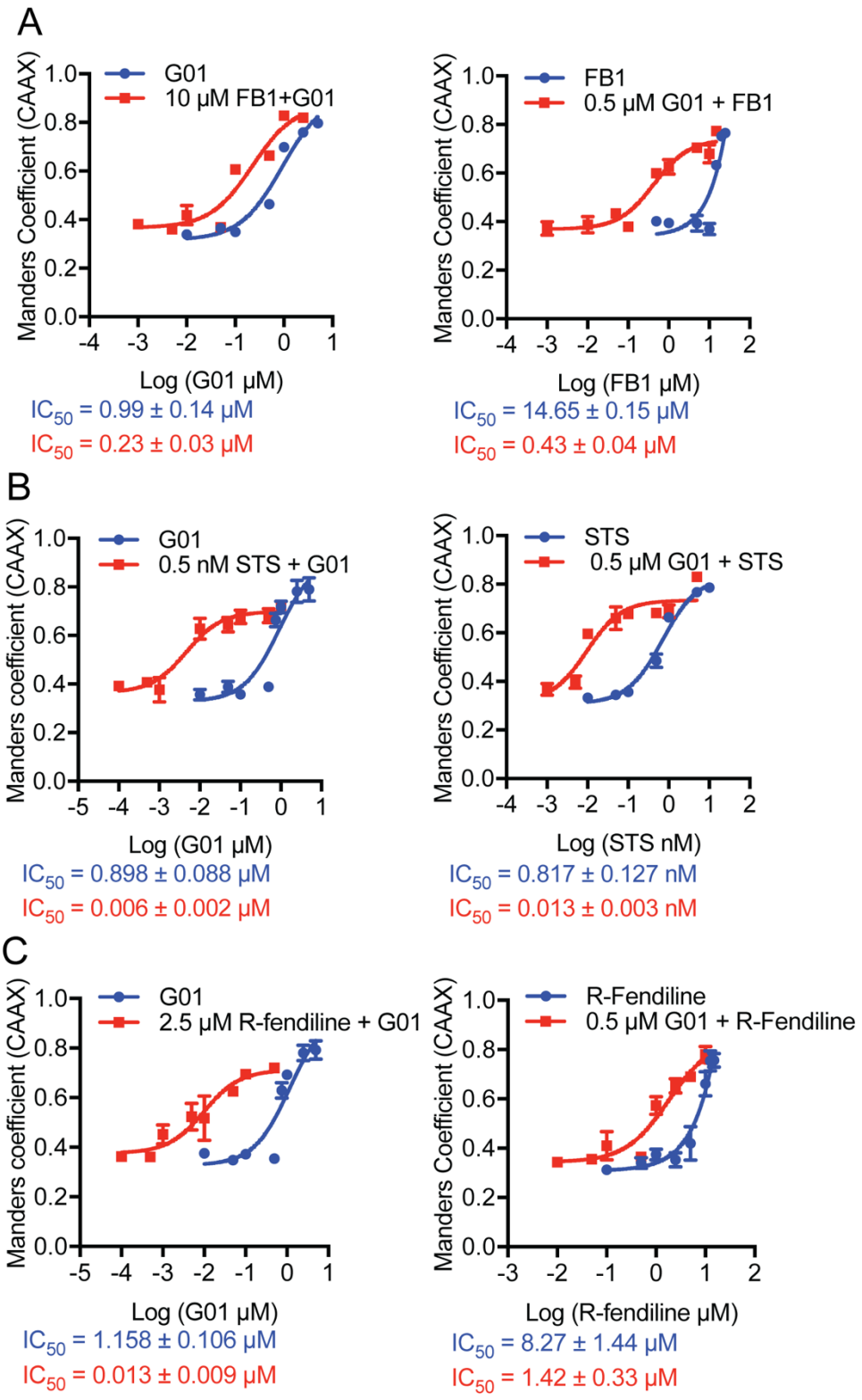

Figure 7. The cocktails of G01 with other compounds are more potent for PM mislocalization of KRAS. (A) MDCK cells stably coexpressing mCherry-CAAX and mGFP-KRASG12V were treated with 10 μM FB1 with variable concentrations

of G01, or 0.5 μM G01 with variable concentrations of FB1. Cells were fixed and imaged in a confocal microscope. The colocalization between mGFP-LactC2 and mCherry-CAAX was quantified by Manders coefficients (± s.e.m. *n*= *3*). IC_{50} values were estimated from the Manders coefficient dose-response plots. (B) MDCK cells stably coexpressing mCherry-CAAX and mGFP-KRASG12V were treated with 0.5nM STS with variable concentrations of G01, or 0.5 μM G01 with variable concentrations of STS. Manders coefficients (± s.e.m. *n*= *3*) were quantified and IC_{50} values were estimated. (C) MDCK cells stably coexpressing mCherry-CAAX and mGFP-KRASG12V were treated with 2.5 μM R-fendiline with variable concentrations of G01, or 0.5 μM G01 with variable concentrations of R-fendiline. Manders coefficients (± s.e.m. *n*= *3*) were quantified and IC_{50} values were estimated.

A

FB1 (μM)	G01 (μM)	CI
10	0.001	9.82
10	0.005	12.65
10	0.01	6.64
10	0.05	12.69
10	0.1	0.97*
10	0.5	0.84*
10	1	0.11*
10	2.5	0.26*

*Synergism between two compounds

G01 (μM)	FB1 (μM)	CI
0.5	0.001	11.05
0.5	0.01	9.31
0.5	0.05	5.52
0.5	0.1	10.29
0.5	0.5	0.95*
0.5	1	0.73*
0.5	5	0.38*
0.5	10	0.69*
0.5	15	0.24*

*Synergism between two compounds

B

STS (nM)	G01 (μM)	CI
0.5	0.0001	7.93
0.5	0.0005	6.51
0.5	0.001	0.59
0.5	0.01	0.46*
0.5	0.5	0.42*
0.5	0.1	0.31*
0.5	0.5	0.56*
0.5	1	0.52*

*Synergism between two compounds

G01 (μM)	STS (nM)	CI
0.5	0.001	11.73
0.5	0.005	8.37
0.5	0.01	0.96*
0.5	0.05	0.48*
0.5	0.1	0.40*
0.5	0.5	0.57*
0.5	1	0.71*
0.5	5	0.23*

*Synergism between two compounds

C

R-fendiline (μM)	G01 (μM)	CI
2.5	0.0001	4.43
2.5	0.0005	4.49
2.5	0.001	3.61
2.5	0.005	0.83*
2.5	0.01	0.92*
2.5	0.05	0.35*
2.5	1	0.19*
2.5	0.5	0.30*

*Synergism between two compounds

G01 (μM)	R-fendiline (μM)	CI
0.5	0.05	13.57
0.5	0.1	7.28
0.5	0.5	12.99
0.5	1	1.39
0.5	2.5	0.69*
0.5	5	0.58*
0.5	10	0.25*
0.5	12.5	0.35*

*Synergism between two compounds

Table 1. G01 synergizes with modulators of SM metabolism for KRAS mislocalization. Synergism was quantified by the Chou and Talalay method using Compusyn software (Version 1.0; ComboSyn, Inc.). Combination indexes (CI)

were calculated using the mean value of Manders coefficients from three independent experiments (Synergism, CI <1; additive effect, CI = 1; antagonism, CI > 1).

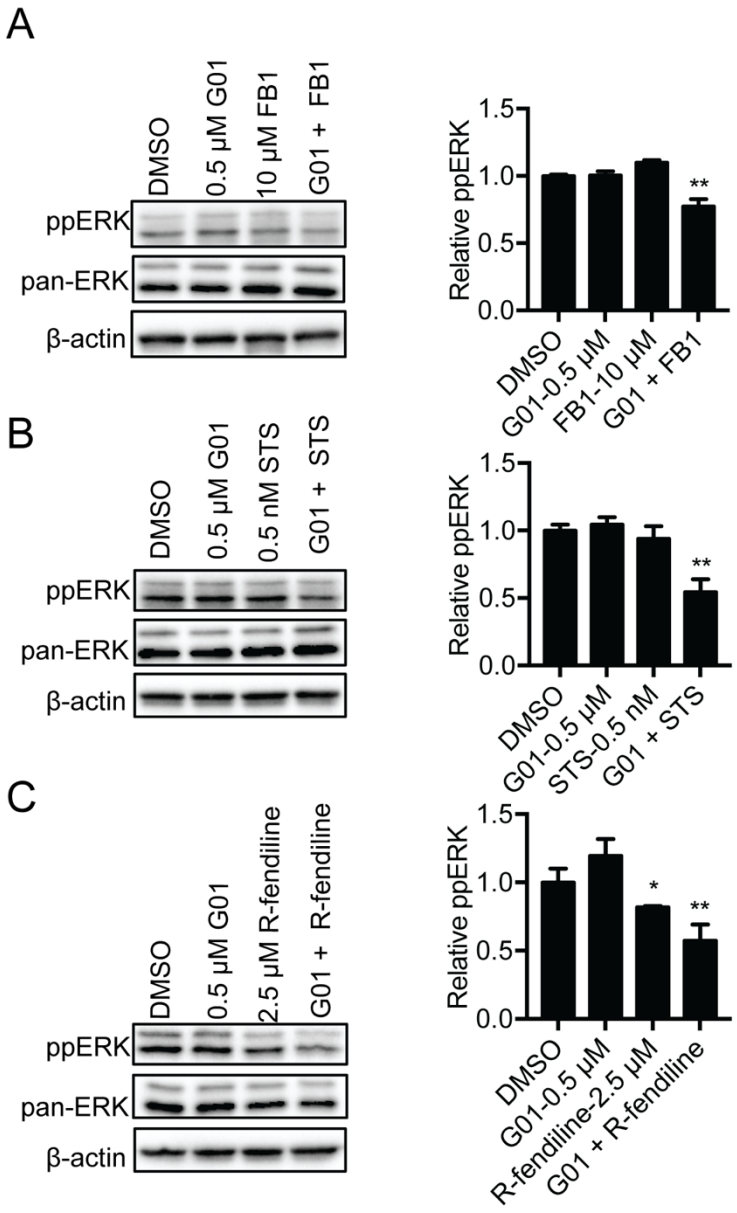

Figure 8. The cocktails of G01 with other compounds are more potent for inhibition of oncogenic KRAS signaling. MDCK cells stably expressing mGFP-

KRASG12V were treated for 48h with vehicle (DMSO), low dose G01 alone, low dose FB1 alone, or a combination of low dose FB1 with G01 (A), or staurosporine (STS) alone, or a combination of STS with G01 (B), or low dose R-fendiline alone or a combination of low dose R-fendiline with G01 (C). Levels of ppERK were measured by quantitative immunoblotting and normalized to the total level of ERK. Representative western blots are shown. The significance of differences between mean (± s.e.m. *n= 3*) drug-treated and control ppERK levels were assessed using one-way ANOVA (*, $P < 0.05$; **, $P < 0.01$).

4.2.3 G01 disrupts the endocytic recycling of epidermal growth factor receptor and transferrin receptor

Normal function of the RE is required to maintain KRAS, HRAS, and NRAS on the PM [46, 51]. We therefore examined whether G01 compromises the cellular distribution of other proteins that recycle through the RE. We first observed the localization and trafficking of epidermal growth factor receptor (EGFR) [106-108]. Chinese hamster ovary (CHO) cells stably expressing mGFP-EGFR were treated with G01 for 48h (or left untreated), serum starved and incubated with EGF on ice for 15mins and then imaged by confocal microscopy at intervals following warming to 37°C. For control cells with no G01 treatment, mGFP-EGFR was predominantly localized to the PM at 0 min and then rapidly endocytosed, such that at 15 min and 30 min, the majority of mGFP-EGFR was localized to intracellular vesicles, before being substantially returned to the PM by 60mins (Figure 9A). In G01 treated cells,

a large fraction of mGFP-EGFR was already redistributed from the PM at 0 min, and at subsequent time points the remaining PM bound mGFP-EGFR was internalized. In striking contrast to control cells at 60 min, mGFP-EGFR was concentrated in the perinuclear region (Figure 9A). In parallel experiments, we quantified the amount of mGFP-EGFR on the PM during EGF-induced endocytosis using anti-GFP immunogold labeling and EM of PM sheets. The results are concordant with the confocal imaging and show significantly lower levels of mGFP-EGFR on the PM in G01-treated cells at 0 min and 60 min (Figure 9B). Together these data illustrate that G01 inhibits the endocytic recycling of EGFR, most probably, given the perinuclear accumulation of internalized EGFR, by inhibiting the exit of EGFR from the RE.

We next examined endocytic recycling of the transferrin receptor (TfR). Alexa Fluor 555 conjugated transferrin (Tf-555) was bound to the surface of MDCK cells that had been treated for 48h with G01 or left untreated. Excess Tf-555 was removed by washing and the cells immediately imaged. The surface fluorescence intensity was much lower in the G01-treated cells, indicating less bound Tf-555 and thus a lower density of TfR on the PM (Figure 10A). MDCK cells stably expressing mGFP-LactC2 were treated with G01 for 48 h, incubated with Tf-555 on ice then imaged by confocal microscopy at intervals following warming to 37°C. PtdSer is not mislocalized by 1μM G01 therefore GFP-LactC2 can be used as a PM marker for quantification. In control cells Tf-555 was rapidly internalized and substantially returned to the PM by 60mins; as shown in the images in Figure 10B that were quantified using Manders coefficients to evaluate the extent of co-

localization between mGFP-LactC2 and Tf-555. Whereas in G01 treated cells Tf-555 was rapidly internalized but not returned to the PM (Figure 10, B and C). These results together suggest that the endocytic recycling of TfR is inhibited by G01. We next conducted similar experiments with Alexa Fluor 647 conjugated cholera toxin b subunit (CTB-647), using A431 cells that express the ganglioside G_{M1}, which is the surface receptor for cholera toxin [109]. After initial incubation with CTB-647 we observed no difference in PM fluorescence intensity between G01 treated and untreated cells, suggesting that the level of G_{M1} expressed on the surface of A431 cells was unchanged by G01 treatment (Figure 10A). To quantify the internalization of CTB-647 we stained fixed cells with the impermeable PM marker Alexa Fluor 488 conjugated to wheat germ agglutinin (WGA-488) that binds N-acetylglucosamine and N-acetylneuraminic acid. Manders coefficients were then used to measure the rate of loss of CTB-647 from the PM. This analysis revealed no difference in the kinetics of CTB-647 internalization in A431 cells after G01 treatment (Figure 11, A and B). We therefore conclude that the internalization of G_{M1}, which is not dependent on RE function, was unaffected by G01 treatment.

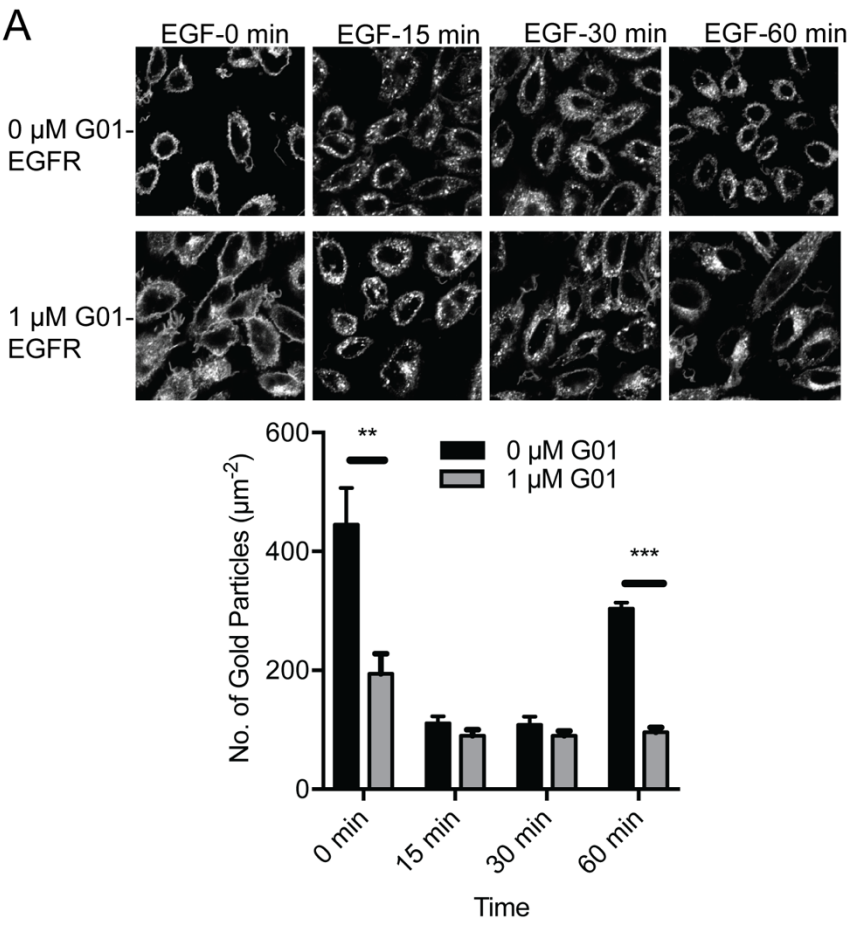

Figure 9. EGFR endosomal recycling is inhibited by G01. (A) CHO cells stably expressing mGFP-EGFR were treated with vehicle (DMSO) or 1 μM G01 for 48 h. Cells were serum-starved for 2 h and incubated with 50ng/ml EGF on ice for 20 min. Excess EGF was washed away with ice-cold PBS. Cells were then incubated with fresh warm medium with vehicle (DMSO), or 1 μM G01 at 37 °C and fixed at different time points. Cells were imaged in a confocal microscope. Representative images of vehicle (DMSO) and 1 μM G01 were shown. (B) In parallel identical experiments PM sheets were generated from the CHO cells under identical conditions as in (A), labeled with anti-GFP antibody conjugated to 4.5 nm gold and imaged by EM. Mean gold density on the PM sheets was determined. The

statistical significance of differences in mean (± s.e.m. $n \geq 12$) gold labeling density at each time point was evaluated using Student's t test (**, $P < 0.01$; ***, $P < 0.001$).

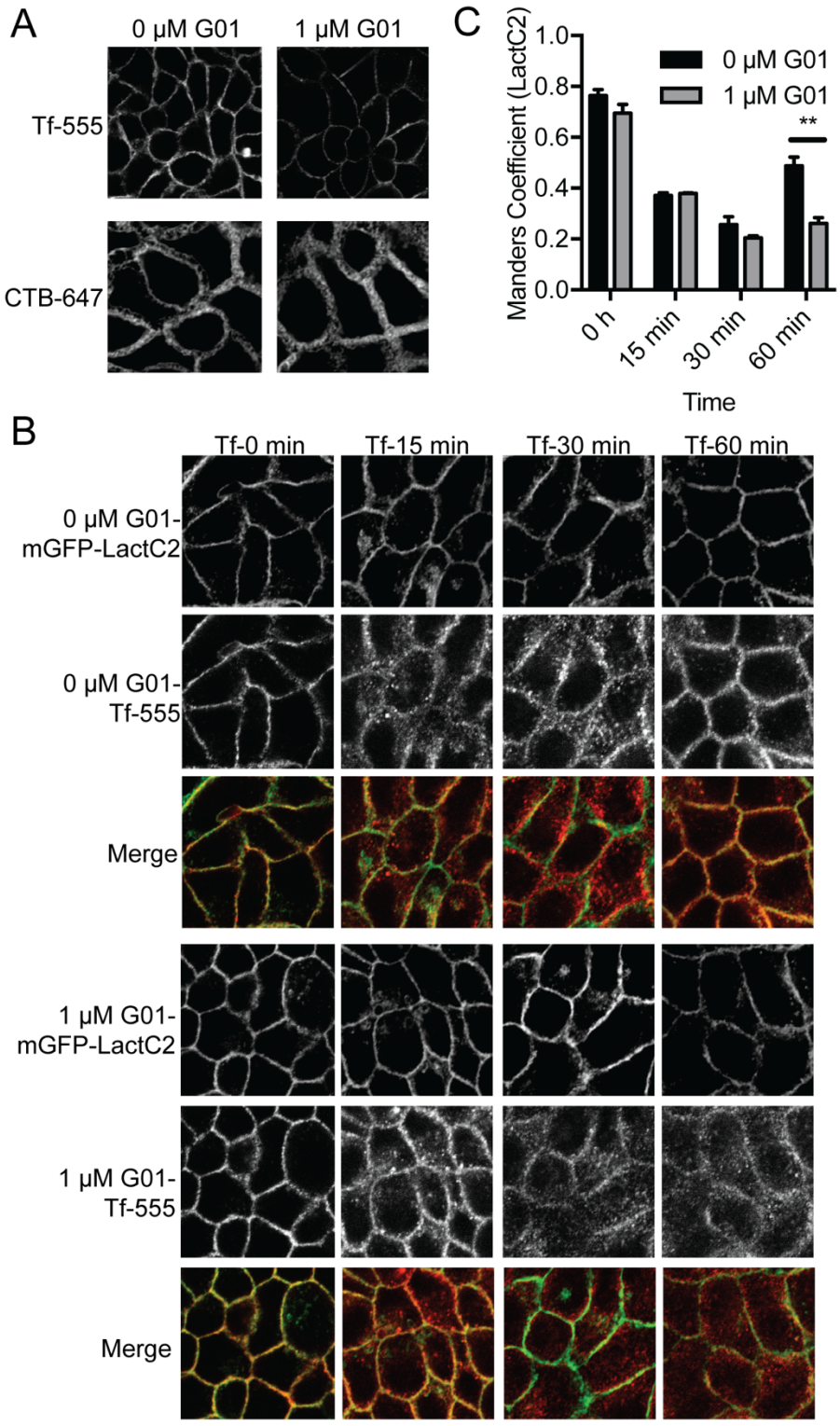

Figure 10. Transferrin receptor endocytic recycling is disrupted by G01. (A) Wild-type MDCK or A431 cells were treated with vehicle (DMSO) or 1 μM G01 for 48 h. MDCK and A431 Cells were incubated with Tf-555 or CTB-647 on ice respectively for 20min. Excess Tf-555 or CTB-647 was washed away with ice-cold PBS. Cells were fixed and observed under a confocal microscope with fixed imaging parameters to assess comparative fluorescent intensities.. Representative images were shown. (B) MDCK cells stably expressing mGFP-LactC2 were treated with vehicle (DMSO) or 1 μM G01 for 48 h. Cells were incubated with Tf-555 on ice for 20min. Excess Tf-555 was washed away with ice-cold PBS. Cells were then incubated with fresh warm medium with vehicle (DMSO) or 1 μM G01 at 37 °C and fixed at different time points. Cells were imaged in a confocal microscope and representative images of vehicle (DMSO), 1 μM G01 are shown. (C) Images were analyzed using Manders coefficients to quantify the extent of colocalization of mGFP-LactC2 and Tf-555. The statistical significance of differences between mean Manders coefficients (± s.e.m. *n*= *3*) at each time point was evaluated using Student's *t* tests (**, $P < 0.01$).

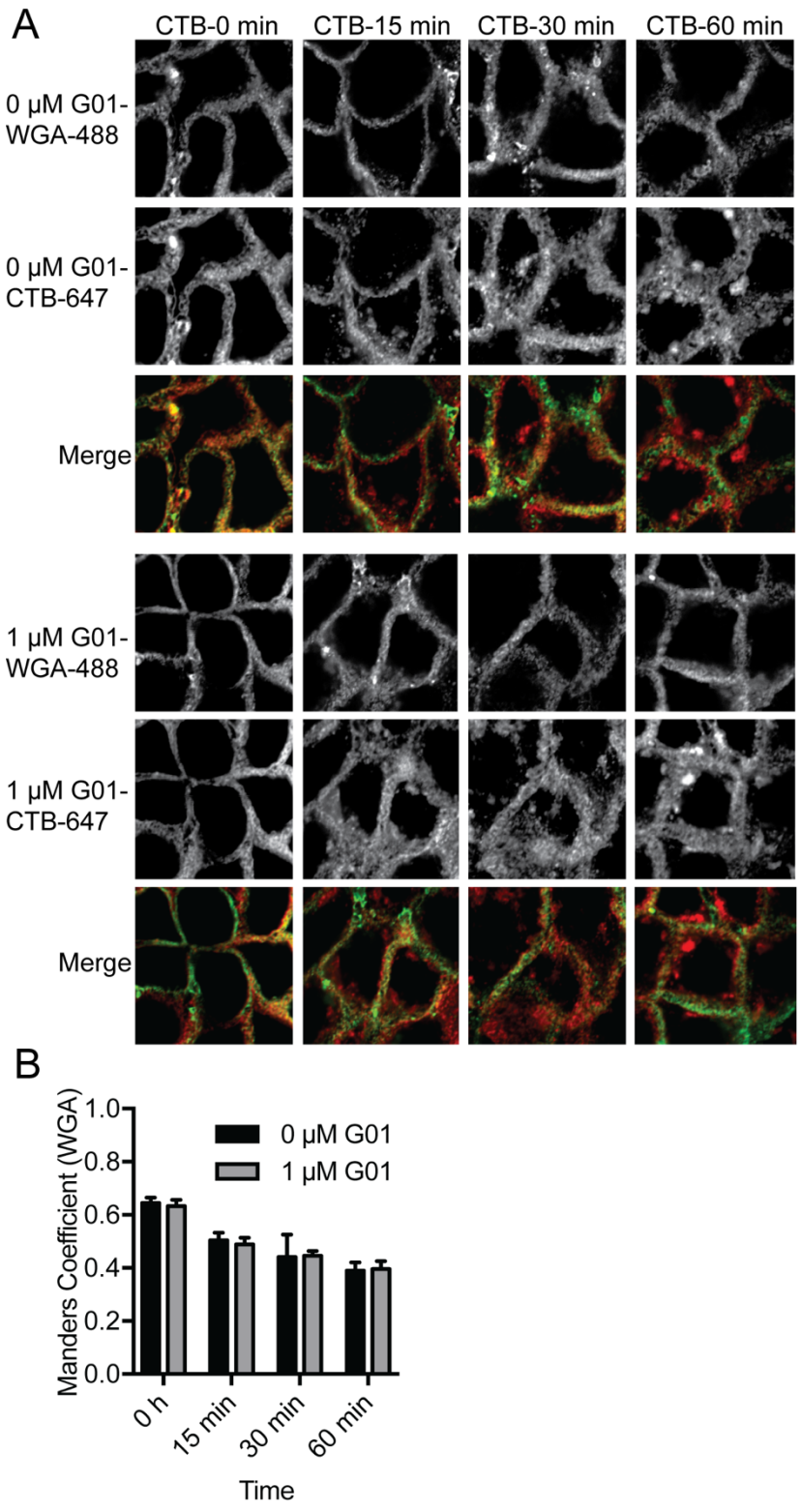

Figure 11. Endocytosis of cholera toxin is unaffected by G01. (A) A431 cells were treated with vehicle (DMSO) or 1 μM G01 for 48 h. Cells were incubated with

CTB-647 on ice for 20min. Excess CTB-647 was washed away by ice-cold PBS. Cells were then incubated with fresh warm medium with vehicle (DMSO) or 1 μM G01 at 37 °C and fixed at different time points. Cells were incubated with WGA-488 for 10min and mounted. Cells were imaged in a confocal microscope and representative images of vehicle (DMSO), 1 μM G01 are shown. (B) Images were analyzed using Manders coefficients to quantify colocalization of the PM marker, WGA-488 and CTB-647. The statistical significance of differences between mean Manders coefficients (± s.e.m. *n= 3*) at each time point was evaluated using Student's *t* tests.

4.2.4 G01 does not affect RAB11A localization or function

RAB11 includes three isoforms, RAB11A, RAB11B, and RAB11C, which are expressed in different tissues. Previous reports showed that HRAS was recycled via RAB11-positive endomembrane compartments, suggesting that HRAS PM localization may be mediated by RAB11 [110]. RAB11 is also important for the recycling of KRAS. Expression of inactive RAB11 or knockdown of endogenous RAB11 reduced KRAS localization on the PM [51]. We propose that HRAS and KRAS PM localization is disrupted when G01 alters RAB11 activity.

First, we determined the role of RAB11 in KRAS PM localization. Because RAB11A, but not RAB11B or RAB11C, is expressed in MDCK cells, we employed point mutagenesis to generate constitutively active (RAB11A-Q70L) and dominantly negative mCherry-RAB11A (RAB11A-S25N) from wild-type mCherry-Rab11A (RAB11A-WT). mCherry-RAB11A mutants and mGFP-KRASG12V were

transfected into MDCK cells. Cells stably expressing both fluorescence-tagged proteins were observed by confocal microscopy. KRASG12V appeared mislocalized in MDCK cells expressing RAB11A-Q70L or RAB11A-S25N, but not in cells expressing RAB11A-WT, indicating that normal RAB11A biological function was critical for maintaining KRAS on the PM (Figure 12A). Both activation and inactivation of RAB11A reduced the PM localization of KRAS.

RAB11A is concentrated in the perinuclear area for the biogenesis of the RE, indicating that its localization is crucial for RE biogenesis [111]. We next tested whether G01 disrupted RAB11A localization. MDCK cells stably expressing mGFP-KRASG12V and mCherry-RAB11A mutants were treated with 1 μM G01 for 48 h and observed by fluorescence microscopy. In control cells, RAB11A was concentrated in the perinuclear area (Figure 12B). In G01-treated cells, KRASG12V was mislocalized from the PM, but no changes to RAB11A localization were observed, suggesting that G01 does not affect RAB11A cellular distribution (Figure 12B).

Next, we tested whether G01 affected RAB11A activated status. We used a pull-down assay with a fragment of FIP3, a protein that binds to RAB11-GTP [101]. First, we validated the assay by obtaining lysates of MDCK cells stably expressing mCherry-RAB11A-WT, mCherry-RAB11A-Q70L, or mCherry-RAB11A-S25N. RAB11A-GTP was then pulled down with the FIP3 fragment and analyzed by immunoblotting. The ratio of mCherry-RAB11A-GTP in samples of mCherry-RAB11A-WT, mCherry-RAB11A-Q70L, and mCherry-RAB11A-S25N was approximately 1: 4: 0.1, confirming the validity and sensitivity of the assay for

measuring RAB11A-GTP cellular levels (Figure 12C). Next, MDCK cells were treated with G01 for 48 h and the relative RAB11-GTP level was determined. An approximately equal amount of RAB11-GTP was observed irrespective of G01 treatment, indicating that G01 did not affect the level of active RAB11 (Figure 12D).

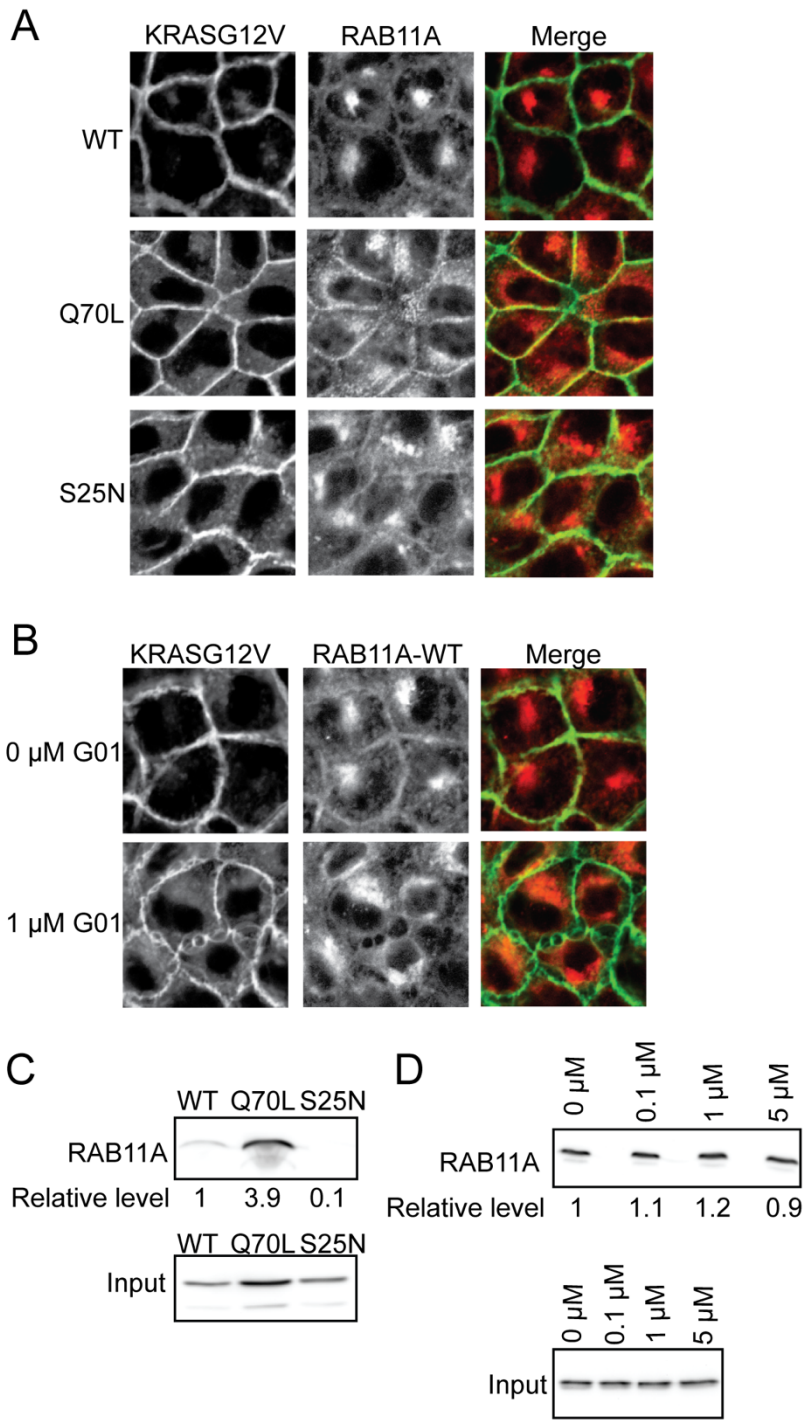

Figure 12. The localization or activity of RAB11A is not affected by G01. (A) MDCK cells stably expressing mGFP-KRASG12V and mCherry-RAB11A-WT or mCherry-RAB11A-Q70L or mCherry-RAB11A-S25N were fixed by 4% PFA and

imaged in a confocal microscope. Representative images are shown. (B) MDCK cells stably expressing mGFP-KRASG12V and mCherry-RAB11A-WT were treated with vehicle (DMSO) or 1 μM G01 for 48 h. Cells were fixed by 4% PFA and imaged in a confocal microscope. Representative images are shown. (C) MDCK cells stably expressing mGFP-KRASG12V and mCherry-RAB11A-WT or mCherry-RAB11A-Q70L or mCherry-RAB11A-S25N were lysed. GTP-loaded mCherry-RAB11A was pulled down and its level was measured by quantitative immunoblotting. The level of GTP-loaded mCherry-RAB11A was normalized to the total level of mCherry-RAB11A. Representative western blots are shown. (D) MDCK cells stably expressing mGFP-KRASG12V were treated with vehicle (DMSO) or G01 for 48 h. GTP-loaded endogenous RAB11A was pulled down and its level was measured by quantitative immunoblotting. The level of GTP-loaded RAB11A was normalized to the total level of RAB11A. Representative western blots are shown.

4.2.5 G01 binds to and inhibits the enzyme acylpeptide hydrolase

To determine the protein target of G01, a compound named as B-G01 was synthesized, whose structure consists of a biotin and G01 moiety. We incubated vehicle (DMSO) or B-G01 with CaCO2 cell lysate. B-G01 along with its bound proteins was pulled down by streptavidin-conjugated beads and analyzed by silver staining. A band of ~75 kDa was detected in the sample incubated with B-G01 but not in the control sample incubated with streptavidin-conjugated beads alone (Figure 13A). The silver stained band was excised and identified by mass

spectrometry as acylpeptide hydrolase (APEH). Protein identity was then confirmed by immunoblotting (Figure 13B).

APEH, is a prolyl-oligopeptidase which is responsible for catalyzing the removal of Nα-acylated amino acids from peptides and has a general role in protein degradation [112-115]. APEH is also capable of breaking down oxidized and glycated proteins and has been alternately named oxidized protein hydrolase [116, 117]. To biochemically verify this result we measured the enzymatic activity of APEH by analyzing the release of p-nitroaniline (pNA) from a synthetic peptide, acetyl-Alanine-p-nitroaniline (ac-Ala-pNA). The released pNA was detected by measuring absorbance at 410 nm (A410). At 15, 60, or 120 min, A410 was significantly lower in the G01-treated cell lysate than in the control, indicating a significant decrease of APEH enzymatic activity following G01 addition (Figure 13C).

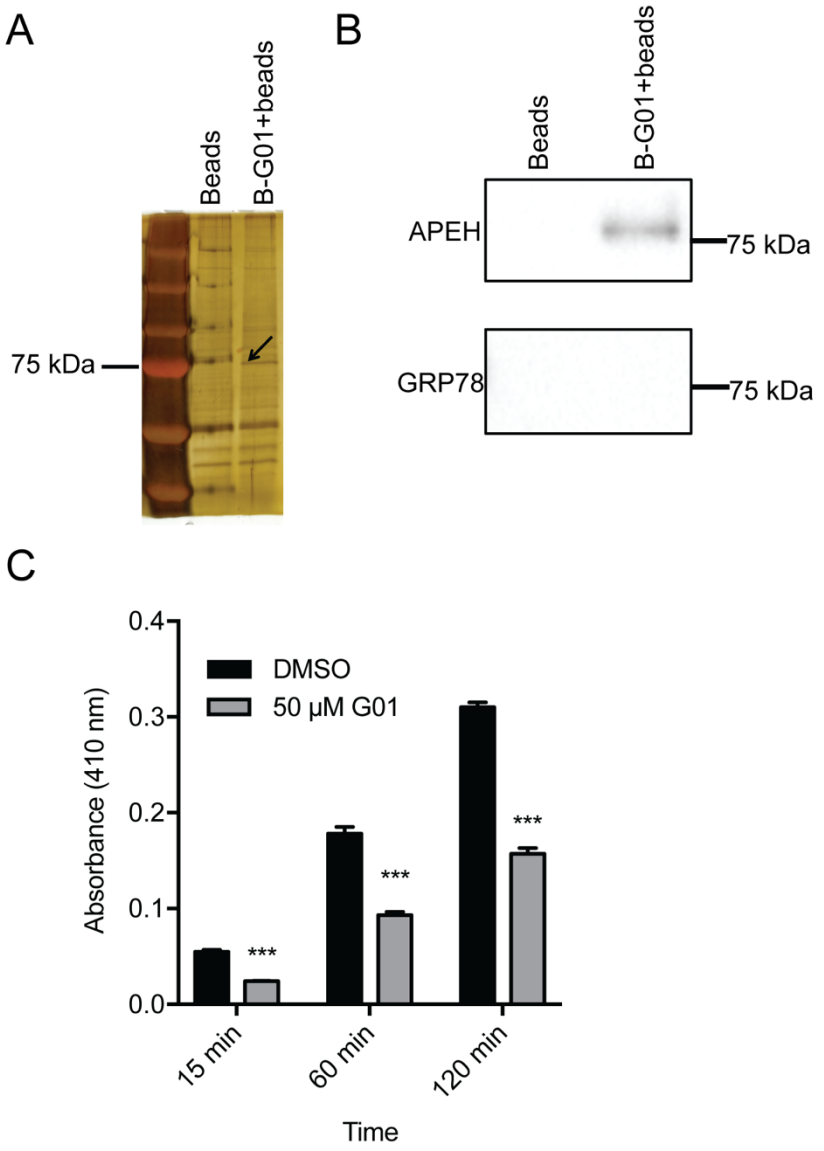

Figure 13. APEH is bound to and inhibited by G01. (A) The cell lysate of CaCO2 cells were incubated with streptavidin beads with DMSO or streptavidin beads with B-G01. The proteins that bind streptavidin beads and DMSO or B-G01 were analyzed by silver staining (*n= 3*). Representative silver-stained gel is shown. The gel area of 75kDa was cut and analyzed by mass spectrometry. (B) The cell lysate of CaCO2 cells were incubated with streptavidin beads with DMSO or streptavidin beads combined with B-G01. The proteins that bind streptavidin beads and DMSO

or B-G01 were analyzed by immunoblotting. (C) Ac-Ala-pNA was incubated with the MDCK cell lysate and absorbance was measured under 410 nm. The statistical significance of differences between mean absorbance (± s.e.m. $n = 3$) at each time point was evaluated using Student's t tests (***, $P < 0.001$).

4.2.6 Inhibition or knockdown of APEH mislocalizes oncogenic KRAS and PtdSer from the PM

To determine whether downregulation of APEH inhibits PM localization of KRASG12V, we knocked down APEH with NT shRNA or APEH shRNAs in MDCK cells stably expressing mGFP-tagged KRASG12V and mCherry-tagged CAAX, an endomembrane marker (Figure 14A). The cells with stable knockdown of APEH were imaged in a confocal microscope. In cells transfected with APEH shRNAs, we observed a mislocalization of KRASG12V from the PM, whereas KRASG12V was predominantly localized on the PM in cells transfected with NT shRNA (Figure 14B). The mislocalization of mGFP-KRASG12V from the PM was quantified by Manders coefficients [95], which evaluate the extent of colocalization between mGFP-KRASG12V and mCherry-CAAX. We observed a significant increase in the Manders coefficient in APEH-knockdown cells, indicating a significant mislocalization of KRASG12V from the PM (Figure 14C). Previous work has identified ebelactone A (ebelactone) as a commercially-available APEH inhibitor [114, 118]. We therefore treated MDCK cells stably expressing mGFP-KRASG12V and mCherry-CAAX with ebelactone. Similar to the observation in APEH-knockdown cells, mGFP-KRASG12V localization to the PM was inhibited by

ebelactone (Figure 14B) with an IC_{50} of 206 μM (Figure 14C), which is similar to the concentration at which ebelactone inhibited APEH and downstream proteasomal function in previous studies [114].

Next, we confirmed that reduced expression of APEH is causative to KRAS mislocalization. MDCK cells stably expressing mGFP-KRASG12V and mCherry-CAAX with or without APEH knockdown were transfected with APEH cDNA, and imaged with confocal microscopy. mGFP-KRASG12V was localized predominantly on the PM in the cells transfected with NT shRNA and mislocalized from the PM in cells transfected with APEH shRNAs (Figure 15, A to C). The PM localization of mGFP-KRASG12V was rescued by the restoration of ectopic APEH expression using exogenous cDNA (Figure 15, A to C). These observations confirmed that the KRAS mislocalization was induced by the knockdown of APEH and not by other off-target effects.

To explore potential molecular mechanisms for how APEH maintains KRAS PM localization and organization we investigated whether APEH regulates the PM localization of PtdSer and cholesterol, which are in turn critically important for the PM localization and clustering of KRAS and HRAS [31]. APEH was knocked down in MDCK cells stably expressing mGFP-LactC2 and mCherry-D4H, which are probes of PtdSer and cholesterol respectively. The localization of mGFP-LactC2 and mCherry-D4H was imaged in a confocal microscope. In control cells, the majority of mGFP-LactC2 and mCherry-D4H was localized on the PM. However, in APEH-knockdown cells, mGFP-LactC2 and mCherry-D4H were redistributed to endomembrane, suggesting a disruption of PtdSer and cholesterol localization

(Figure 16A). We next tested whether APEH inhibitors have similar effect on the localization of PtdSer and cholesterol. MDCK cells stably expressing mGFP-LactC2 and mCherry-D4H were treated with ebelactone or G01 for 48 h and imaged. mGFP-LactC2 and mCherry-D4H were mislocalized in G01- or ebelactone-treated cells (Figure 16B).

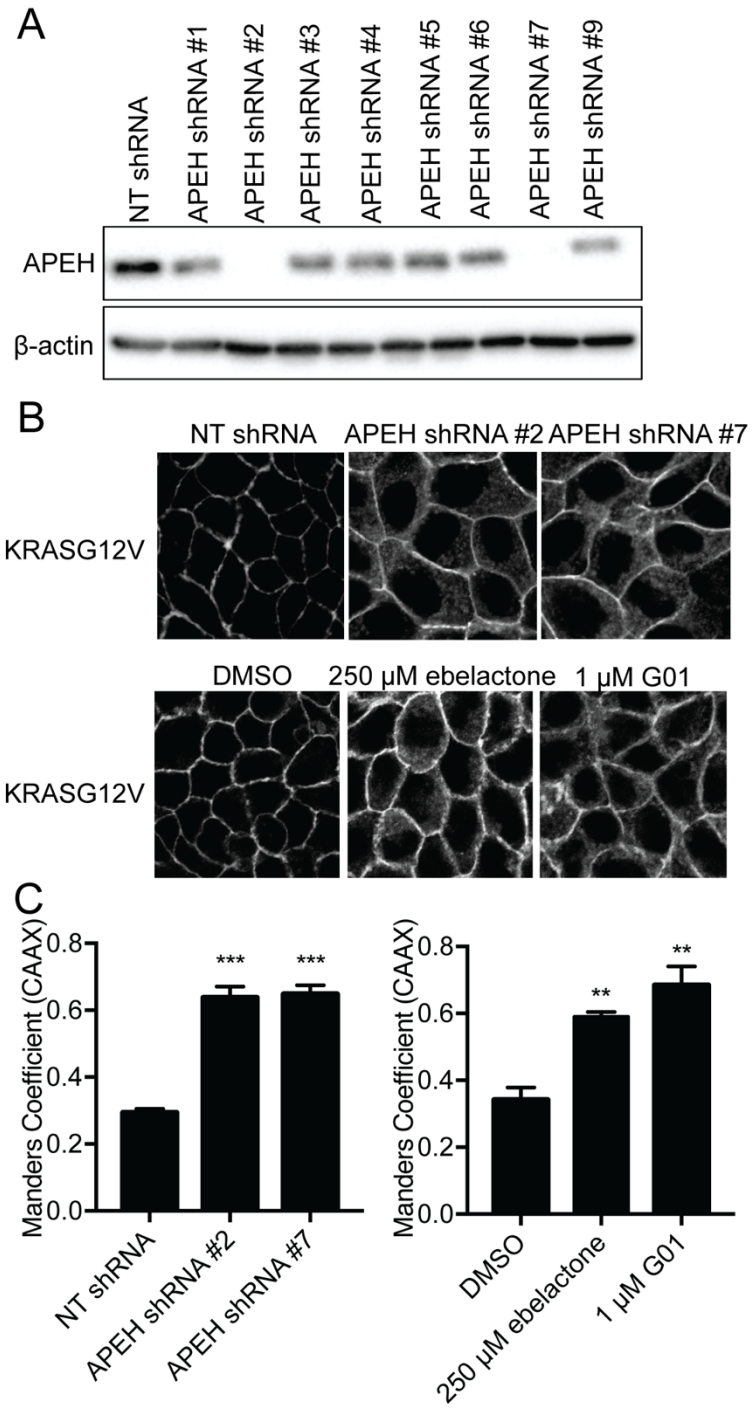

Figure 14. Inhibition or knockdown of APEH redistributes KRASG12V from the PM. (A) APEH was knocked down with APEH shRNAs or non-target (NT) shRNA in MDCK cells stably expressing mGFP-KRASG12V and mCherry-CAAX. Cells were maintained in media containing 5μg/ml puromycin. Level of APEH was

measured by immunoblotting. (B) MDCK cells stably expressing mGFP-KRASG12V and mCherry-CAAX with or without the knockdown of APEH, and MDCK cells stably expressing mGFP-KRASG12V and mCherry-CAAX with 48 h treatment of vehicle (DMSO) or ebelactone or G01 were imaged in a confocal microscope. Representative images were shown. (C) The extent of RAS mislocalization was quantified with Manders coefficients. The significance of differences (± s.e.m. $n = 3$) were assessed using one-way ANOVA (**, $P < 0.01$; ***, $P < 0.001$).

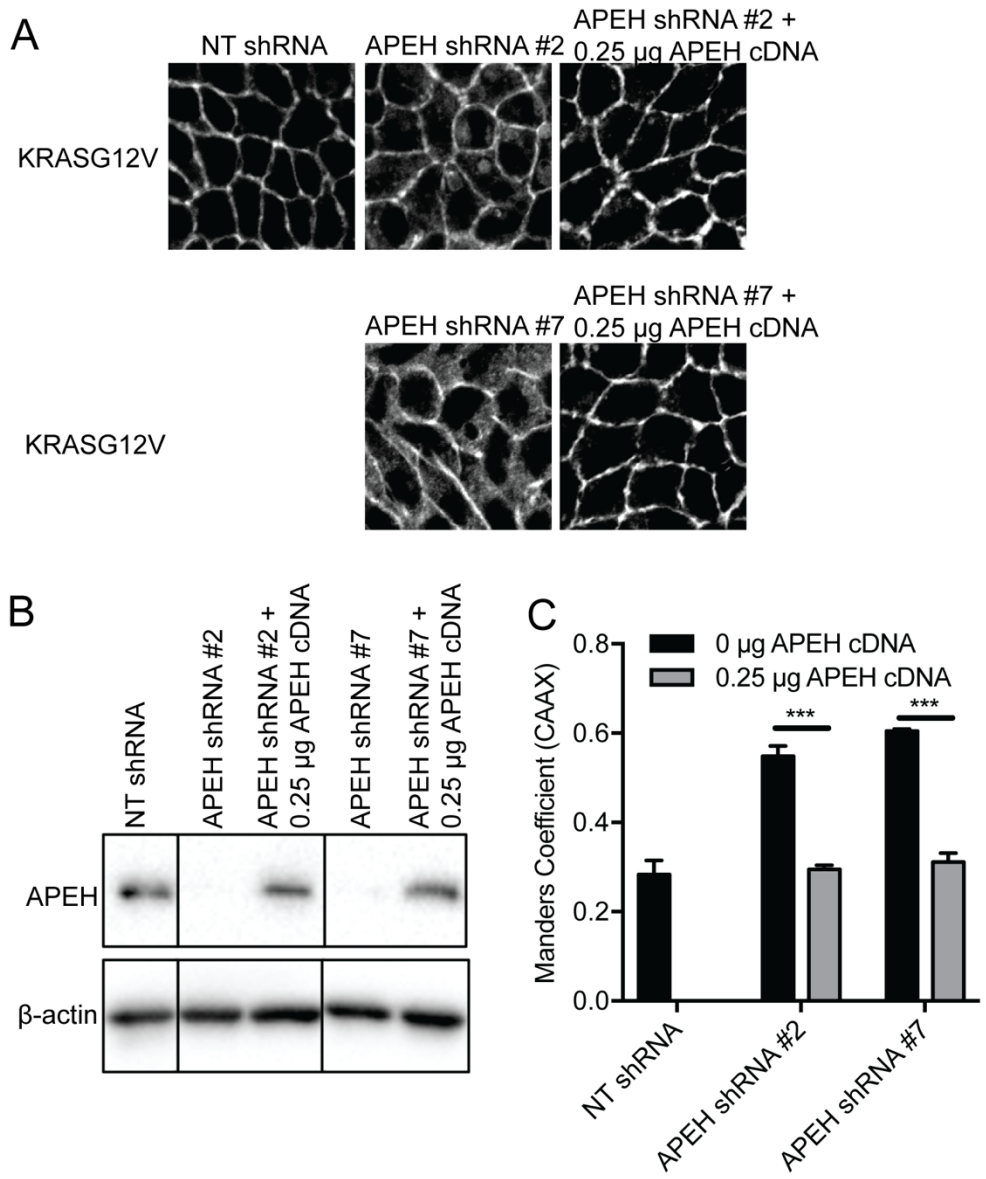

Figure 15. The mislocalization of KRASG12V induced by APEH knockdown is rescued by the expression of exogenous APEH. (A) APEH was knocked down with APEH shRNAs or non-target (NT) shRNA in MDCK cells stably expressing mGFP-KRASG12V and mCherry-CAAX. Cells were maintained in media containing 5µg/ml puromycin. Cells were seeded in 12-well plates and transfected with 0ug or 0.25ug APEH cDNA. Cells were imaged in a confocal microscope and representative images are shown. (B) APEH level was measured

with immunoblotting. (C) Manders coefficients were calculated for representation of the extent of RAS mislocalization. The significance of differences (± s.e.m. *n*= *3*) were assessed using Student's *t* tests (***, $P < 0.001$).

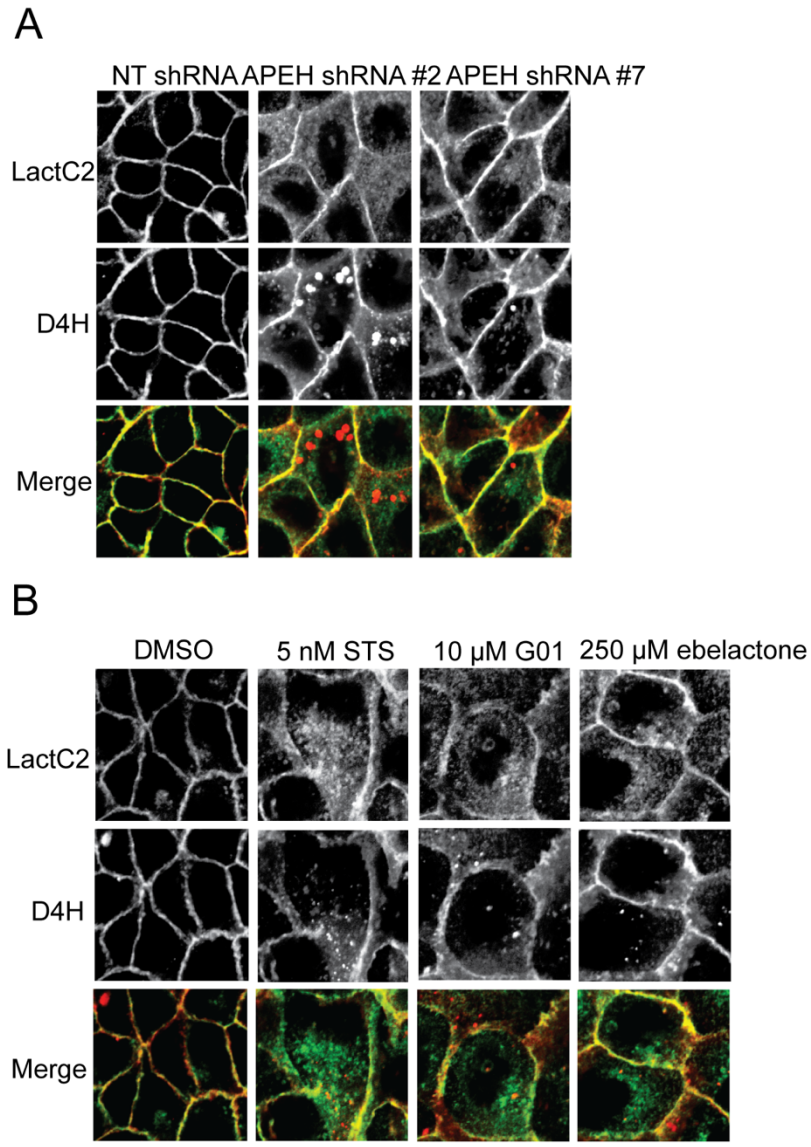

Figure 16. PtdSer and cholesterol are mislocalized from the PM by inhibition or knockdown of APEH. (A) APEH was knocked down with APEH shRNAs or non-target (NT) shRNA in MDCK cells stably expressing mGFP-LactC2 and mCherry-D4H. Cells were grown in media with 5μg/ml puromycin and were

observed in a confocal microscope. Representative images are shown. (B) MDCK cells stably expressing mGFP-LactC2 and mCherry-D4H were treated with vehicle (DMSO) or STS or ebelactone or G01 for 48 h. Cells were imaged and representative images are shown.

4.3 Discussion

Several lines of evidence suggest that the mechanism of action of G01 involves disruption of RE function. Firstly, we observed mislocalization of palmitoylated HRAS and KRAS4A, as well as non-palmitoylated KRAS4B with approximately equal potency. This result implicates a common component of their respective spatial organizing systems that maintains PM localization after posttranslational processing, namely the RE [51]. Secondly, the EGFR and TfR were aberrantly distributed in G01 treated cells concordant with abnormal endocytic recycling [46, 51, 106-108], this was most evident with the EGFR, which accumulated in the RE after G01 treatment in EGF stimulated CHO cells.

We further show that the molecular target of G01 is the enzyme APEH. G01 bound to APEH with sufficient avidity to allow affinity purification from cell lysates and G01 inhibited the enzymatic activity of APEH in biochemical assays. Concordant with the biological effect of G01 [119], shRNA knock down of APEH expression resulted in KRAS mislocalization from the PM, which was rescued by the restoration of ectopic APEH expression. Together these observations reveal that APEH is a novel regulator of KRAS PM localization. Two major cellular processes are required for the fidelity of KRAS PM targeting: First, the

maintenance of a high concentration of PtdSer on the inner leaflet of the PM, which is required because the KRAS membrane anchor exhibits exquisite binding specificity for this phospholipid [31, 120]. Second, a functioning spatial organization system, which in the case of KRAS requires the RE operating in concert with the chaperone PDEδ and its regulator ARL2 [40, 46, 51]. We show here that both of these components are compromised when APEH expression is suppressed. PM inner leaflet PtdSer is reduced, resulting in redistribution of the PtdSer probe, LactC2 to endomembrane. In addition, our recent results show that there is malfunction of the RE as evidenced by aberrant endosomal recycling of the EGFR and TfR. It seems likely that the failure to maintain PM PtdSer content in APEH-knockdown cells is at least in part also due to aberrant RE function, since lipids as well as proteins must be appropriately sorted and recycled after endocytosis. Therefore, the mechanism of action of APEH knockdown for KRAS mislocalization involves disruption of RE function, concordant with observations in G01-treated cells and impairment of the KRAS spatial organizing system and reduced PtdSer content of PM are causative of KRAS mislocalization. These results were recapitulated by a previously described, albeit much less potent, APEH inhibitor, ebelactone [114, 118], which we show here also mislocalized KRAS and reduced the PtdSer content of the inner PM. Concordant with the effects on KRAS PM localization, our recent results show that APEH knockdown blocked MAPK signaling downstream of oncogenic mutant KRASG12V and inhibited the proliferation of KRAS-dependent pancreatic cancer cells. By contrast APEH

knockdown had minimal effect on the proliferation of pancreatic cancer cells that expressed wild type KRAS.

Of note, our recent results show that APEH knockdown was less efficacious at inhibiting pancreatic cancer cell growth than treatment with G01. Moreover, whereas G01 elevates cellular SM levels [119], knockdown of APEH had no such effect, suggesting that G01 may have other cellular targets in addition to APEH. Consistent with this interpretation of the results biochemical assays indeed showed that G01 can inhibit both ASMase and NSMase whereas the activity of these enzymes was unaffected in APEH-knockdown cells. Interestingly ebelactone also elevated cellular SM levels and inhibited NSMase. Previous work has shown that inhibition of SMases is of itself sufficient to impair KRAS PM localization [39, 40, 96], it therefore seems likely that simultaneous perturbation of SM metabolism and RE function via APEH inhibition results in the increased potency of G01 for inhibition of KRAS-dependent pancreatic cancer cell proliferation.

We recently identified multiple enzymes in the SM metabolic pathway whose pharmacological inhibition, or in some cases pharmacological activation, mislocalize KRAS and PtdSer from the PM. In this context we now show in KRAS mislocalization assays that G01 synergizes with three inhibitors of different SM metabolic enzymes. We propose therefore that G01 modulates SM metabolism, but through a molecular target different from those of FB1, R-fendiline and STS. Interestingly this synergy was observed with inhibitors that both up regulate and down regulate SM levels, indicating the critical importance of PM SM lipid homeostasis in maintaining KRAS function. Most interestingly, the synergistic

effects on KRAS mislocalization also extended to synergistic inhibition of oncogenic KRAS driven MAPK activation. Together these results strongly suggest that G01 may have utility in drug cocktails for future anti-RAS therapies.

Alpha-acetylation of the amino-terminal amino acid of proteins (Nα acetylation) is a highly prevalent post-translational modification in eukaryotic cells [121]. The function of Nα acetylation is not fully understood, but there are examples where the modification can regulate protein stability, enzymatic activity and protein-protein interactions. Nα acetylation is irreversible, unlike amino acid side chain acetylation. In eukaryotic cells APEH, a ubiquitously expressed cytosolic enzyme, catalyzes removal of the Nα-acetylated amino acid from peptides and therefore regulates the overall cellular levels of Nα acetylated proteins [114]. APEH is also able to hydrolyze oxidized or glycated proteins and has been alternately named as oxidized protein hydrolase in older literature [116, 117]. Recent studies have shown that knockdown or inhibition of APEH blocks the chymotrypsin-like activity of the proteasome [114, 122, 123]. Thus, APEH has been advocated to operate as a regulator of proteasome that degrades of poly-ubiquitinated and/or oxidized proteins. Separately, APEH has also been identified as a component of an enzyme complex that repairs DNA single-strand breaks and concordantly was shown to translocate into the cell nucleus in response to DNA damage [115].

Linking these disparate activities of APEH to the perturbation of RE function and consequent mislocalization of KRAS that we have described is not immediately straightforward. Taken together, the previous studies broadly suggest that APEH is a regulator of cellular protein quality control, given its peptidase

activity and role in proteasomal regulation. We therefore speculate that aberrant protein quality control causes damage to the endolysosome, which is in turn critical for the recycling of RAS and PM lipids [39, 40]. This may be a consequence of oxidative stress induced by accumulation of oxidatively damaged proteins [124, 125], that in turn causes oxidative damage to the endolysosome and / or dysregulation of specific proteins involved in regulating of RE function [126-128]. Identifying the precise molecular target(s) may prove elusive, but in support of the general mechanism that aberrant protein quality control is involved we show that treatment of cells with the proteasome inhibitor, bortezomib phenocopies the effect of G01 on KRAS mislocalization.

Finally, it is interesting to note that APEH is expressed at higher levels in cancers expressing oncogenic mutant KRAS than in cancers expressing wild type KRAS. This correlation, when taken in the context of our observations that APEH activity is required to maintain KRAS and PtdSer on the inner leaflet of the PM, highlights the potential utility of APEH inhibitors and perhaps proteasomal inhibitors in the treatment of KRAS-dependent pancreatic cancer.

Chapter 5 Addition of a farnesyl or geranyl moiety potentiates the inhibitory effect of G01 on plasma membrane localization as well as biological function of oncogenic KRAS

5.1 Introduction

To enhance the effect of G01 on oncogenic KRAS PM mislocalization, a series of oxanthroquinone derivatives were synthesized based on the original structure of G01. The addition of a geranyl or farnesyl moiety to proteins usually augments their hydrophobicity, facilitating their attachment to the cell membrane. Accordingly, we hypothesized that addition of a geranyl (D01) or farnesyl (D02) moiety to G01 could increase its attachment to cell membranes and absorption, ultimately potentiating KRAS mislocalization. In addition, given the synergistic action of STS, FB1, or R-fendiline with G01, we speculated that a chimera of STS and G01 was more effective at mislocalizing KRAS than G01 alone. Based on this assumption, we attached G01 to an STS moiety (D04). During the synthesis of D01, D02, and D04, a series of intermediate chemical products were generated. As they all shared the G01 backbone, we tested their ability to mislocalize oncogenic KRAS from the PM as well.

5.2 Results

5.2.1 D01 or D02 is more potent than G01 at mislocalizing oncogenic KRAS

MDCK cells stably co-expressing mGFP-KRASG12V and mCherry-CAAX

were treated with oxanthroquinone derivatives for 48 h. We show that C10 or C11 or C12 mislocalized KRAS from the PM with IC_{50} ~1 μM, while H09 or D04 did not mislocalize KRAS (Figure 17 and 18). Interestingly, D01 or D02 mislocalized KRAS with IC_{50} ~0.006 μM or ~0.06 μM, respectively (Figure 19). Therefore, we conclude that D01 or D02 is more effective than G01 at mislocalizing KRAS from the PM.

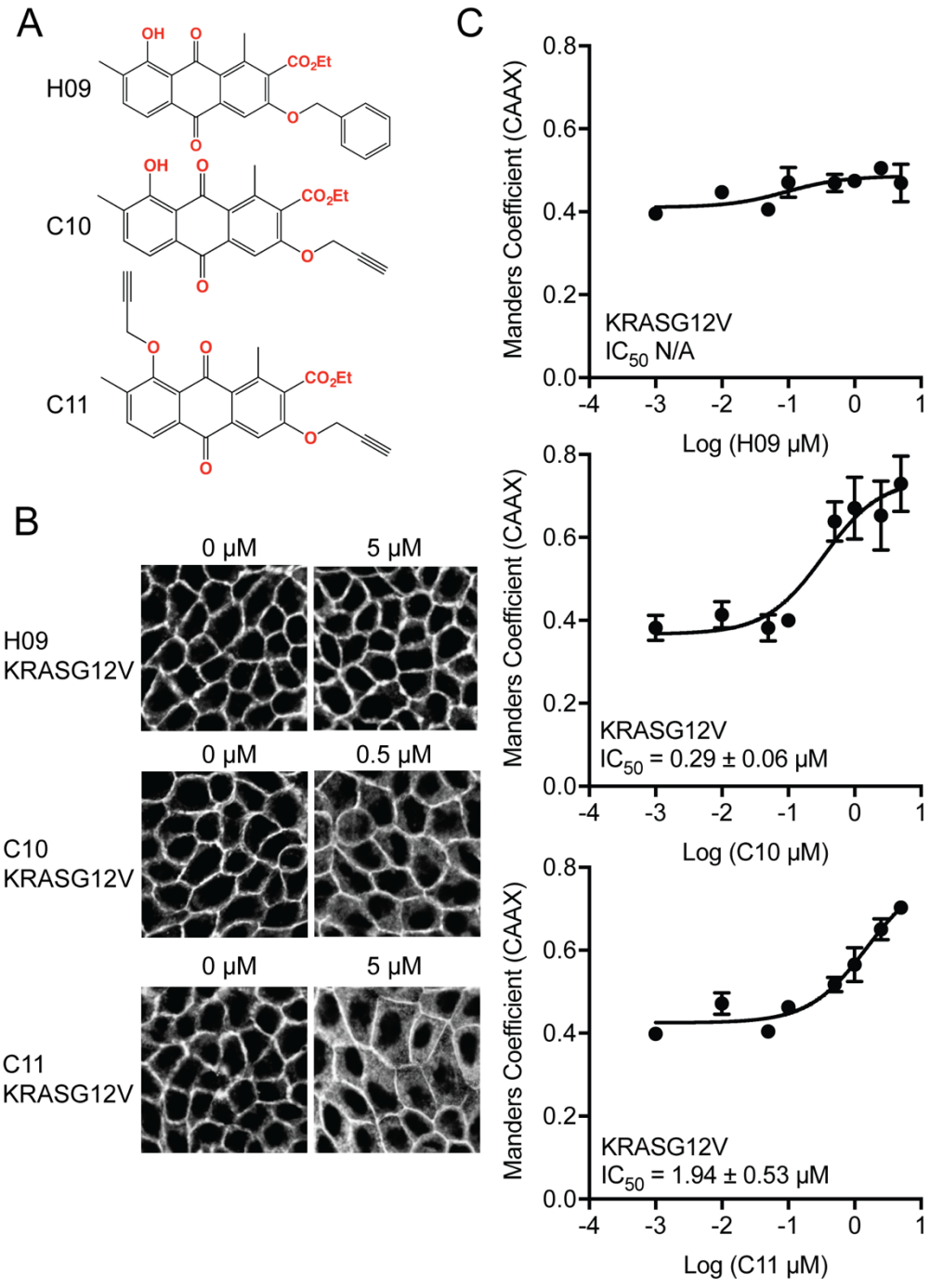

Figure 17. KRASG12V is mislocalized by C10 or C11 but not by H09. (A) Structure of H09, C10, and C11. (B) MDCK cells stably expressing mGFP-KRASG12V and mCherry-CAAX were treated with vehicle (DMSO) or H09 or C10

or C11 for 48 h and imaged in a confocal microscope. Representative images are shown. (C) The extent of RAS mislocalization was quantified with Manders coefficients. Estimated IC_{50} values were obtained from the Manders coefficient (± s.e.m. *n*= *3*) dose-response plots.

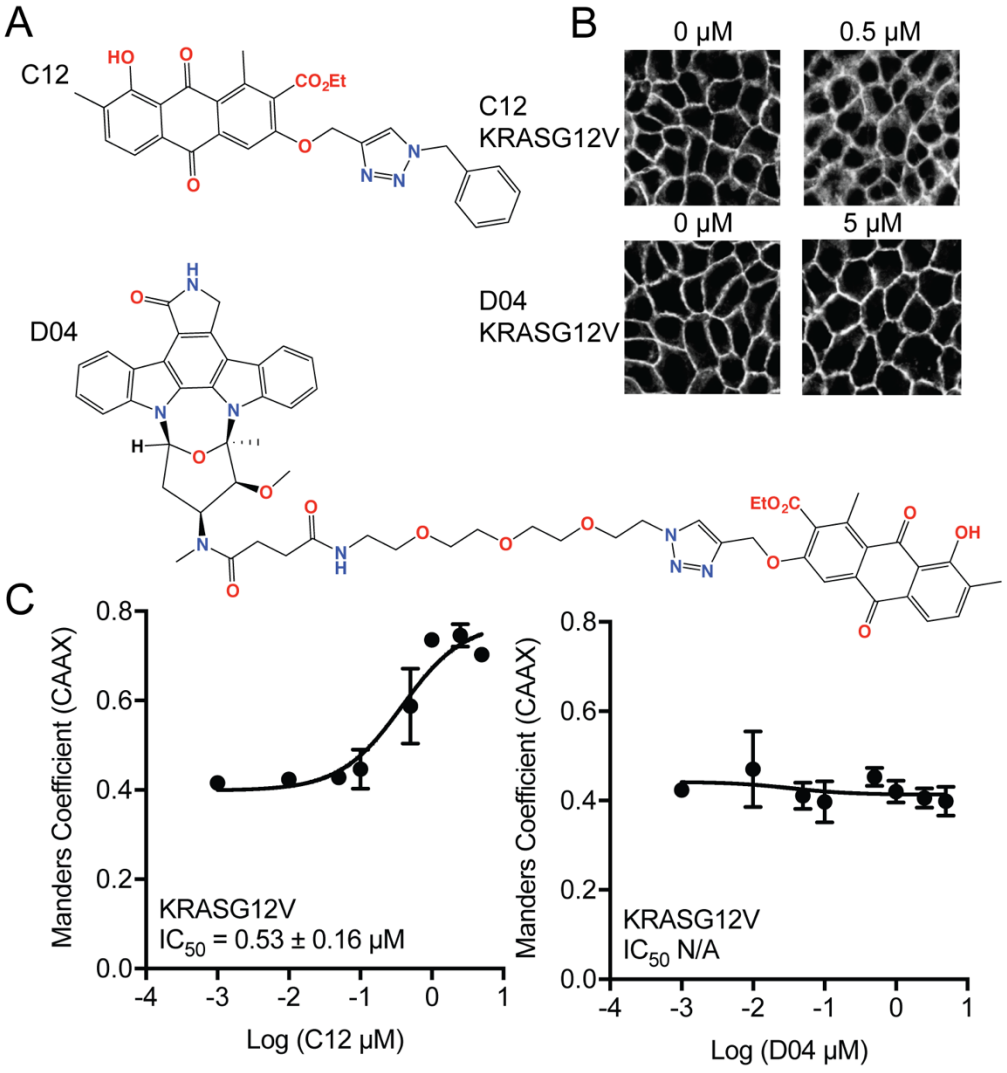

Figure 18. KRASG12V is mislocalized by C12 but not by D04. (A) Structure of C12 and D04. (B) MDCK cells stably expressing mGFP-KRASG12V and mCherry-CAAX were treated with vehicle (DMSO) or C12 or D04 for 48 h and imaged in a confocal microscope. Representative images are shown. (C) The extent of RAS

mislocalization was quantified with Manders coefficients. Estimated IC_{50} values were obtained from the Manders coefficient (± s.e.m. *n*= *3*) dose-response plots.

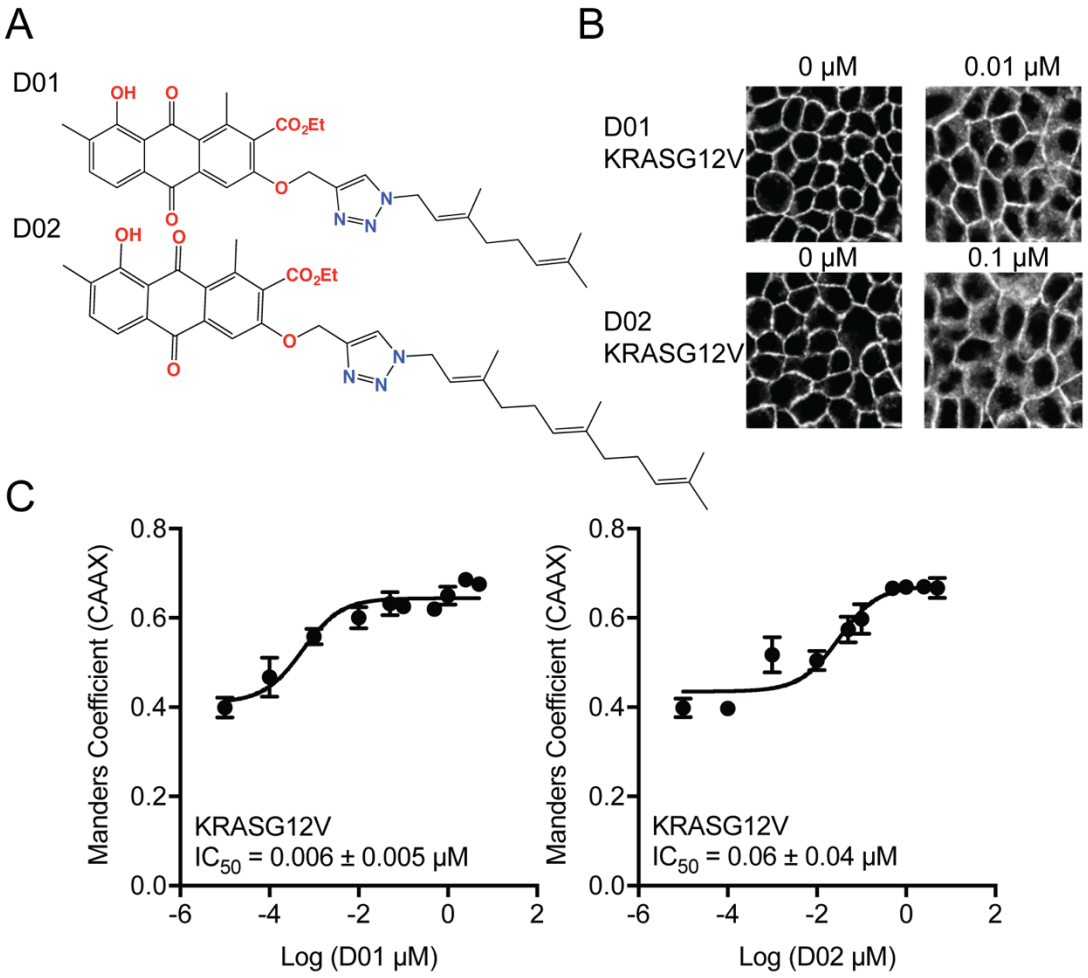

Figure 19. KRASG12V is mislocalized by D01 or D02. (A) Structure of D01 and D02. (B) MDCK cells stably expressing mGFP-KRASG12V and mCherry-CAAX were treated with vehicle (DMSO) or D01 or D02 for 48 h and imaged in a confocal microscope. Representative images are shown. (C) The extent of RAS mislocalization was quantified with Manders coefficients. Estimated IC_{50} values were obtained from the Manders coefficient (± s.e.m. *n*= *3*) dose-response plots.

5.2.2 D01 or D02 disrupts the spatial organization of KRAS on the

PM

We next tested whether D01 or D02 disrupted KRAS nanocluster formation. We treated MDCK cells stably expressing mGFP-KRASG12V with 0.01 μM D01 or 0.1 μM D02. Intact PM sheets were prepared and incubated with anti-GFP antibodies conjugated with 4.5-nm gold particles. EM images were analyzed by Ripley's K-function. A significant decrease in the L_{max} value was observed in D01- or D02-treated cells, indicating significant disruption of KRAS nanoclusters (Figure 20A). This was accompanied by a significant decrease in the number of gold particles and confirmed with results showing that 0.01 μM D01 and 0.1 μM D02 effectively mislocalized KRASG12V from the PM (Figure 20B).

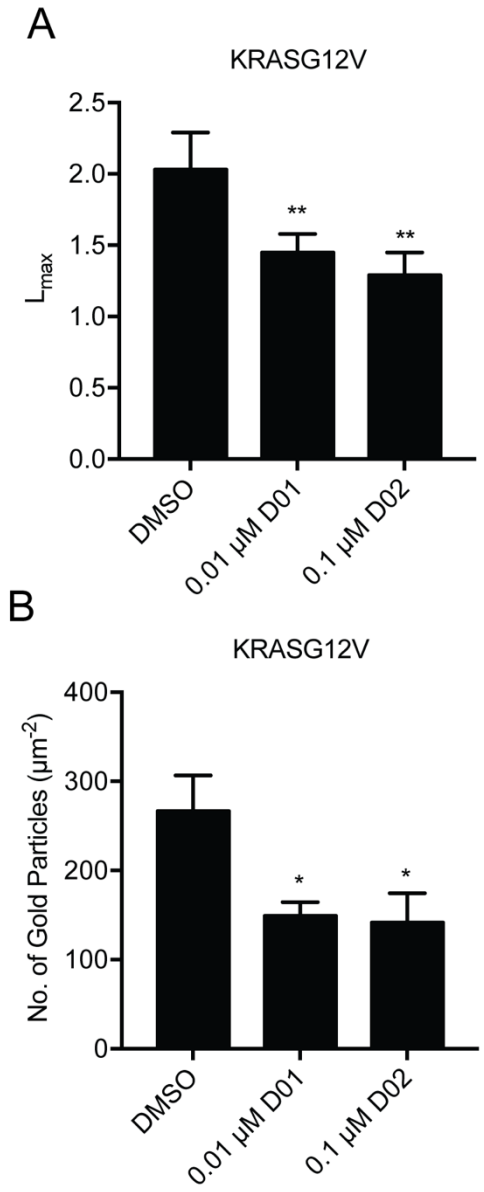

Figure 20. D01 or D02 disrupts the PM nanoscale organization of KRASG12V. (A) MDCK cells stably expressing mGFP-KRASG12V were treated with vehicle (DMSO) or 0.01 μM D01 or 0.1 μM D02 for 24 h. Basal PM sheets were generated from the drug-treated cells and imaged by EM after labeling with anti-GFP antibody conjugated to 4.5 nm gold. The extent of clustering of the gold particles was analyzed using Ripley's K-function. Values of L_{max} above the CI indicates nanoclustering. L_{max} value represents the extent of nanoclustering. At least 12 PM

sheets were evaluated for each condition. Significant differences from the control pattern for D01- or D02-treated cells were assessed using bootstrap tests (**, $P < 0.01$). (B) Average mean (± s.e.m. $n \geq 12$) gold labeling density on the PM sheets was calculated and the statistical significance of differences in gold labeling density was evaluated using one-way ANOVA (*, $P < 0.05$).

5.2.3 D01 or D02 inhibits MAPK signaling downstream of oncogenic KRAS

To assess whether D01 or D02 was more effective than G01 at inhibiting oncogenic KRAS signaling, we measured ppERK in MDCK cells stably expressing KRASG12V with D01 or D02 treatment. Treatment with 0.01 μM D01 or 0.1 μM D02 significantly reduced ppERK levels without affecting oncogenic KRAS levels, indicating significant inhibition of MAPK signaling downstream of oncogenic KRAS (Figure 21 and 22). Notably, the same concentrations of G01 did not have any effect on ppERK level (Figure 21). These observations confirm that D01 and D02 are more potent than G01 at inhibiting oncogenic KRAS function.

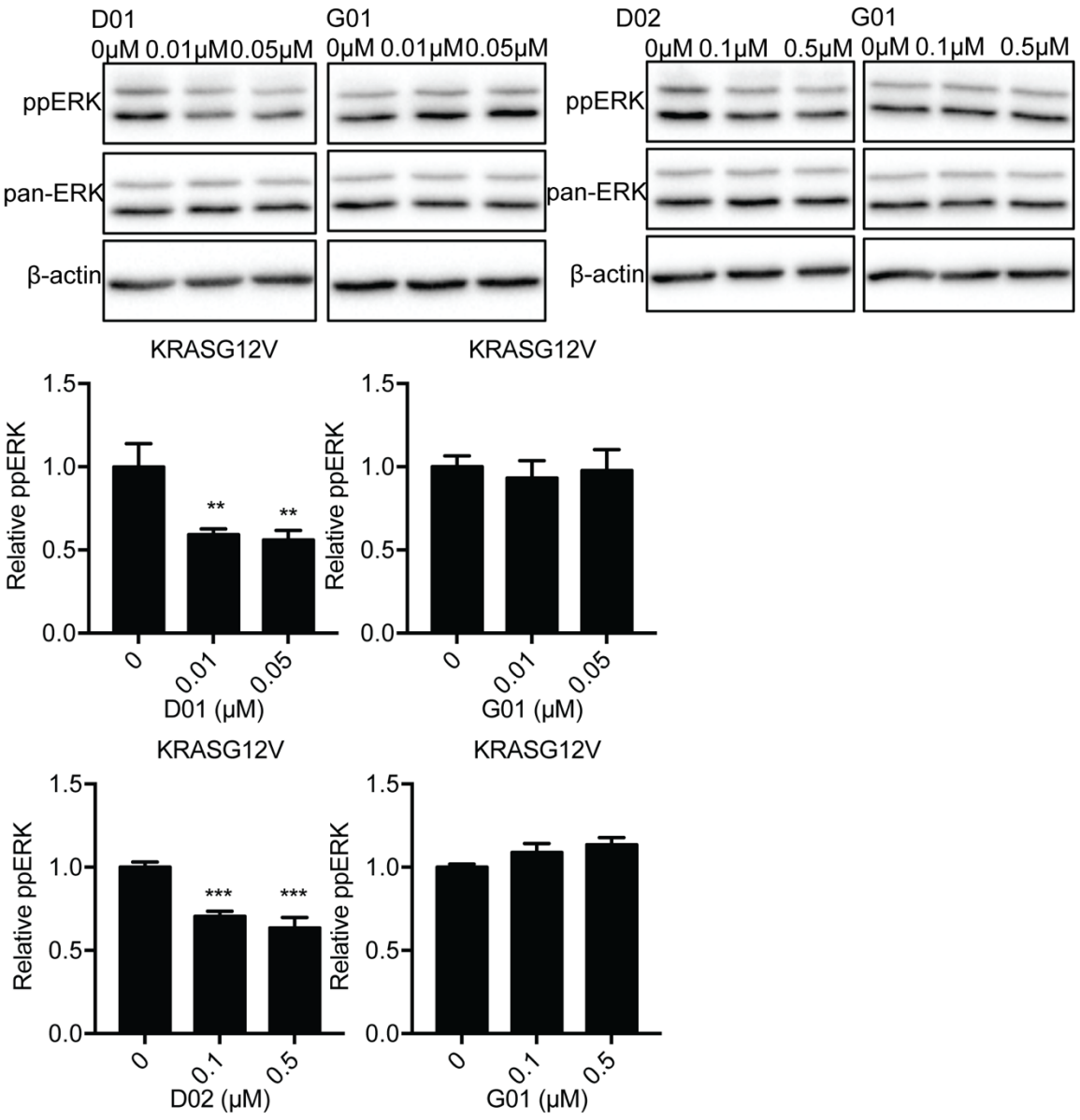

Figure 21. Oncogenic KRAS signaling is more potently inhibited by D01 or D02. MDCK cells stably expressing mGFP-KRASG12V were treated with vehicle (DMSO) or D01 or D02 or G01 for 48 h. ppERK levels were measured by quantitative immunoblotting. The relative ppERK level was obtained by normalizing ppERK level to pan-ERK level. Statistical significance of differences was evaluated using one-way ANOVA (**, $P < 0.01$; ***, $P < 0.001$).

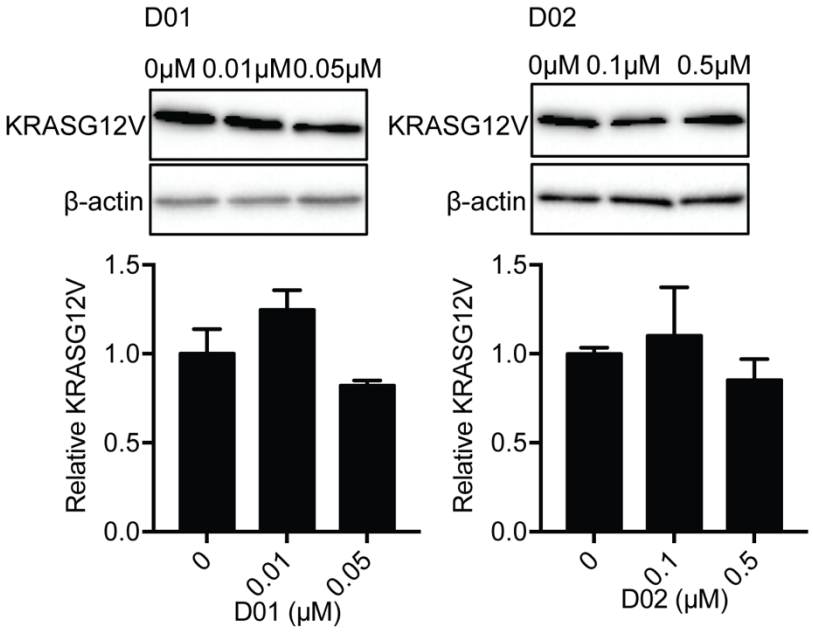

Figure 22. Oncogenic KRAS level is not affected by D01 or D02. MDCK cells stably expressing mGFP-KRASG12V were treated with vehicle (DMSO) or D01 or D02 for 48 h. KRASG12V levels were measured by quantitative immunoblotting. The relative KRASG12V level was obtained by normalizing KRASG12V level to β-actin level. Statistical significance of differences was evaluated using one-way ANOVA.

5.2.4 D01 or D02 selectively inhibits the proliferation of oncogenic KRAS-dependent cell lines

We next tested whether D01 or D02 inhibited the proliferation of RAS-less MEFs expressing oncogenic KRAS or BRAF. Treatment with D01 or D02 inhibited the proliferation of KRASG12V-expressing RAS-less MEFs, but not those expressing BRAFV600E (Figure 23A).

Finally, we tested whether D01 or D02 inhibited the proliferation of oncogenic

KRAS-dependent MiaPaCa-2 pancreatic tumor cell lines. The latter were compared to BxPC3 cells, which express wild-type KRAS and are therefore KRAS-independent. The two cell lines were treated with D01 or D02 for 72 h. We report that proliferation of BxPC3 cells was not affected, whereas that of MiaPaCa-2 cells were significantly inhibited, indicating that D01 or D02 selectively inhibited the proliferation of KRAS-dependent pancreatic tumor cells (Figure 23B).

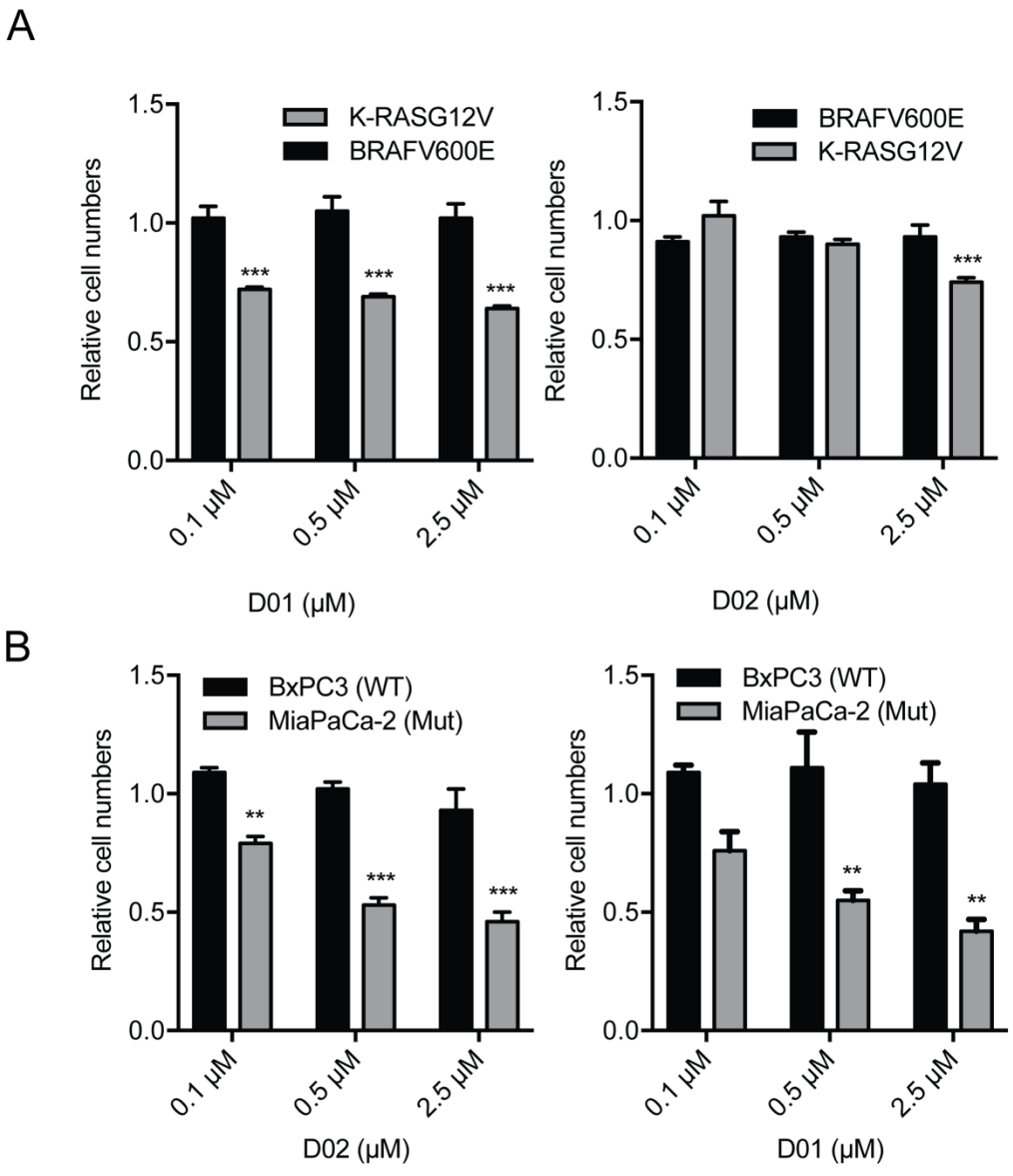

Figure 23. The proliferation of KRAS-dependent cell lines is selectively inhibited by D01 or D02. RAS-less MEF cells rescued by expressing KRASG12V or BRAFV600E (A), and pancreatic cancer cells (B) were seeded in 24-well plates and treated with vehicle (DMSO) or D01 or D02 for 72 h. Cells were detached and counted. Relative cell numbers were obtained by normalizing numbers of drug-treated cells to DMSO-treated cells. Statistical significance of differences was evaluated using one-way ANOVA (**, $P < 0.01$; ***, $P < 0.001$).

5.2.5 D01 did not affect SMase activity

We have reported in the previous chapter that G01 enhanced cellular SM levels, which contributed to G01-induced KRAS mislocalization from the PM [119]. Our recent finding shows that G01 inhibited acid SMase (ASMase) and neutral SMase (NSMase), which are responsible for catalyzing the breakdown of SM. To test whether D01 also affects SMase function, we tested SMase enzymatic activity in D01-treated MDCK cells. We show that D01 did not affect SMase activity in both neutral and acidic pH environments, suggesting no inhibitory activity towards ASMase or NSMase.

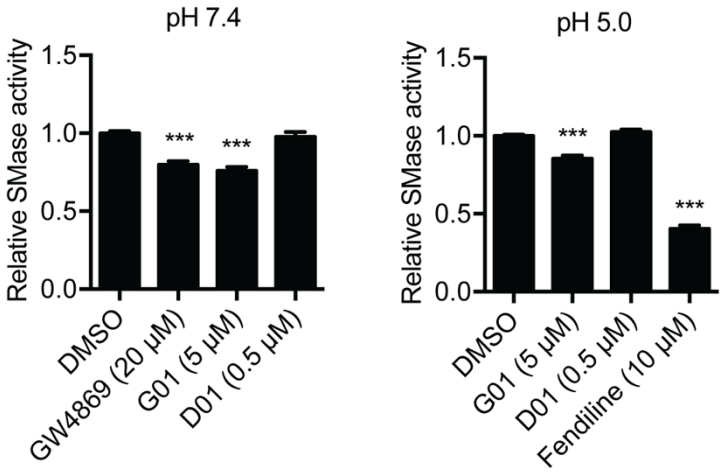

Figure 24. SMase function is not affected by D01. MDCK cells were treated with vehicle (DMSO) or GW4869 or G01 or D01 or fendiline for 48 h and lysed. Cell lysates were analyzed for neutral and acid SMase activity. The significance of differences was determined using one-way ANOVA (***, $P < 0.001$).

5.3 Discussion

We show that addition of a geranyl or farnesyl moiety to G01, resulting in D01 or D02, respectively, further inhibits oncogenic KRAS PM localization and signaling. The observed increased potency for KRAS mislocalization indicates enhanced intake of these compounds by the cells, which is consistent with previous studies showing that farnesyl or geranyl groups improved proteins' hydrophobicity [129].

Our recent experiments show that G01 treatment is more efficacious at inhibiting pancreatic cancer cell proliferation than APEH knockdown. This is because G01 not only inhibits APEH function, but perturbs SM metabolism as well. The simultaneous disruption of APEH function and SM metabolism may be

causative to the enhanced potency of G01 for inhibiting the proliferation of KRAS-dependent cancer cells. In this chapter, we show that D01 did not cause inhibition of cellular SMase function. This may be the reason why D01 is not very efficacious at inhibiting the proliferation of KRAS-dependent pancreatic cancer cells, even at a concentration that is much higher than that for mislocalizing KRAS.

Besides prenylation, fatty-acetyl modification such as N-myristoylation and palmitoylation, also contribute to proteins' hydrophobicity and membrane binding capacity. Therefore, the addition of N-myristoyl or palmitoyl groups to pharmacological agents may represent a promising avenue for enhancing the cellular uptake of drugs.

Chapter 6 Discussion and future directions

In this study, we identified G01 as a potential anti-RAS therapeutic. G01 mislocalized KRAS, HRAS, and KRAS4A from the PM and disrupted the nanoclusters of RAS proteins remaining on the PM. Previous studies indicated that RAS must localize on the PM and assemble into nanoclusters to recruit downstream effectors [18, 31]. Concordant with these studies, MAPK signaling downstream of RAS was disrupted by G01-induced PM mislocalization of RAS.

We further identified the molecular target of G01 to be APEH. G01 bound to APEH and inhibited the enzymatic activity of APEH. Concordant with the biological effect of G01, APEH knockdown or inhibitors mislocalized KRAS from the PM, inhibited the nanoclusters of KRAS remaining on the PM, and abrogated the MAPK signaling downstream of KRAS.

KRAS PM targeting requires two major cellular processes. First, a high concentration of PtdSer is required to be maintained on the inner leaflet of the PM, because KRAS binds specifically to PtdSer [31, 120]. Second, a functioning spatial organization system, which involves the RE operating in concert with PDEδ and ARL2, is needed [40, 46, 51]. In this study, we show that both of these two cellular processes are compromised in APEH-knockdown or -inhibited cells. It seems likely that the mislocalization of PtdSer is at least partially induced by the aberrancy of RE function because lipids must be properly sorted and recycled after endocytosis.

Concordant with the effect on KRAS PM localization, APEH knockdown or inhibition selectively blocked the proliferation of oncogenic KRAS-dependent cancer cells, but have minimal effect on the proliferation of cancer cells expressing

wild-type KRAS. Interestingly, G01 inhibited the proliferation of KRAS-dependent cancer cells more potently than APEH knockdown. Moreover, G01 increased cellular SM level and inhibited SMase function [119], which was not observed in APEH-knockdown cells. These observations suggest that G01 have other cellular targets in addition to APEH. Recently we have reported that inhibition of SMases is of itself sufficient to impair KRAS PM localization [39, 40, 96]. Therefore, the simultaneous perturbation of SM metabolism and RE function via APEH inhibition is likely to result in the increased potency of G01 for inhibition of KRAS-dependent pancreatic cancer cell proliferation.

In our recent studies, several inhibitors of enzymes in the SM metabolism have been identified [39]. This study further shows that G01 synergized with three of these inhibitors, which target different SM metabolic enzymes, for mislocalizing KRAS and inhibiting MAPK signaling pathway. We therefore propose that G01 modulates SM metabolism through a molecular target different from those of FB1, R-fendiline, and STS, and that G01 may be used in drug cocktails for future anti-RAS therapies.

Previous studies suggest that APEH regulates cellular protein quality control, due to its peptidase activity and its role in the proteasomal regulation [114]. APEH and proteasome are responsible for the removal of oxidized proteins in cells [116, 117]. Therefore, we speculate that the aberrant protein quality control causes damage to the endolysosome, which is crucial for the recycling of RAS and PM lipids (Figure 25) [39, 40]. This may be a consequence of oxidative stress induced by accumulation of oxidatively damaged proteins [124, 125], that in turn causes

oxidative damage to the endolysosome and/or dysregulation of specific proteins involved in regulating of RE function (Figure 25) [126-128]. This speculation is further supported by our recent observation of KRAS PM mislocalization in cells treated with proteasome inhibitor, bortezomib.

APEH is more expressed in cancers expressing oncogenic mutant KRAS than in cancers expressing wild type KRAS. This correlation, when taken in the context of our observations that APEH activity is required to maintain KRAS and PtdSer on the inner leaflet of the PM, highlights the potential utility of APEH inhibitors and perhaps proteasomal inhibitors in the treatment of KRAS-dependent pancreatic cancer. Therefore, the future direction of this study is to test APEH inhibitors, such as ebelactone and G01, and perhaps proteasome inhibitors for inhibition of oncogenic KRAS-dependent xenograft tumors in mice. Due to our observation of the synergism effect between G01 and other compounds, we will also test drug cocktails *in vivo*. Besides G01, we have developed D01 and D02, which are more potent than G01 for mislocalizing KRAS from the PM. We will test them in combination with other pharmacological agents for inhibition of oncogenic KRAS-dependent xenograft tumors in mice as well.

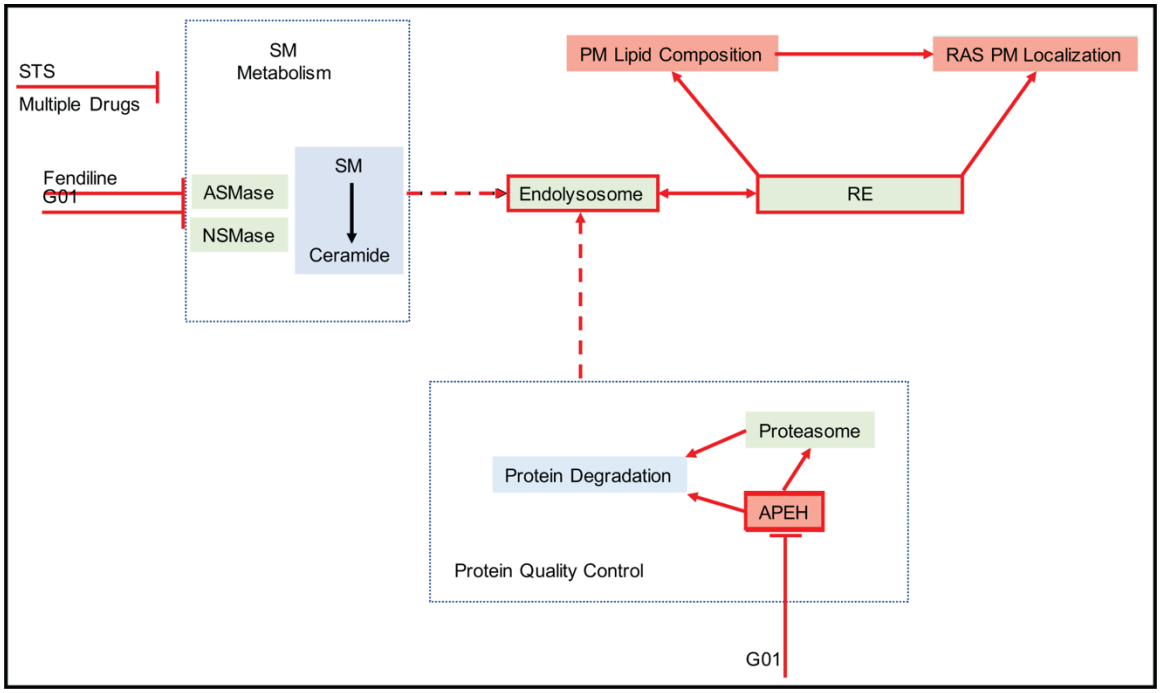

Figure 25. Molecular machineries involved in maintaining RAS PM localization targeted by G01. APEH inhibition by G01 and the subsequent proteasome inhibition impair cellular protein degradation. Thus, cellular protein quality control is compromised. The abberant protein quality control causes damage to the endolysosome, which is critical for the RE-mediated endosomal recycling of RAS and PM lipids. Besides APEH, SMase activity is inhibited by G01 as well. Because SMases are responsible for breaking down SM to ceramide, the inhibition of SMases by G01 increases cellular SM level and causes aberrant endolysosomal function, perturbing the endosomal recycling of KRAS and PM lipids. Besides G01, a disruption of KRAS and PM lipids was also observed in cells treated with other compounds targeting SM metabolism.

References

1. Bos JL, Rehmann H and Wittinghofer A (2007) GEFs and GAPs: critical elements in the control of small G proteins. Cell 129:865-877.

2. Freedman TS, Sondermann H, Friedland GD, Kortemme T, Bar-Sagi D, Marqusee S and Kuriyan J (2006) A Ras-induced conformational switch in the Ras activator Son of sevenless. Proceedings of the National Academy of Sciences 103:16692-16697.

3. Roberts PJ and Der CJ (2007) Targeting the Raf-MEK-ERK mitogen-activated protein kinase cascade for the treatment of cancer. Oncogene 26:3291.

4. Yordy JS and Muise-Helmericks RC (2000) Signal transduction and the Ets family of transcription factors. Oncogene 19:6503.

5. Rodriguez-Viciana P, Warne PH, Dhand R, Vanhaesebroeck B, Gout I, Fry MJ, Waterfield MD and Downward J (1994) Phosphatidylinositol-3-OH kinase direct target of Ras. Nature 370:527.

6. Pacold ME, Suire S, Perisic O, Lara-Gonzalez S, Davis CT, Walker EH, Hawkins PT, Stephens L, Eccleston JF and Williams RL (2000) Crystal structure and functional analysis of Ras binding to its effector phosphoinositide 3-kinase γ. Cell 103:931-944.

7. Datta SR, Brunet A and Greenberg ME (1999) Cellular survival: a play in three Akts. Genes & development 13:2905-2927.

8. Khwaja A, Rodriguez‐Viciana P, Wennström S, Warne PH and Downward J (1997) Matrix adhesion and Ras transformation both activate a phosphoinositide

3 - OH kinase and protein kinase B/Akt cellular survival pathway. The EMBO journal 16:2783-2793.

9. De Ruiter ND, Burgering BM and Bos JL (2001) Regulation of the Forkhead transcription factor AFX by Ral-dependent phosphorylation of threonines 447 and 451. Molecular and cellular biology 21:8225-8235.

10. Kelley GG, Reks SE, Ondrako JM and Smrcka AV (2001) Phospholipase Cϵ: a novel Ras effector. The EMBO journal 20:743-754.

11. Malumbres M and Barbacid M (2003) RAS oncogenes: the first 30 years. Nature Reviews Cancer 3:459.

12. Karnoub AE and Weinberg RA (2008) Ras oncogenes: split personalities. Nature reviews Molecular cell biology 9:517.

13. Cox AD, Fesik SW, Kimmelman AC, Luo J and Der CJ (2014) Drugging the undruggable RAS: Mission Possible? Nature Reviews Drug Discovery 13:828. doi: 10.1038/nrd4389

https://www.nature.com/articles/nrd4389 - supplementary-information

14. Forbes SA, Bindal N, Bamford S, Cole C, Kok CY, Beare D, Jia M, Shepherd R, Leung K and Menzies A (2010) COSMIC: mining complete cancer genomes in the Catalogue of Somatic Mutations in Cancer. Nucleic acids research 39:D945-D950.

15. Prior IA, Lewis PD and Mattos C (2012) A Comprehensive Survey of Ras Mutations in Cancer. Cancer Research 72:2457-2467. doi: 10.1158/0008-5472.can-11-2612

16. Haigis KM, Kendall KR, Wang Y, Cheung A, Haigis MC, Glickman JN, Niwa-Kawakita M, Sweet-Cordero A, Sebolt-Leopold J and Shannon KM (2008) Differential effects of oncogenic K-Ras and N-Ras on proliferation, differentiation and tumor progression in the colon. Nature genetics 40:600.

17. Keller JW, Franklin JL, Graves‐Deal R, Friedman DB, Whitwell CW and Coffey RJ (2007) Oncogenic KRAS provides a uniquely powerful and variable oncogenic contribution among RAS family members in the colonic epithelium. Journal of cellular physiology 210:740-749.

18. Hancock JF (2003) Ras proteins: different signals from different locations. Nature Reviews Molecular Cell Biology 4:373. doi: 10.1038/nrm1105

19. Hancock JF, Magee AI, Childs JE and Marshall CJ (1989) All ras proteins are polyisoprenylated but only some are palmitoylated. Cell 57:1167-1177. doi: https://doi.org/10.1016/0092-8674(89)90054-8

20. Omerovic J, Laude AJ and Prior IA (2007) Ras proteins: paradigms for compartmentalised and isoform-specific signalling. Cellular and molecular life sciences 64:2575.

21. Hancock JF, Paterson H and Marshall CJ (1990) A polybasic domain or palmitoylation is required in addition to the CAAX motif to localize p21ras to the plasma membrane. Cell 63:133-139. doi: https://doi.org/10.1016/0092-8674(90)90294-O

22. Laude AJ and Prior IA (2008) Palmitoylation and localisation of RAS isoforms are modulated by the hypervariable linker domain. Journal of Cell Science 121:421-427. doi: 10.1242/jcs.020107

23. Prior IA, Muncke C, Parton RG and Hancock JF (2003) Direct visualization of Ras proteins in spatially distinct cell surface microdomains. The Journal of cell biology 160:165-170.

24. Plowman SJ, Muncke C, Parton RG and Hancock JF (2005) H-ras, K-ras, and inner plasma membrane raft proteins operate in nanoclusters with differential dependence on the actin cytoskeleton. Proceedings of the National Academy of Sciences 102:15500-15505.

25. Murakoshi H, Iino R, Kobayashi T, Fujiwara T, Ohshima C, Yoshimura A and Kusumi A (2004) Single-molecule imaging analysis of Ras activation in living cells. Proceedings of the National Academy of Sciences 101:7317-7322.

26. Tian T, Plowman SJ, Parton RG, Kloog Y and Hancock JF (2010) Mathematical modeling of K-Ras nanocluster formation on the plasma membrane. Biophysical journal 99:534-543.

27. Janosi L, Li Z, Hancock JF and Gorfe AA (2012) Organization, dynamics, and segregation of Ras nanoclusters in membrane domains. Proceedings of the National Academy of Sciences 109:8097-8102.

28. Güldenhaupt J, Rudack T, Bachler P, Mann D, Triola G, Waldmann H, Kötting C and Gerwert K (2012) N-Ras forms dimers at POPC membranes. Biophysical journal 103:1585-1593.

29. Lin W-C, Iversen L, Tu H-L, Rhodes C, Christensen SM, Iwig JS, Hansen SD, Huang WY and Groves JT (2014) H-Ras forms dimers on membrane surfaces via a protein–protein interface. Proceedings of the National Academy of Sciences 111:2996-3001.

30. Nan X, Collisson EA, Lewis S, Huang J, Tamgüney TM, Liphardt JT, McCormick F, Gray JW and Chu S (2013) Single-molecule superresolution imaging allows quantitative analysis of RAF multimer formation and signaling. Proceedings of the National Academy of Sciences:201318188.

31. Zhou Y and Hancock JF (2015) Ras nanoclusters: Versatile lipid-based signaling platforms. Biochimica et Biophysica Acta (BBA)-Molecular Cell Research 1853:841-849.

32. Gorfe AA, Hanzal-Bayer M, Abankwa D, Hancock JF and McCammon JA (2007) Structure and dynamics of the full-length lipid-modified H-Ras protein in a 1, 2-dimyristoylglycero-3-phosphocholine bilayer. Journal of medicinal chemistry 50:674-684.

33. Abankwa D, Gorfe AA and Hancock JF (2008) Mechanisms of Ras membrane organization and signaling: Ras on a rocker. Cell cycle 7:2667-2673.

34. Zhou Y, Liang H, Rodkey T, Ariotti N, Parton RG and Hancock JF (2014) Signal integration by lipid-mediated spatial cross talk between Ras nanoclusters. Molecular and cellular biology 34:862-876.

35. Prior IA and Hancock JF (2012) Ras trafficking, localization and compartmentalized signalling. Seminars in Cell & Developmental Biology 23:145-153. doi: https://doi.org/10.1016/j.semcdb.2011.09.002

36. Prior IA and Hancock JF (2001) Compartmentalization of Ras proteins. Journal of cell science 114:1603-1608.

37. Kay JG, Koivusalo M, Ma X, Wohland T and Grinstein S (2012) Phosphatidylserine dynamics in cellular membranes. Molecular biology of the cell 23:2198-2212.

38. Zhou Y, Cho K-J, Plowman SJ and Hancock JF (2012) Nonsteroidal anti-inflammatory drugs alter the spatiotemporal organization of Ras proteins on the plasma membrane. Journal of Biological Chemistry:jbc. M112. 348490.

39. van der Hoeven D, Cho K-j, Zhou Y, Ma X, Chen W, Naji A, Montufar-Solis D, Zuo Y, Kovar SE and Levental KR (2018) Sphingomyelin metabolism is a regulator of K-Ras function. Molecular and cellular biology 38:e00373-17.

40. Cho K-j, van der Hoeven D, Zhou Y, Maekawa M, Ma X, Chen W, Fairn GD and Hancock JF (2016) Inhibition of acid sphingomyelinase depletes cellular phosphatidylserine and mislocalizes K-Ras from the plasma membrane. Molecular and cellular biology 36:363-374.

41. van der Hoeven D, Cho K-j, Ma X, Chigurupati S, Parton RG and Hancock JF (2013) Fendiline inhibits K-Ras plasma membrane localization and blocks K-Ras signal transmission. Molecular and cellular biology 33:237-251.

42. Rocks O, Peyker A, Kahms M, Verveer PJ, Koerner C, Lumbierres M, Kuhlmann J, Waldmann H, Wittinghofer A and Bastiaens PIH (2005) An Acylation Cycle Regulates Localization and Activity of Palmitoylated Ras Isoforms. Science 307:1746-1752. doi: 10.1126/science.1105654

43. Dekker FJ, Rocks O, Vartak N, Menninger S, Hedberg C, Balamurugan R, Wetzel S, Renner S, Gerauer M and Schölermann B (2010) Small-molecule

inhibition of APT1 affects Ras localization and signaling. Nature chemical biology 6:449.

44. Rocks O, Gerauer M, Vartak N, Koch S, Huang Z-P, Pechlivanis M, Kuhlmann J, Brunsveld L, Chandra A, Ellinger B, Waldmann H and Bastiaens PIH (2010) The Palmitoylation Machinery Is a Spatially Organizing System for Peripheral Membrane Proteins. Cell 141:458-471. doi: https://doi.org/10.1016/j.cell.2010.04.007

45. Goodwin JS, Drake KR, Rogers C, Wright L, Lippincott-Schwartz J, Philips MR and Kenworthy AK (2005) Depalmitoylated Ras traffics to and from the Golgi complex via a nonvesicular pathway. The Journal of Cell Biology 170:261-272. doi: 10.1083/jcb.200502063

46. Misaki R, Morimatsu M, Uemura T, Waguri S, Miyoshi E, Taniguchi N, Matsuda M and Taguchi T (2010) Palmitoylated Ras proteins traffic through recycling endosomes to the plasma membrane during exocytosis. The Journal of Cell Biology 191:23-29. doi: 10.1083/jcb.200911143

47. Zhou M, Wiener H, Su W, Zhou Y, Liot C, Ahearn I, Hancock JF and Philips MR (2016) VPS35 binds farnesylated N-Ras in the cytosol to regulate N-Ras trafficking. The Journal of Cell Biology 214:445-458. doi: 10.1083/jcb.201604061

48. Howe CL, Valletta JS, Rusnak AS and Mobley WC (2001) NGF signaling from clathrin-coated vesicles: evidence that signaling endosomes serve as a platform for the Ras-MAPK pathway. Neuron 32:801-814.

49. Jura N, Scotto-Lavino E, Sobczyk A and Bar-Sagi D (2006) Differential modification of Ras proteins by ubiquitination. Molecular cell 21:679-687.

50. Willumsen BM, Christensen A, Hubbert NL, Papageorge AG and Lowy DR (1984) The p21 ras C-terminus is required for transformation and membrane association. Nature 310:583.

51. Schmick M, Vartak N, Papke B, Kovacevic M, Truxius Dina C, Rossmannek L and Bastiaens Philippe IH (2014) KRas Localizes to the Plasma Membrane by Spatial Cycles of Solubilization, Trapping and Vesicular Transport. Cell 157:459-471. doi: https://doi.org/10.1016/j.cell.2014.02.051

52. Berndt N, Hamilton AD and Sebti SM (2011) Targeting protein prenylation for cancer therapy. Nature Reviews Cancer 11:775.

53. Rowinsky EK (2006) Lately, It Occurs to Me What a Long, Strange Trip It's Been for the Farnesyltransferase Inhibitors. Journal of Clinical Oncology 24:2981-2984. doi: 10.1200/JCO.2006.05.9808

54. Sebti SM and Der CJ (2003) Searching for the elusive targets of farnesyltransferase inhibitors. Nature Reviews Cancer 3:945. doi: 10.1038/nrc1234

55. Wahlstrom AM, Cutts BA, Liu M, Lindskog A, Karlsson C, Sjogren A-KM, Andersson KM, Young SG and Bergo MO (2008) Inactivating Icmt ameliorates K-RAS–induced myeloproliferative disease. Blood 112:1357-1365.

56. Amoyel M, Hackman M, Lee KE, Xu R, Miller G, Bar-Sagi D, Bach EA, Bergö MO and Philips MR (2013) Isoprenylcysteine carboxylmethyltransferase deficiency exacerbates KRAS-driven pancreatic neoplasia via Notch suppression. The Journal of clinical investigation 123:4681-4694.

57. Majmudar JD, Hodges-Loaiza HB, Hahne K, Donelson JL, Song J, Shrestha L, Harrison ML, Hrycyna CA and Gibbs RA (2012) Amide-modified prenylcysteine based Icmt inhibitors: structure–activity relationships, kinetic analysis and cellular characterization. Bioorganic & medicinal chemistry 20:283-295.

58. Manandhar SP, Hildebrandt ER and Schmidt WK (2007) Small-molecule inhibitors of the Rce1p CaaX protease. Journal of biomolecular screening 12:983-993.

59. Winter-Vann AM, Baron RA, Wong W, dela Cruz J, York JD, Gooden DM, Bergo MO, Young SG, Toone EJ and Casey PJ (2005) A small-molecule inhibitor of isoprenylcysteine carboxyl methyltransferase with antitumor activity in cancer cells. Proceedings of the National Academy of Sciences 102:4336-4341.

60. Bivona TG, Quatela SE, Bodemann BO, Ahearn IM, Soskis MJ, Mor A, Miura J, Wiener HH, Wright L and Saba SG (2006) PKC regulates a farnesyl-electrostatic switch on K-Ras that promotes its association with Bcl-XL on mitochondria and induces apoptosis. Molecular cell 21:481-493.

61. Cho K-j, Casteel DE, Prakash P, Tan L, van der Hoeven D, Salim AA, Kim C, Capon RJ, Lacey E and Cunha SR (2016) AMPK and eNOS signaling regulates K-Ras plasma membrane interactions via cGMP-dependent Protein Kinase 2. Molecular and Cellular Biology:MCB. 00365-16.

62. Zimmermann G, Papke B, Ismail S, Vartak N, Chandra A, Hoffmann M, Hahn SA, Triola G, Wittinghofer A and Bastiaens PI (2013) Small molecule inhibition of the KRAS–PDEδ interaction impairs oncogenic KRAS signalling. Nature 497:638.

63. Stephen AG, Esposito D, Bagni RK and McCormick F (2014) Dragging ras back in the ring. Cancer cell 25:272-281.

64. Herrmann C, Block C, Geisen C, Haas K, Weber C, Winde G, MoÈroÈy T and MuÈller O (1998) Sulindac sulfide inhibits Ras signaling. Oncogene 17:1769.

65. Waldmann H, Karaguni IM, Carpintero M, Gourzoulidou E, Herrmann C, Brockmann C, Oschkinat H and Müller O (2004) Sulindac‐Derived Ras Pathway Inhibitors Target the Rasoulidou E, Herrmann C, Brockmann C, Oschkinat H and Müller O (2004) Sulindacgnaling. Oncogene

66. Karaguni I-M, Herter P, Debruyne P, Chtarbova S, Kasprzynski A, Herbrand U, Ahmadian M-R, Glüsenkamp K-H, Winde G and Mareel M (2002) The new sulindac derivative IND 12 reverses Ras-induced cell transformation. Cancer research 62:1718-1723.

67. Patgiri A, Yadav KK, Arora PS and Bar-Sagi D (2011) An orthosteric inhibitor of the Ras-Sos interaction. Nature chemical biology 7:585.

68. Ostrem JM, Peters U, Sos ML, Wells JA and Shokat KM (2013) K-Ras (G12C) inhibitors allosterically control GTP affinity and effector interactions. Nature 503:548.

69. Roskoski Jr R (2012) ERK1/2 MAP kinases: structure, function, and regulation. Pharmacological research 66:105-143.

70. Lyons J, Wilhelm S, Hibner B and Bollag G (2001) Discovery of a novel Raf kinase inhibitor. Endocrine-related cancer 8:219-225.

71. Wilhelm SM, Carter C, Tang L, Wilkie D, McNabola A, Rong H, Chen C, Zhang X, Vincent P and McHugh M (2004) BAY 43-9006 exhibits broad spectrum

oral antitumor activity and targets the RAF/MEK/ERK pathway and receptor tyrosine kinases involved in tumor progression and angiogenesis. Cancer research 64:7099-7109.

72. Lito P, Rosen N and Solit DB (2013) Tumor adaptation and resistance to RAF inhibitors. Nature medicine 19:1401.

73. Hatzivassiliou G, Song K, Yen I, Brandhuber BJ, Anderson DJ, Alvarado R, Ludlam MJ, Stokoe D, Gloor SL and Vigers G (2010) RAF inhibitors prime wild-type RAF to activate the MAPK pathway and enhance growth. Nature 464:431.

74. Heidorn SJ, Milagre C, Whittaker S, Nourry A, Niculescu-Duvas I, Dhomen N, Hussain J, Reis-Filho JS, Springer CJ and Pritchard C (2010) Kinase-dead BRAF and oncogenic RAS cooperate to drive tumor progression through CRAF. Cell 140:209-221.

75. Poulikakos PI, Zhang C, Bollag G, Shokat KM and Rosen N (2010) RAF inhibitors transactivate RAF dimers and ERK signalling in cells with wild-type BRAF. Nature 464:427.

76. Oberholzer PA, Kee D, Dziunycz P, Sucker A, Kamsukom N, Jones R, Roden C, Chalk CJ, Ardlie K and Palescandolo E (2012) RAS mutations are associated with the development of cutaneous squamous cell tumors in patients treated with RAF inhibitors. Journal of Clinical Oncology 30:316.

77. Su F, Viros A, Milagre C, Trunzer K, Bollag G, Spleiss O, Reis-Filho JS, Kong X, Koya RC and Flaherty KT (2012) RAS mutations in cutaneous squamous-cell carcinomas in patients treated with BRAF inhibitors. New England Journal of Medicine 366:207-215.

78. Little AS, Balmanno K, Sale MJ, Newman S, Dry JR, Hampson M, Edwards PA, Smith PD and Cook SJ (2011) Amplification of the driving oncogene, KRAS or BRAF, underpins acquired resistance to MEK1/2 inhibitors in colorectal cancer cells. Sci. Signal. 4:ra17-ra17.

79. Kinsey C, Guillen K, Camolotto S, Boespflug A, Shea J, Seipp M, Scaife C and McMahon M (2018) Abstract LB-254: Combined inhibition of MEK and autophagy promotes regression of pancreatic cancer. AACR,

80. Teraishi F, Guo W, Zhang L, Dong F, Davis JJ, Sasazuki T, Shirasawa S, Liu J and Fang B (2006) Activation of sterile20-like kinase 1 in proteasome inhibitor bortezomib–induced apoptosis in oncogenic K-ras-transformed cells. Cancer research 66:6072-6079.

81. Steckel M, Molina-Arcas M, Weigelt B, Marani M, Warne PH, Kuznetsov H, Kelly G, Saunders B, Howell M and Downward J (2012) Determination of synthetic lethal interactions in KRAS oncogene-dependent cancer cells reveals novel therapeutic targeting strategies. Cell research 22:1227.

82. Downward J (2015) RAS Synthetic Lethal Screens Revisited: Still Seeking the Elusive Prize? Clinical Cancer Research 21:1802-1809. doi: 10.1158/1078-0432.ccr-14-2180

83. Amaravadi RK, Lippincott-Schwartz J, Yin X-M, Weiss WA, Takebe N, Timmer W, DiPaola RS, Lotze MT and White E (2011) Principles and current strategies for targeting autophagy for cancer treatment. Clinical cancer research 17:654-666.

84. Mancias JD and Kimmelman AC (2011) Targeting autophagy addiction in cancer. Oncotarget 2:1302.

85. Bryant K, Peng S, Tikunov A, Pierobon M, Gunda V, Tomar G, Singh P, Petricoin E, Macdonald J and Tran N (2018) Inhibition of ERK MAPK signaling increases pancreatic cancer dependency on autophagy. AACR,

86. Ying H, Kimmelman AC, Lyssiotis CA, Hua S, Chu GC, Fletcher-Sananikone E, Locasale JW, Son J, Zhang H and Coloff JL (2012) Oncogenic Kras maintains pancreatic tumors through regulation of anabolic glucose metabolism. Cell 149:656-670.

87. Hannun YA and Obeid LM (2008) Principles of bioactive lipid signalling: lessons from sphingolipids. Nature reviews Molecular cell biology 9:139.

88. Chang K-T, Anishkin A, Patwardhan GA, Beverly LJ, Siskind LJ and Colombini M (2015) Ceramide channels: destabilization by Bcl-xL and role in apoptosis. Biochimica et Biophysica Acta (BBA)-Biomembranes 1848:2374-2384.

89. Mukhopadhyay A, Saddoughi SA, Song P, Sultan I, Ponnusamy S, Senkal CE, Snook CF, Arnold HK, Sears RC and Hannun YA (2009) Direct interaction between the inhibitor 2 and ceramide via sphingolipid-protein binding is involved in the regulation of protein phosphatase 2A activity and signaling. The FASEB Journal 23:751-763.

90. Saddoughi SA, Gencer S, Peterson YK, Ward KE, Mukhopadhyay A, Oaks J, Bielawski J, Szulc ZM, Thomas RJ and Selvam SP (2013) Sphingosine analogue drug FTY720 targets I2PP2A/SET and mediates lung tumour

suppression via activation of PP2A‐RIPK1‐dependent necroptosis. EMBO molecular medicine 5:105-121.

91. Corcelle-Termeau E, Vindeløv SD, Hämälistö S, Mograbi B, Keldsbo A, Bräsen JH, Favaro E, Adam D, Szyniarowski P and Hofman P (2016) Excess sphingomyelin disturbs ATG9A trafficking and autophagosome closure. Autophagy 12:833-849.

92. Sentelle RD, Senkal CE, Jiang W, Ponnusamy S, Gencer S, Selvam SP, Ramshesh VK, Peterson YK, Lemasters JJ and Szulc ZM (2012) Ceramide targets autophagosomes to mitochondria and induces lethal mitophagy. Nature chemical biology 8:831.

93. Ogretmen B (2018) Sphingolipid metabolism in cancer signalling and therapy. Nature Reviews Cancer 18:33.

94. Bayer R and Mannhold R (1987) Fendiline: a review of its basic pharmacological and clinical properties. Pharmatherapeutica 5:103-136.

95. Cho K-j, Park J-H, Piggott AM, Salim AA, Gorfe AA, Parton RG, Capon RJ, Lacey E and Hancock JF (2012) Staurosporines disrupt phosphatidylserine trafficking and mislocalize Ras proteins. Journal of Biological Chemistry 287:43573-43584.

96. Maekawa M, Lee M, Wei K, Ridgway ND and Fairn GD (2016) Staurosporines decrease ORMDL proteins and enhance sphingomyelin synthesis resulting in depletion of plasmalemmal phosphatidylserine. Scientific reports 6:35762.

97. Salim AA, Xiao X, Cho K-J, Piggott AM, Lacey E, Hancock JF and Capon RJ (2014) Rare Streptomyces sp. polyketides as modulators of K-Ras localisation. Organic & biomolecular chemistry 12:4872-4878.

98. Ripley B (1977) Modelling spatial patterns (with discussion). JR Statist. Soc. B 39,172-212. Ripley17239J. R. Statist. Soc B 1977.

99. Hancock JF and Prior IA (2005) Electron microscopic imaging of Ras signaling domains. Methods 37:165-172.

100. Diggle PJ, Mateu J and Clough HE (2000) A comparison between parametric and non-parametric approaches to the analysis of replicated spatial point patterns. Advances in Applied Probability 32:331-343.

101. Franco I, Gulluni F, Campa CC, Costa C, Margaria JP, Ciraolo E, Martini M, Monteyne D, De Luca E and Germena G (2014) PI3K class II α controls spatially restricted endosomal PtdIns3P and Rab11 activation to promote primary cilium function. Developmental cell 28:647-658.

102. Choy E, Chiu VK, Silletti J, Feoktistov M, Morimoto T, Michaelson D, Ivanov IE and Philips MR (1999) Endomembrane trafficking of ras: the CAAX motif targets proteins to the ER and Golgi. Cell 98:69-80.

103. Zhou Y and Hancock JF (2015) Ras nanoclusters: Versatile lipid-based signaling platforms. Biochimica et Biophysica Acta (BBA) - Molecular Cell Research 1853:841-849. doi: https://doi.org/10.1016/j.bbamcr.2014.09.008

104. Drosten M, Dhawahir A, Sum EYM, Urosevic J, Lechuga CG, Esteban LM, Castellano E, Guerra C, Santos E and Barbacid M (2010) Genetic analysis of Ras

signalling pathways in cell proliferation, migration and survival. The EMBO Journal 29:1091-1104. doi: 10.1038/emboj.2010.7

105. Chou T-C (2010) Drug combination studies and their synergy quantification using the Chou-Talalay method. Cancer research 70:440-446.

106. Ghosh RN and Maxfield FR (1995) Evidence for nonvectorial, retrograde transferrin trafficking in the early endosomes of HEp2 cells. The Journal of Cell Biology 128:549-561.

107. Rodman JS and Wandinger-Ness A (2000) Rab GTPases coordinate endocytosis. J Cell Sci 113:183-192.

108. Roepstorff K, Grandal MV, Henriksen L, Knudsen SLJ, Lerdrup M, Grøvdal L, Willumsen BM and Van Deurs B (2009) Differential effects of EGFR ligands on endocytic sorting of the receptor. Traffic 10:1115-1127.

109. Parton RG (1994) Ultrastructural localization of gangliosides; GM1 is concentrated in caveolae. Journal of Histochemistry & Cytochemistry 42:155-166. doi: 10.1177/42.2.8288861

110. Gomez GA and Daniotti JL (2005) H-Ras Dynamically Interacts with Recycling Endosomes in CHO-K1 Cells INVOLVEMENT OF Rab5 AND Rab11 IN THE TRAFFICKING OF H-Ras TO THIS PERICENTRIOLAR ENDOCYTIC COMPARTMENT. Journal of Biological Chemistry 280:34997-35010.

111. Welz T, Wellbourne-Wood J and Kerkhoff E (2014) Orchestration of cell surface proteins by Rab11. Trends in cell biology 24:407-415.

112. Gonen H, Smith CE, Siegel NR, Kahana C, Merrick WC, Chakraburtty K, Schwartz AL and Ciechanover A (1994) Protein synthesis elongation factor EF-1

alpha is essential for ubiquitin-dependent degradation of certain N alpha-acetylated proteins and may be substituted for by the bacterial elongation factor EF-Tu. Proceedings of the National Academy of Sciences 91:7648-7652.

113. Hershko A, Heller H, Eytan E, Kaklij G and Rose IA (1984) Role of the alpha-amino group of protein in ubiquitin-mediated protein breakdown. Proceedings of the National Academy of Sciences 81:7021-7025.

114. Palmieri G, Bergamo P, Luini A, Ruvo M, Gogliettino M, Langella E, Saviano M, Hegde RN, Sandomenico A and Rossi M (2011) Acylpeptide hydrolase inhibition as targeted strategy to induce proteasomal down-regulation. PloS one 6:e25888.

115. Zeng Z, Rulten SL, Breslin C, Zlatanou A, Coulthard V and Caldecott KW (2017) Acylpeptide hydrolase is a component of the cellular response to DNA damage. DNA repair 58:52-61.

116. Fujino T, Ando K, Beppu M and Kikugawa K (2000) Enzymatic removal of oxidized protein aggregates from erythrocyte membranes. The Journal of Biochemistry 127:1081-1086.

117. Fujino T, Watanabe K, Beppu M, Kikugawa K and Yasuda H (2000) Identification of oxidized protein hydrolase of human erythrocytes as acylpeptide hydrolase1. Biochimica et Biophysica Acta (BBA)-Protein Structure and Molecular Enzymology 1478:102-112.

118. Sandomenico A, Russo A, Palmieri G, Bergamo P, Gogliettino M, Falcigno L and Ruvo M (2012) Small peptide inhibitors of acetyl-peptide hydrolase having

an uncommon mechanism of inhibition and a stable bent conformation. Journal of medicinal chemistry 55:2102-2111.

119. Tan L, Cho K-J, Neupane P, Capon RJ and Hancock JF (2018) An oxanthroquinone derivative that disrupts RAS plasma membrane localization inhibits cancer cell growth. Journal of Biological Chemistry 293:13696-13706.

120. Zhou Y, Prakash P, Liang H, Cho K-J, Gorfe AA and Hancock JF (2017) Lipid-sorting specificity encoded in K-Ras membrane anchor regulates signal output. Cell 168:239-251. e16.

121. Zhang X, Ye J, Engholm-Keller K and Højrup P (2011) A proteome-scale study on in vivo protein Nα-acetylation using an optimized method. PROTEOMICS 11:81-93. doi: doi:10.1002/pmic.201000453

122. Bergamo P, Palmieri G, Cocca E, Ferrandino I, Gogliettino M, Monaco A, Maurano F and Rossi M (2016) Adaptive response activated by dietary cis9, trans11 conjugated linoleic acid prevents distinct signs of gliadin-induced enteropathy in mice. European journal of nutrition 55:729-740.

123. Palumbo R, Gogliettino M, Cocca E, Iannitti R, Sandomenico A, Ruvo M, Balestrieri M, Rossi M and Palmieri G (2016) APEH inhibition affects osteosarcoma cell viability via downregulation of the proteasome. International journal of molecular sciences 17:1614.

124. Shimizu K, Fujino T, Ando K, Hayakawa M, Yasuda H and Kikugawa K (2003) Overexpression of oxidized protein hydrolase protects COS-7 cells from oxidative stress-induced inhibition of cell growth and survival. Biochemical and biophysical research communications 304:766-771.

125. Shimizu K, Kiuchi Y, Ando K, Hayakawa M and Kikugawa K (2004) Coordination of oxidized protein hydrolase and the proteasome in the clearance of cytotoxic denatured proteins. Biochemical and biophysical research communications 324:140-146.

126. Aits S and Jäättelä M (2013) Lysosomal cell death at a glance. The Company of Biologists Ltd,

127. Berndtsson M, Beaujouin M, Rickardson L, Havelka AM, Larsson R, Westman J, Liaudet‐Coopman E and Linder S (2009) Induction of the lysosomal apoptosis pathway by inhibitors of the ubiquitin‐proteasome system. International journal of cancer 124:1463-1469.

128. Yeung BH, Huang D-C and Sinicrope FA (2006) PS-341 (bortezomib) induces lysosomal cathepsin B release and a caspase-2-dependent mitochondrial permeabilization and apoptosis in human pancreatic cancer cells. Journal of Biological Chemistry.

129. Zhang FL and Casey PJ (1996) Protein prenylation: molecular mechanisms and functional consequences. Annual review of biochemistry 65:241-269.

Vita

Lingxiao Tan was born and grew up in the City of Qingdao, Shandong Province in China. He went to Qingdao Agricultural University for bachelor degree in Biological Sciences from September 2008 to June 2012. He joined the PhD program in Cell and Regulatory Biology in the University of Texas MD Anderson Cancer UTHealth Graduate School of Biomedical Sciences in August 2012.

Permanent address:

3707 Main Poplar Drive

Houston, Texas, USA, 77025